Aston University

If you have discovered material in AURA which is unlawful e.g. breaches copyright, (either yours or that of a third party) or any other law, including but not limited to those relating to patent, trademark, confidentiality, data protection, obscenity, defamation, libel, then please read our Takedown Policy and contact the service immediately

SYNTHESIS AND BIOLOGICAL PROPERTIES OF 2-PHENYLBENZOTHIAZOLE DERIVATIVES

CAROL JANE McCALL

Doctor of Philosophy

THE UNIVERSITY OF ASTON IN BIRMINGHAM

June 1990

This copy of the thesis has been supplied on the condition that anyone who consults it is understood to recognise that its copyright rests with the author and that no quotation from the thesis and no information derived from it may be published without the author's prior written consent.

The University of Aston in Birmingham

SYNTHESIS AND BIOLOGICAL PROPERTIES OF 2-PHENYLBENZOTHIAZOLE DERIVATIVES

Carol Jane McCall
Doctor of Philosophy
1990

2-Phenylbenzothiazoles have structural similarities to the antioestrogenic 2-phenylindole, zindoxifene and to the oestrogenic isoflavone, genistein which also inhibits tyrosine kinases. Hydroxylated 2-phenylbenzothiazole derivatives were therefore produced and tested for oestrogenic and tyrosine kinase inhibitory activity.

Synthesis of methoxy substituted 2-phenylbenzothiazoles was via the Jacobson method, demethylation being effected by boron tribromide at -70°C. Three amino substituted 2-phenylbenzothiazoles were also synthesised and tested for activity.

Data are presented for oestrogen receptor binding activity, aromatase inhibitory activity, epidermal growth factor receptor tyrosine kinase (EGFRTK) inhibitory activity and cytotoxicity to ANN-1, 3T3, MCF-7 and WIDR cells.

Oestrogen receptor binding affinity was shown by five of the nine compounds tested. 2-(4-hydroxy)-6-hydroxybenzothiazole was the most active of the benzothiazoles tested (RBA 0.7). This is low but comparable to that of genistein.

EGFRTK inhibitory activity was shown by four of the six benzothiazole derivatives tested; activity was comparable to that of genistein.

Cytotoxicity assays have shown no selective toxicity of 2-phenylbenzothiazoles to any of the cell lines tested. Toxicity to MCF-7 cells was similar to that for other cell lines despite some compounds showing oestrogen receptor binding capacity. Amino-substituted 2-phenylbenzothiazoles showed selective toxicity towards "transformed" ANN-1 cells compared to "normal" 3T3 cells but the mechanism of this selectivity has not been established.

Molecular modelling techniques, including CHEM-X, QUANTA and MOPAC were used to compare known ATP-competitive tyrosine kinase inhibitors with a model of ATP built from the crystal structure of the ATP-phosphoglycerate kinase complex. Structural features thought to be important to kinase inhibition were found and used to suggest further 2-phenylbenzothiazole analogues which may have improved activity.

KEYWORDS: antioestrogen, tyrosine kinase, modelling, synthesis, 2-phenylbenzothiazole

Acknowledgements

I should like to thank Prof. Malcolm Stevens for his guidance and for his support throughout my prolonged illness.

I thank my collegues Dr. Clare Sansom, Dr. Ian Dale, Tony O'Brian, Janet Cresswell and Dr. Paul Yates for their work on various parts of this project and Dr. Sally Freeman, Dr. Carl Schwalbe, Dr. Mike Threadgill and Prof. Andy Gesher for helpful discussions and advice.

I acknowledge the assistance of Dr. Martin Rowlands, The Insitute of Cancer Research, Sutton, Surrey in performing aromatase inhibition assays, Prof. Erwin von Angerer, University of Regensburg, West Germany in performing oestrogen receptor binding assays and Dr. Peter Lelieveld, EORTC screening and pharmacology group, Rijswijk, Netherlands in performing MCF-7 and WIDR cytotoxicity assays.

I should also like to thank Dr. Mike Perry and Karen Farrow for their technical support.

Finally, thanks to all the other staff and postgraduates for making the department a great place to study and socialize.

CONTENTS

ABBREVIATIONS

3-D	three dimensional
ADP	adenosine diphosphate
aq	aqueous
ATCC	American Tissue Culture Collection
ATP	adenosine triphosphate
BPDB	Brookhaven protein databank
c-AMP	cyclic adenosine monophosphate
CCDB	Cambridge crystallographic database
$CDCl_3$	deuterochloroform
$CHCl_3$	chloroform
CMT	catechol O-methyl transferase
CNDO	complete neglect of differential overlap
CO_2	carbon dioxide
CRC	Cancer Research Campaigm
CSCC	cholesterol side-chain cleavage enzyme
DES	diethylstilbestrol
DMF	dimethylformamide
DMBA	7,12-dimethylbenz[a]anthracene
DMEM	Dulbecco's modified Eagle medium
DMSO	dimethyl sulphoxide
$DMSO\text{-}D_6$	deuterodimethyl sulphoxide
DNA	deoxyribose nucleic acid
d.r.	diffuse reflectance
EDTA	ethylene diamine tetraacetic acid
eg.	for example

EGF	epidermal growth factor
EGFR	epidermal growth factor receptor
EORTC	European Organisation for Research and Treatment of Cancer
ER	oestrogen receptor
e.s.d	estimated standard deviation
EtOH	ethanol
eV	electron volts
fig.	figure
FT IR	fourier-transformation infra-red
Gly	glycine
h	hour
Hal	halogen
HEPES	N-2-hydroxyethylpiperazine-N'-2-ethanesulphonic acid
IC_{50}	concentration required to decrease activity/growth by 50%
INDO	intermediate neglect of differential overlap
i.r.	infra-red
KBr	potassium bromide
kcal	kilocalories
$K_3Fe(CN)_6$	potassium ferricyanide
LCAO	linear combination of atomic orbitals
lit.	literature
M^+	molecular ion
MeOH	methanol
Mg-ATP	Adenosine triphosphate complexed with magnesium

MgCl	magnesium chloride
min	minutes
M.M.	molecular mechanics
MNDO	modified neglect of diatomic differential overlap
M.O.	molecular orbital
mol. equiv.	molar equivalent
m.p.	melting point
mRNA	messenger ribose nucleic acid
NaCl	sodium chloride
NADP	nicotinamide adenine dinucleotide phosphate
NADPH	reduced nicotinamide adenine dinucleotide phosphate
NaOH	sodium hydroxide
NDDO	neglect of diatomic differential overlap
NIMR	National Institute for Medical Research
NMR	nuclear magnetic resonance
NMU	N-methylnitrosourea
PBS	phosphate buffered saline
PDGF	platelet derived growth factor
PDGFR	platelet derived growth factor receptor
PGK	phosphoglycerate kinase
pkC	protein kinase C
ppm	parts per million
PR	progesterone receptor
RBA	relative binding affinity
RSV	Rous sarcoma virus

SCF	self-consistent field
TCA	trichloroacetic acid
t.l.c.	thin layer chromatography
U.S.A.	United States of America

LIST OF FIGURES

Fig. Page

LIST OF TABLES

LIST OF PLATES

Plate Page

1 INTRODUCTION

1.1 Oestrogen and Cancer

Breast cancer is best considered a systemic disease as about 33% of the 110,000 new cases diagnosed each year in the U.S.A. will die of the systemic manifestations of the disease[1]. Despite advances in the early detection of tumours, surgical procedures and radiotherapy, the overall mortality rate for this disease has remained unchanged for several decades. In the majority of cases the tumour will have metastasised prior to the initial diagnosis. For this reason systemic therapy of some kind will be given, if not in the first line of treatment with surgery or radiation therapy, then later on when metastatic disease has become apparent.

Systemic therapy in the clinical management of breast cancer can take two forms, cytotoxic chemotherapy and hormonal manipulation. Clinical trials of combinations of chemotherapeutic agents rarely exceed 65-70% response rates and these are mainly partial responses, the average duration of response being less than one year[1]. It must also be remembered that these trials exclude patients unlikely to respond because of widespread metastatic

disease or poor performance status. The overall response of patients with metastatic breast cancer has been disappointing.

Endocrine manipulation is the other option available when systemic therapy is indicated. Two antioestrogens currently available for the palliation of advanced breast cancer; tamoxifen (1), which acts at the oestrogen receptor, blocking the effect of endogenous oestrogen;

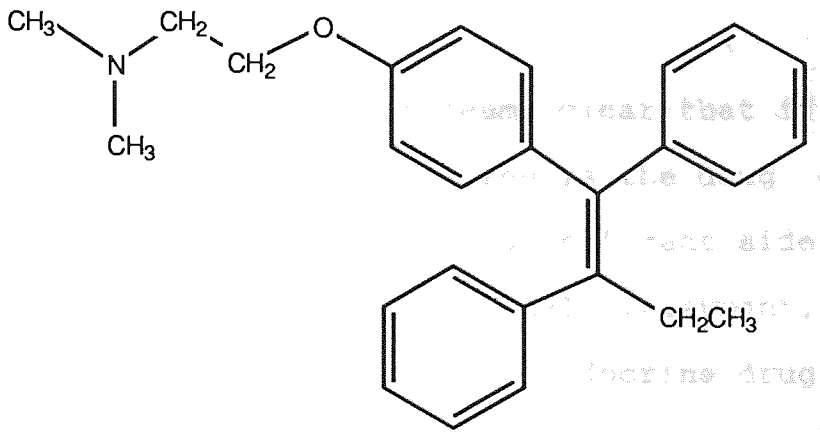

(1)

and aminoglutethimide (2), which lowers the levels of endogenous oestrogens by inhibiting the aromatisation of androstenedione and testosterone to oestrone and oestradiol respectively.

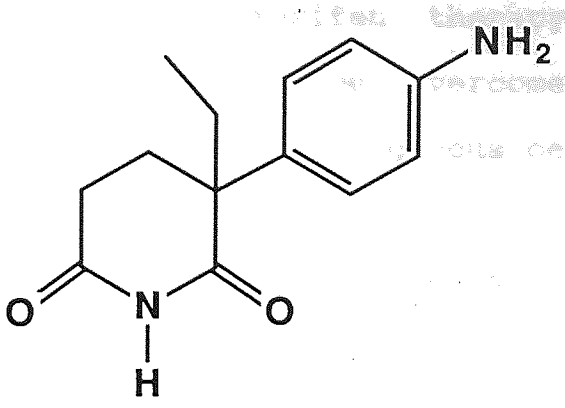

(2)

The treatments available for advanced breast cancer are palliative therefore quality of life for the patient is an important factor. There is debate as to which therapy should be used as first line treatment in the post-menopausal patient. It seems clear that if hormonal therapy is indicated then tamoxifen is the drug of choice because of its low incidence of significant side effects. The overall response rate to hormonal treatment, however, does not vary greatly with the endocrine drug chosen[2]. Trials have shown that when a second endocrine therapy is required after relapse, the highest overall response rate is for patients who had tamoxifen as first line therapy. Cytotoxic therapy can be given after first line tamoxifen therapy with the same overall results as with combination therapy or first line cytotoxic therapy followed by tamoxifen[3]. For the patient this would mean the more unpleasant cytotoxic therapy being given at a later stage

in disease progression where it may be more acceptable. In pre-menopausal women, the increase in circulating oestradiol levels with tamoxifen therapy[2] must be taken into account, but this may be overcome by oophorectomy, removing the main source of endogenous oestrogen.

Biopsies of breast cancer samples have shown that 50% contain oestrogen receptors (ER), but only 55-60% of these receptor positive tumours responded to hormonal manipulation[4]. There are several ways of determining the hormone receptor status of a tissue sample and results can be variable. Several bodies including the European Organisation for Research and Treatment of Cancer (EORTC) have set up quality assurance programmes which should help to eliminate discrepancies and allow comparison of results between centres[5]. After four years of this programme, coefficient of variation has been reduced from nearly 30% to 10% with centres using the same assay procedure. In comparing clinical trials which include determination of receptor status it must be remembered that a variety of assay procedures are used as well as different ER levels being used to designate whether a sample is receptor positive or receptor negative.

The presence of progesterone receptor (PR) in tumour biopsies has been used as a marker of the hormone dependency of the tumour[5]. Oestrogen can stimulate the

production of progesterone receptors therefore the presence of this receptor shows that the tissue has functional oestrogen receptors. In an analysis of a combination of studies response to endocrine therapy was correlated with ER and PR status (Table 1)[5].

Table 1: Overall Response of Advanced Breast Cancer to Endocrine Therapy

Receptor status	Overall response to hormonal therapy (%)
ER+	55
ER+/PR+	71
ER+/PR-	32
ER-	13
ER-/PR+	53
ER-/PR-	9

These results suggest that presence of ER and PR is a good predictor of response to endocrine therapy, but up to 12% of patients with tumours containing very few or no detectable oestrogen receptors still respond to tamoxifen therapy[2]. This may be because of the problems associated with measuring receptor levels in heterogeneous samples such as those from breast tumours or because tamoxifen exerts some other antitumour effect independent

of oestrogen receptor blockade, for example inhibition of protein kinase C (pkC)[6].

There have been several reports of the use of oestrogen and antioestrogens to synchronise the cell cycle of hormone dependent cells within mammary tumours in order to increase the fraction of cells susceptible to chemotherapy. Oestrogen priming, as it is called, seems to produce no increase in toxicity over chemotherapy alone. Despite one study showing a good response[7], this has not been confirmed by other workers[8].

It has been suggested that the induction of mammary tumours by chemical carcinogens is dependent on the presence of undifferentiated tissue. After full term pregnancy or some other hormonal therapies which lead to differentiation of the mammary tissues, induction of tumours by 7,12-dimethylbenz[a]anthracene (DMBA) is reduced or completely inhibited. Differentiated cells in alveolar buds and lobules have reduced proliferative capacity, DNA repair is more efficient and less polar metabolites are formed. These factors influence the susceptibility of cells to transformation[9]. The prevention of breast cancer by induction of differentiation of the breast tissue at an early stage is theoretically possible but much more needs to be known about the events leading up to carcinogenesis as it is

possible that the same treatment would accelerate development of tumours in any cells already exposed to the carcinogenic stimulus.

Prevention of the development of breast tumours in "at risk" patients may be possible with the advent of relatively non-toxic hormonal therapies. It has been shown that the development of DMBA-induced mammary tumours in rats is significantly reduced with tamoxifen treatment[10]. The prophylactic use of tamoxifen would necessitate long term administration and the side effects associated with such use are largely unknown. The level of side effects tolerated by "well" patients is much less than by those who already have diagnosed disease. Leucopenia, thrombo-cytopenia, gastrointestinal complaints, hot flushes and peripheral oedema have been reported after up to five years treatment but have necessitated withdrawal of therapy in less than 3% of patients[2]. The possibility that antioestrogens will lead to osteoporosis on long term exposure has been studied but the evidence so far suggests that this is not the case and there may even be a protective effect[11].

Tamoxifen is metabolised to 4-hydroxytamoxifen (3) which has greater oestrogen receptor binding affinity than the parent compound, but has less antitumour activity.

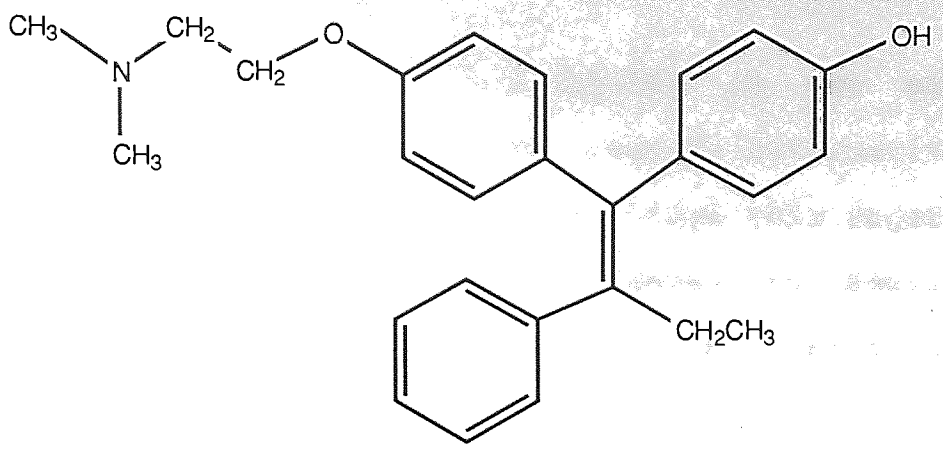

(3)

This difference can be partially explained by the shorter duration of action of 4-hydroxytamoxifen[12]. In vitro, 4-hydroxytamoxifen and oestradiol have been shown to stimulate MCF-7 cells to produce collagenase IV and to increase their ability to invade through a reconstituted basement membrane gel[13]. The clinical significance of this is not clear but it is theoretically possible that tamoxifen treatment could induce tumours to metastasise, a major disadvantage in prophylactic therapy.

Despite the vast increase in knowledge about the progression of breast cancers and prognostic factors, it is still not possible to say definitely that an ER negative tumour biopsy means the patient will not respond to endocrine therapy or that chemotherapy will give better results in this particular case. Several factors may be involved; it may be that the sample was not processed swiftly; that the frozen sample thawed during transit to

the laboratory; that the variability in the assay procedures led to a false negative result; alternatively that the patient is one of the 10% where this negative result does not reflect unresponsiveness to tamoxifen therapy. The determination of receptor content gives a guide to the outcome of treatment and prognosis but the actual treatment instigated is a matter for the judgement of the clinician.

There is no consistent relationship between receptor status and aromatase activity. This enzyme is the target for another group of agents used for treatment of hormone dependent cancer. The most widely used drug of this class, aminoglutethimide, inhibits the aromatisation of androstenedione to oestrone in peripheral tissues which is a major source of oestrogens in post-menopausal women (Fig. 1). The oestrone produced is then either converted to the inactive sulphate conjugate or to the active oestradiol. The aromatisation step is thought to be rate limiting in the production of oestradiol as the conversion by 17β-hydroxysteroid dehydrogenase of oestrone to oestradiol is more expedient[14]. Oestradiol may also be produced by the action of sulphatase and 17β-hydroxysteroid dehydrogenase on circulating oestrone sulphate[14]. Both of these enzymes are found in human breast cancer samples and could give the tumour a direct source of oestradiol, but as oestrone sulphate is

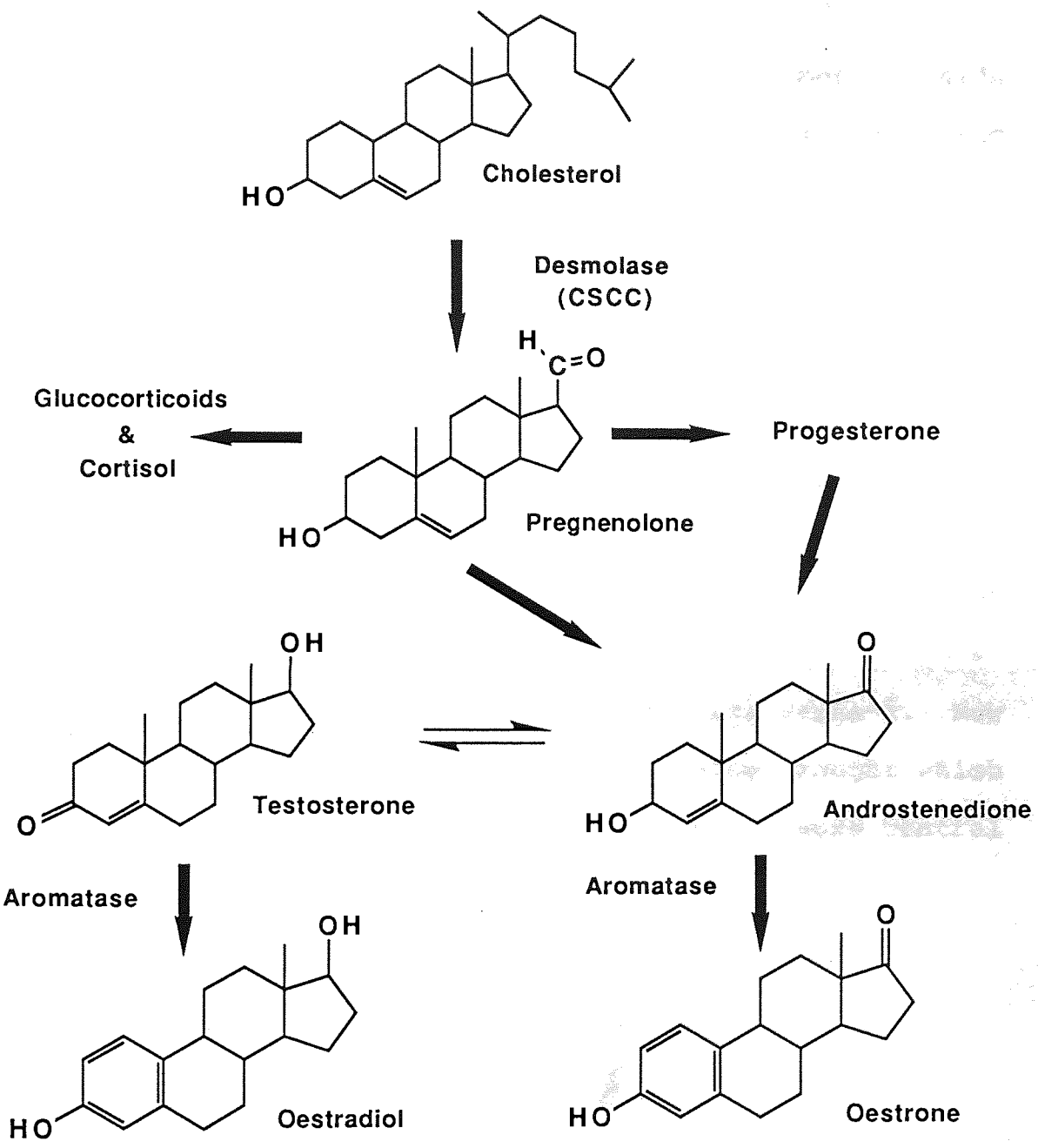

FIG. 1: Formation of oestrogens from cholesterol

originally produced by aromatisation, aminoglutethimide therapy should decrease the pool of this precursor.

Aminoglutethimide therapy induces a number of side effects including skin rashes, drowsiness, ataxia and drug induced fever but these generally abate after six weeks of therapy[15]. The action of aminoglutethimide against aromatase is not specific as it also inhibits desmolase (cholesterol side-chain cleavage enzyme) which is involved in cortisol production. Hydrocortisone or dexamethasone supplements are therefore given concurrently with aminoglutethimide therapy. Aminoglutethimide is usually given as a second line treatment for hormone dependent tumours as there is a greater chance of a further response after failure of tamoxifen therapy than vice versa[14]. New specific inhibitors of aromatase are being sought which will not require cortisol supplementation or cause central nervous system side effects.

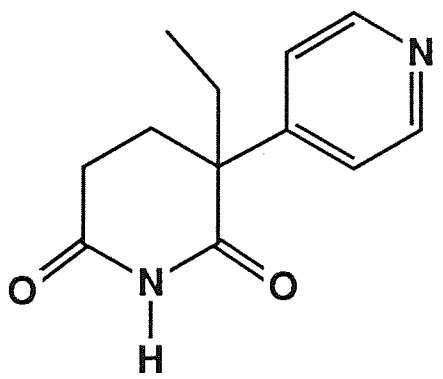

(6)

One of the compounds under development is pyridoglutethimide (6), an analogue of aminoglutethimide (2) which is more selective towards aromatase[16].

As can be seen from the above brief overview there remains much scope for improvement in the field of systemic treatment of breast cancer, both cytotoxic and endocrine.

1.2 Tyrosine Kinases and Cancer

Phosphorylation on tyrosine is a rare event in cells. Most protein phosphorylation occurs on serine and threonine residues, phosphorylation on tyrosine occurring in about 0.06% of cases[17].

Epidermal growth factor receptor (EGFR), platelet derived growth factor receptor (PDGFR) and insulin receptor have tyrosine kinase activity and are involved in the control of normal cell growth[18]. Stimulation of the receptor by its respective growth factor leads to phosphorylation on tyrosine of the receptor itself and other cellular proteins. Autophosphorylation of EGFR on its carboxy terminal end[19] and phosphorylation on threonine by pkC[20] is implicated in the modulation of receptor behavior. Any change in this normal regulatory system could lead to the uncontrolled growth of malignant cells.

The v-erb-B oncogene protein is very similar to EGFR in its transmembrane and cytosolic components but is truncated in the EGF binding region[21]. The v-erb-B protein can be considered as an altered receptor which has the capacity to phosphorylate itself and other cellular proteins but does not need external stimulation from a

growth factor. Tyrosine kinase activity of this protein has been demonstrated[22].

Tyrosine kinase activity has been associated with proto-oncogenes including *src*, *yes*, *fes*, *fps* and *abl*, which are at present increasingly implicated in the pathogenesis of cancer. The expression of these "housekeeping" genes is thought to be essential in normal development[23] but is under strict control. Breakdown of this control mechanism leading to overexpression of these gene products could be a precipitating factor in human malignancies.

Tyrosine kinases have a role in the development and continuation of some transformed states. Infection of cells with the Rous sarcoma virus (RSV) leads to the expression of the protein product of the *src* gene which possesses tyrosine kinase activity. The state of phosphorylation of cellular proteins in cells infected by a temperature sensitive mutant of RSV is closely linked to the transformed state of those cells[17].

HER-2/*neu* is an oncogene closely related to but different from c-*erb*-B[24] which as stated before codes for a protein with many similarities to EGFR. Amplification of the HER-2/*neu* gene is significantly correlated with the prognosis and survival time for patients with breast

cancer, but its role in the pathogenesis and/or maintenance of this disease is not known.

The expression of the protein product of c-erb-B_2 which has tyrosine kinase activity is a significant independent indicator of poor long term prognosis in breast cancer[25]. In patents whose tumours expressed c-erb-B_2, those also ER positive had the worst prognosis. As the 20% of patients whose tumours are c-erb-B_2 positive have a significantly worse prognosis it is interesting to speculate on the possibility of inhibiting this tyrosine kinase in the treatment of these breast cancers although a causal link to the maintainence of the disease has not been established.

In the case of chronic myeloid leukaemia a chromosomal aberration leads to the fusion of part of the abl oncogene with another gene which is normally expressed. The protein product of this aberrant gene has tyrosine kinase activity and phosphorylates at least one protein that is also phosphorylated after stimulation of the cells by EGF and PDGF[26]. This observation leads to the possibility that this altered tyrosine kinase activity is, at least in part, responsible for transformation of these cells.

Phosphorylation on tyrosine is detectable in fibroblasts transfected with the oncogenes v-src, v-abl, v-fps, and v-fes but not in control fibroblasts[27]. The phosphoproteins detected were the protein products of these genes along with some others. It is not clear how this observation is linked with controlled or uncontrolled growth, however, one possibility is that phosphorylation on the receptor itself initiates a cascade of events which eventually leads to the cellular response. Alternatively, it could be the intracellular proteins, which are also phosphorylated by these receptors, that go on to initiate the cascade. In normal cells phosphorylation of the receptor itself and of other proteins would be transient, stimulated by binding of the specific growth factor. In untransformed 3T3 fibroblasts, phosphotyrosine could only be detected immediately after stimulation with PDGF or EGF but not in growth arrested cells[27].

Human tumour cell lines have been assessed for their expression of proteins phosphorylated on tyrosine. Giodano et al[28] tested 18 such cell lines including HEPG2, HT29, A549, and MCF-7 and normal epithelium, bone marrow and untransformed fibroblasts. Abnormal levels of phosphotyrosine were seen in all tumour cell lines except HEPG2. None of the normal tissues showed detectable phosphotyrosine. It is still not clear if these elevated levels of phosphotyrosine cause the production and

maintenance of the transformed state but there is mounting evidence of their involvement somewhere in the deregulation of cell growth.

Production of tyrosine kinase inhibitors will enable researchers to study the mechanisms of control exerted by these enzymes and may lead to potential anticancer agents. At present there are two types of tyrosine kinase inhibitors, those which compete with the protein substrate and those that compete with the phosphate donor.

Substrate inhibitors of tyrosine kinases are derived from a natural product, erbstatin (7) which inhibits autophosphorylation of EGFR with an IC_{50} of 14μM[29].

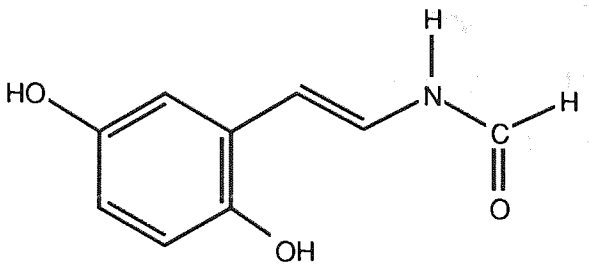

(7)

ST 638 (8), a 4-hydroxycinnamide derivative, shows differential inhibition of EGFR and $pp60^{v\text{-}src}$ kinases the IC_{50} values being 1.1μM and 87μM respectively[30] . This is not surprising, as the kinases will phosphorylate

different proteins giving rise to their own specific cellular response.

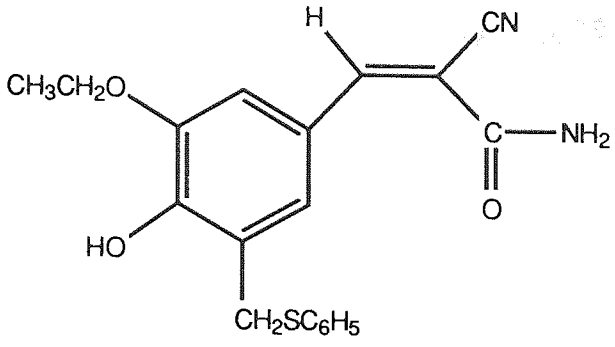

(8)

Levitzki's group have taken on the challenge of producing substrate inhibitors specific for each tyrosine kinase. The EGF receptor preferentially phosphorylates a polyGAT peptide available from Sigma, Poole, England, so this was used to assess the tyrosine kinase inhibitory activity of a number of benzylidenemalonitriles including 1,1-dicyano-2-(3,4,5-trihydroxyphenyl)ethene (9).

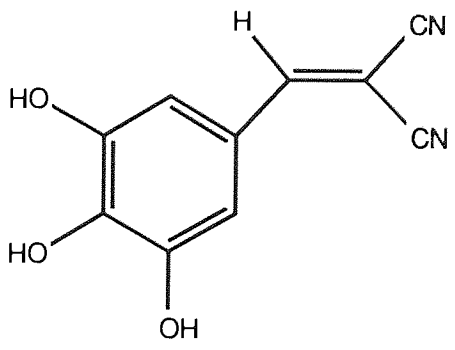

(9)

The range of activities were very wide and one of the trends noted was that increasing the number of hydroxy groups lead to increased activity. Compound (9) had an IC_{50} against EGFR tyrosine kinase of 3μM[29].

The other class of tyrosine kinase inhibtors act by competing with the phosphate donor usually adenosine triphosphate (ATP) (10)[31].

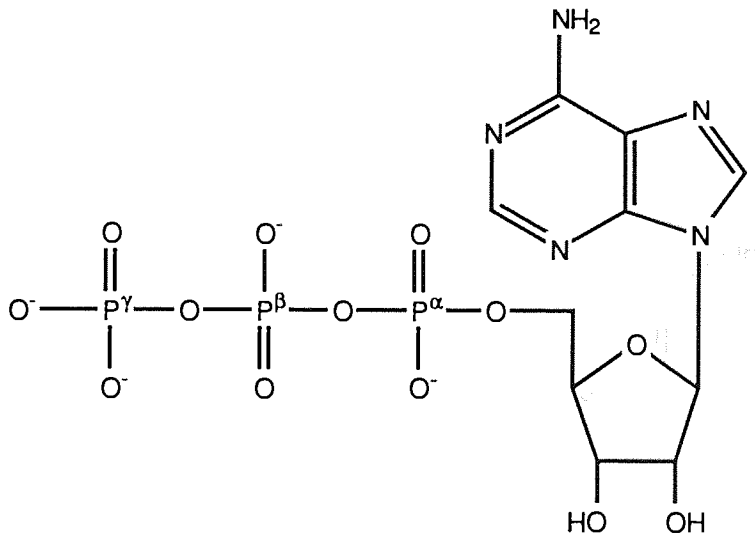

(10)

Quercetin (11) inhibits the phosphorylation on tyrosine by the protein product of the Rous Sarcoma virus ($pp60^{v\text{-}src}$), ATPases, phosphorylase kinase and other protein phosphorylations by type two casein kinases but

not cyclic-adenosine monophosphate (c-AMP) dependent kinases[32].

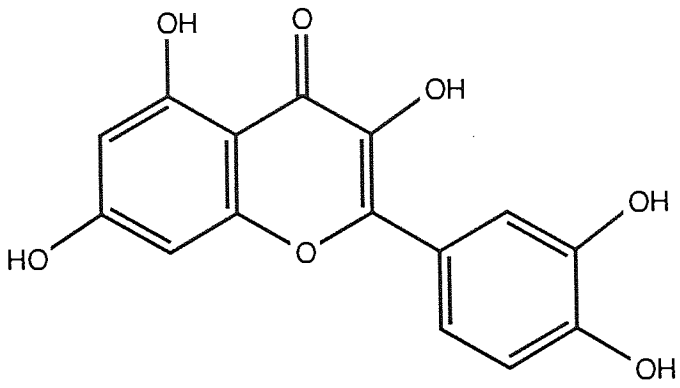

(11)

Kinase inhibition by Genistein (12) is much more specific to tyrosine phosphorylation. It does not inhibit pkC or phosphorylase kinase[33].

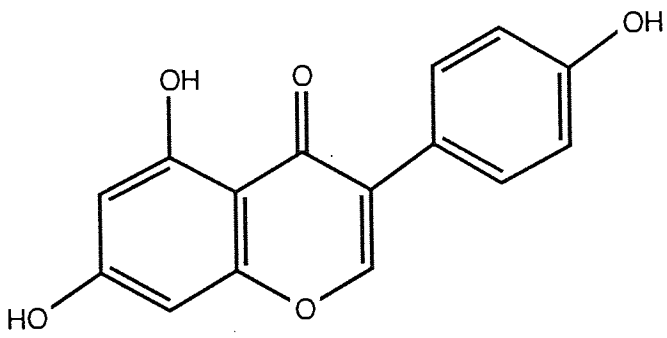

(12)

Amiloride (13), a commonly used potassium sparing diuretic, inhibits the tyrosine kinase activity of EGFR, PDGFR and insulin receptor[34] along with c-AMP dependent protein kinase, casein kinase type 1 and a number of others.

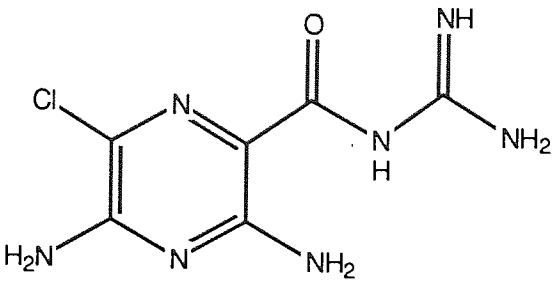

(13)

Table 2: Activity of protein kinase inhibitors

Compound	ref.	ENZYME			
		EGFR IC_{50} (μM)	$pp60^{v-src}$ IC_{50} (μM)	pkC IC_{50} (μM)	phosphorylase kinase IC_{50} (μM)
ST638 (8)	30	1.1	87		
(9)	29	3			
quercetin (11)	33	27	27	83	83
genistein (12)	33	22	26	>370	>370
amiloride (13)	34	500			

Within the group of tyrosine kinase inhibitors which compete with ATP there is some selectivity between enzymes[35]. Part of the study described in this thesis will try to define why this selectivity exists and to suggest new compounds which will have a greater selectivity.

1.3 Relationship between Oestrogens and Tyrosine Kinases

An area of interest to this project is how oestrogenic, antioestrogenic and tyrosine kinase inhibitory effects coincide. At first sight there is little area of overlap but some flavones and isoflavones have effects on both systems.

The lead compound in the relationship between oestrogens and tyrosine kinase inhibitors is genistein (12), the most potent of a group of isoflavone oestrogens[36].

This group of compounds is plant derived and occurs in foodstuffs including soyabeans, chick peas and most importantly for farmers, clover[37]. Eating of clovers containing these compounds, particularly formononetin (14), by sheep leads to "Clover disease" which is characterised by a marked loss of fertility.

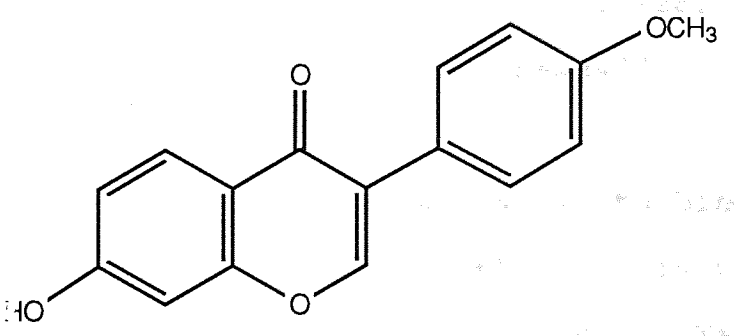

(14)

Formononetin (14) itself is inactive but in sheep 70% of a dose is metabolised to equol (15).

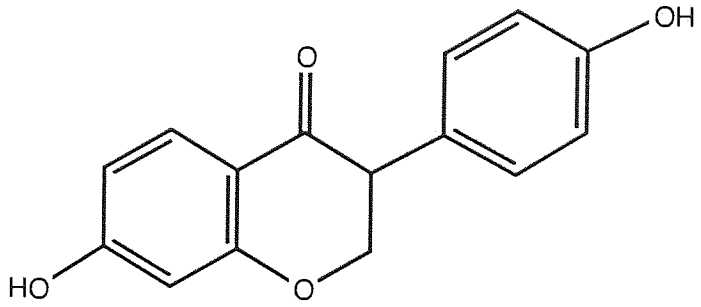

(15)

Equol (15), unlike genistein (12), is not extensively degraded in the rumen and is therefore available for absorption[37].

Only a few of the large number of naturally occuring isoflavones isolated have oestrogenic properties and these are weak compared to animal derived and synthetic oestrogens. Genistein (12) has a relative binding affinity (RBA) to MCF-7 cell oestrogen receptor of 2 with respect to oestradiol (RBA = 100)[37] and is also a potent and specific inhibitor of tyrosine kinase, having little effect on serine and threonine kinases[33].

Some isoflavenes have been shown to bind to oestrogen receptors and to have uterotrophic activity. The most active in a series of compounds tested by Wani et al[38] was 2-methyl-3-(4-acetoxyphenyl)-4-ethyl-7-acetoxy-isoflavene

(16). Assays performed were designed to show general antifertility effects so give little information on antioestrogenic effects[38].

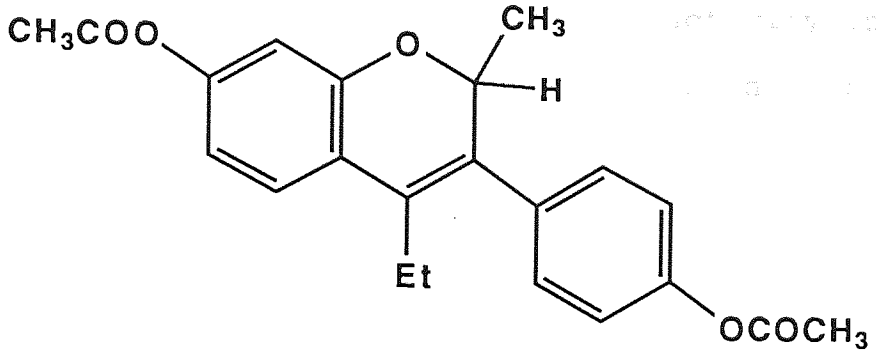

(16)

It is interesting to compare the substitution patterns of these compounds and the 2-phenylindene and 2-phenylindole derivatives; this will be discussed in Section 1.4.1.

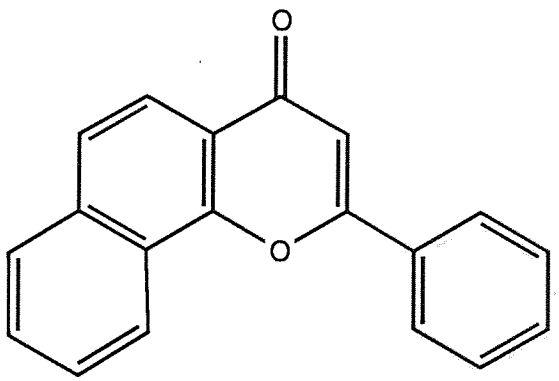

(17)

Flavones have a completely different mechanism of interaction with oestrogen biochemistry. 7,8-Benzoflavone

(17) is an inhibitor of aromatase, ten times more potent than aminoglutethimide (2)[39].

Oestrone produced from androstenedione by this enzyme is an important source of oestrogenic activity in post-menopausal women and as such it is a valid target for anti-hormonal anti-cancer agents (see Section 1.1). Other flavones with substantial aromatase inhibitory activity are shown in Table 3[39].

Table 3: Inhibition of human placental aromatase

Compound	IC_{50}(μM) (substrate androstenedione 40nM)
7,8-Benzoflavone (17)	0.07
Chrysin (18)	0.5
Apigenin (19)	1.2
Flavone (20)	8
Quercetin (11)	12

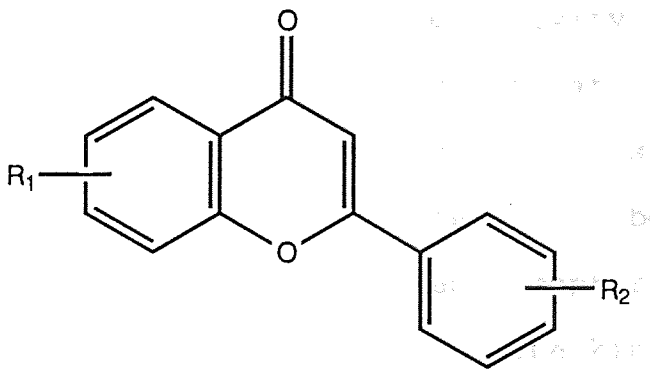

	R1	R2
(18)	H	5,7-di-OH
(19)	5,7-di-OH	4-OH
(20)	H	H

Inhibition of aromatase by flavones is proposed to be by competition with substrate, this being confirmed for 7,8-benzoflavone (17) and chrysin (18)[39].

Quercetin (11) is a potent inhibitor of aromatase and is also a widely studied inhibitor of protein kinases[31].

The interactions of oestrogens with tyrosine kinases described above have been based on compounds possessing activity in both systems. It is also true that the systems themselves interact.

As has previously been pointed out, phosphorylation of enzymes and proteins on tyrosine is involved in the regulation of the activity of these enzymes and proteins. Auricchio's group have shown that the oestrogen receptor itself is only able to bind oestrogen when it is phosphorylated on tyrosine[40]. The activity of partially purified receptor kinase is present at low levels in oestrogen responsive tissues and is stimulated by oestradiol. The stimulation seems to be effected by binding to an already phosphorylated receptor as there is no specific binding of oestradiol to the kinase itself[41]. Kinase activity is calmodulin-dependent and is not stimulated by the hormones progesterone, dexamethasone or testosterone which do not bind to the oestrogen receptor. Tamoxifen at its IC_{50} for inhibiting oestradiol binding causes a 45% reduction in the oestradiol induced

stimulation of this kinase[41]. Some of the antioestrogenic activity of tamoxifen (1) could be due to binding non-productively to oestrogen receptors which in turn would limit the number of phosphorylated oestrogen receptors capable of binding oestrogens.

In addition to receptor kinase there is an ER phosphotyrosine phosphatase which is present in the nuclei of oestrogen sensitive tissues. This phosphatase acts on the oestrogen-receptor complex leading to deactivation of the complex and abolition of oestrogen binding[42]. This phosphatase does not act on tamoxifen-receptor complex so would cause the antioestrogenic effects described above to last longer[43].

Oestrogens have effects on other tyrosine kinases including growth factor receptors which may explain some aspects of oestrogen induced cell growth. Administration of oestrogens has been shown to lead to a downregulation of insulin receptors and a reduction in the basal level of tyrosine kinase activity of these receptors[44]. The decrease in kinase activity 12 hours after the last oestradiol injection was not as substantial as would be expected from the reduction in insulin receptor numbers so it seems likely that oestrogens have other effects on tyrosine kinases or on phosphatase activity. Another receptor with tyrosine kinase activity, EGFR, is induced

by acute administration of oestradiol within the same time scale[45]. The insulin receptors used by[44] were only partially purified so some EGFR could have been present.

In immature rat uteri EGFR production is increased three fold within 12 hours of administration of a single dose of oestradiol and levels remain high for 18-24 hours. Oestradiol seems to be acting at the transcriptional level as within six hours of administration before the amount of EGFR increases, EGFR mRNA levels are raised by 3-4 fold[46]. Autophosphorylation and phosphorylation of exogenous substrates on tyrosine is increased by 2-3 fold 18 hours after oestradiol administration[45]. As these experiments were performed <u>in vivo</u> it is difficult to interpret these results because many other endogenous products may be implicated, but it is known that EGFR is not induced by dexamethasone, dihydrotestosterone or progesterone under the conditions used.

Eighteen hours after oestradiol administration to immature, ovariectomised rats, there is an increase in DNA production. This effect is preceded by EGFR production but this increase in EGFR production does not always lead to increased DNA synthesis. For example, when oestradiol is administered with dexamethasone, EGFR levels induced are comparable to oestradiol administration alone but the great increase in DNA synthesis is not seen[46].

The physiological significance of the ability of oestrogen to alter EGFR levels is supported by the observation that EGFR levels vary throughout the oestrus cycle and that EGF may be implicated in contraction of myometrial tissues[46]. It is still not clear whether oestrogen induced growth is mediated via EGFR and its tyrosine kinase activity.

1.4 Rationale for the Preparation of 2-Phenylbenzothiazole Derivatives

1.4.1 Oestrogenic activity

One of the aims of this project was to prepare and test new chemical entities which may be antioestrogenic in character and therefore useful in the treatment of hormone dependent breast cancer. The 2-phenylbenzothiazole nucleus (21) was chosen because of its similarity to some indoles[47] and indenes[48] already shown to have anti-oestrogenic activity.

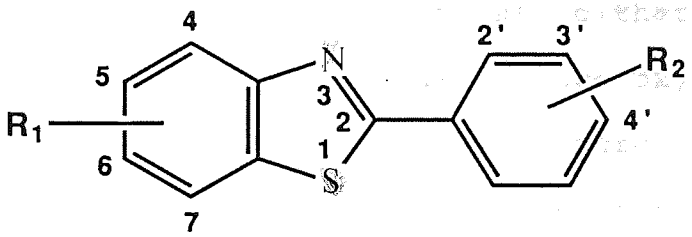

(21)

Structural features in these compounds thought to be important to oestrogen receptor binding, and agonist/antagonist activity are discussed below.

One antioestrogen currently under development is 5-acetoxy-2-(4-acetoxyphenyl)-1-ethyl-3-methylindole, (zindoxifene or D16726) (22)[49].

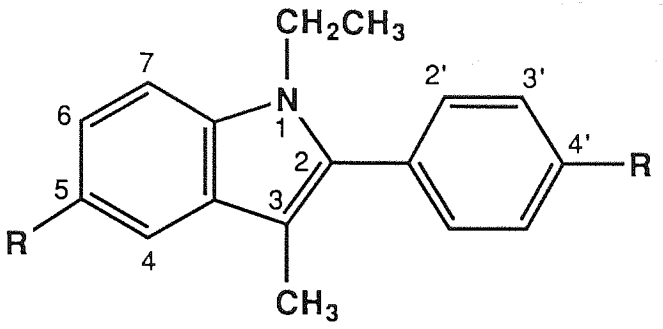

(22) R = $OCOCH_3$

(23) R = OH

This is a compound based on the 2-phenylindole nucleus with one oxygen function at either end. This compound acts as a prodrug as the acetoxy moieties are cleaved readily <u>in vivo</u> to give hydroxy substituted compound D15414 (23). The free hydroxyl groups are believed to be important in oestrogen receptor binding. D15414 (23) has a relative binding affinity (RBA) of 10 (oestradiol RBA = 100)[49]. The RBA is defined as the molar ratio of test compound required to decrease binding of radiolabelled 17β-oestradiol by 50% multiplied by 100. Administration of zindoxifene (22) to immature mice does not lead to a marked oestrogenic response and has been shown to inhibit the increase in uterine weight caused by administration of oestrone[47]. Growth inhibition of MCF-7

cells in culture by D15414 (23) is similar to that caused by tamoxifen but no activity is seen in hormone independent models[49]. This fact, coupled with the inhibitory activity of zindoxifene (22) against DMBA-induced rat mammary carcinoma, N-methylnitrosourea (NMU) induced rat mammary tumour and transplanted MXT tumours of mouse[49] has led to zindoxifene being selected as a potential therapeutic agent for hormone dependent cancers.

Structure activity relationships in this group of compounds suggest that several features are necessary for oestrogen receptor binding. All active compounds had a small alkyl chain at N1, a methyl or an ethyl group being favoured at C3 of the indole nucleus but not essential. A standard requirement for oestrogenic and antioestrogenic agents is the presence of two hydroxy groups at either end of the molecule and it is possible that the distance between these oxygen atoms is important for binding - this will be discussed in Section 2.3.1. Active indoles have hydroxy substituents at 4'- and 5- or 6-positions. An oxygen function in position 7 interferes with binding[47].

A two carbon bridge has been built between C3 of the indole nucleus and the ortho position of the 2-phenyl ring to form 11-alkylbenzo[a]carbazoles (24 and 25) and their 5,6-dihydro derivatives (26 and 27).

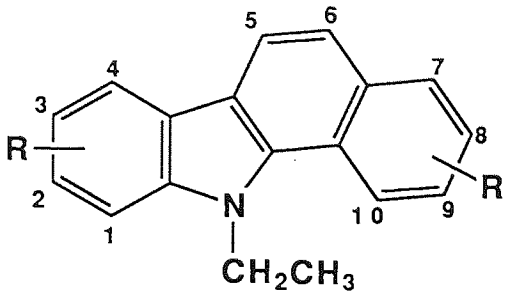

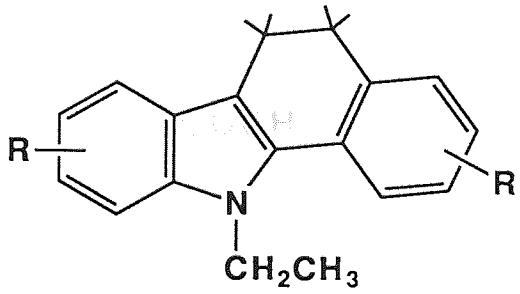

(24) R = $OCOCH_3$

(25) R = OH

(26) R = $OCOCH_3$

(27) R = OH

The purpose of this modification was to make the ring system more rigid, as in endogenous oestrogens, and to introduce the potential to intercalate into DNA. Compounds with oxygen functions at positions 3 and 8 or 9 had high RBAs; 3, 9-disubstituted compounds had oestrogenic character while 3, 8-disubstitution gave only low agonist activity[50].

2-Phenylindenes have also been studied for oestrogenic activity, using the same substituents (small alkyl groups at C1 and C3, and one oxygen function on each of the A and C rings) and also catechol type structures eg. 1-methyl-2-(3,4-diacetoxyphenyl)-3-ethyl-5,6-diacetoxyindene (28)[48].

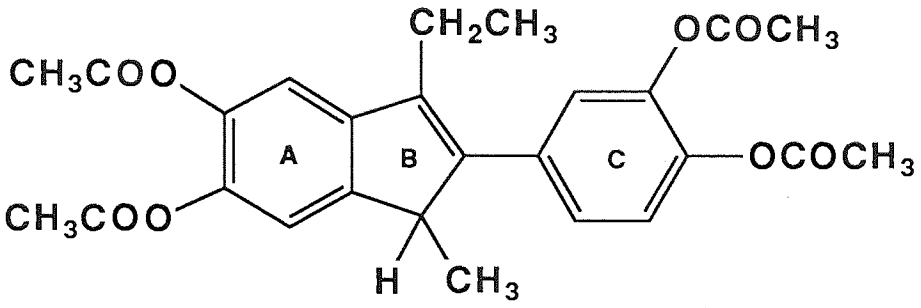

(28)

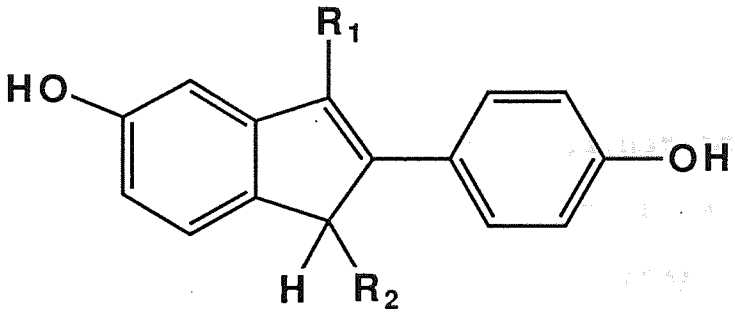

(29) R1 = Et R2 = Me

(30) R1 = Me R2 = Et

Compound 28 was derived from the oestrogenic compounds indenestrol A (29) and indenestrol B (30) which are metabolites of diethylstilbestrol (DES)(31)[51].

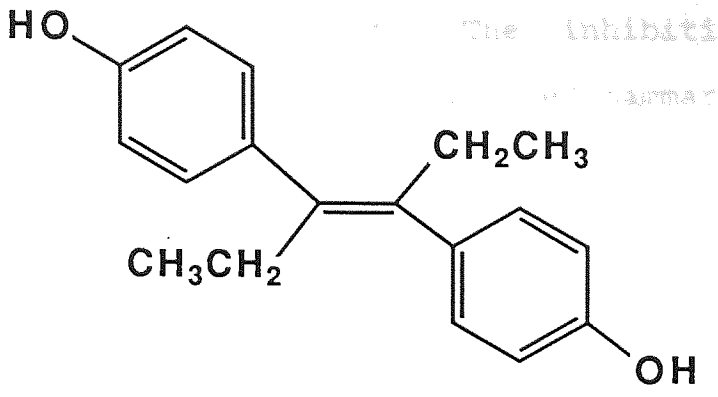

(31)

Indenes have a potential chiral centre at C1 and the isomers of Indenestrol A (29) have been shown to vary greatly in binding affinity for the oestrogen receptor. Compound (28) is a partial agonist, having antioestrogenic activity, and antitumour activity against transplantable MXT hormone-dependent mammary carcinoma, but also oestrogenic activity measured by increase in uterine weight. The antitumour effect decreases with increasing dose but the oestrogenic effect does not, which may suggest agonist properties predominate at higher doses[48]. It would be interesting to see if oestrogenic and antioestrogenic properties were due to the different isomers present.

Antitumour activity has also been found in 2-phenylbenzo[b]thiophene analogues of zindoxifene. The most active in this series was 2-(4-hydroxyphenyl)-3-

methyl-5-hydroxybenzothiophene (32). This compound binds strongly to ER (RBA = 59.6) and exhibits both oestrogenic and antioestrogenic properties. The inhibition of MXT-transplantable tumours and DMBA induced mammary carcinoma in rats was significant and comparable to that caused by zindoxifene (22)[52].

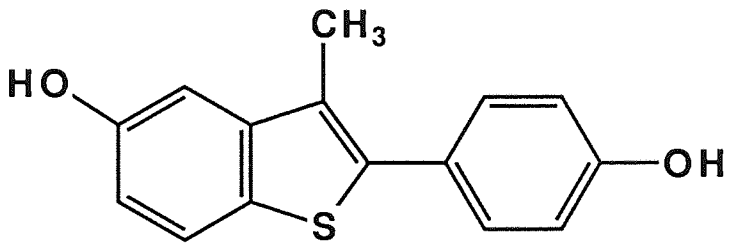

(32)

Catechol substitution patterns on endogenous oestrogens have been associated with the regulation of oestrogen receptor stimulation within cells[53]. The growth inhibitory action of adding 2-hydroxyoestrone (33) to MCF-7 cells in culture is antagonised when oestradiol was added concurrently and quinalizarin was present to block the action of catechol O-methyl transferase (CMT).

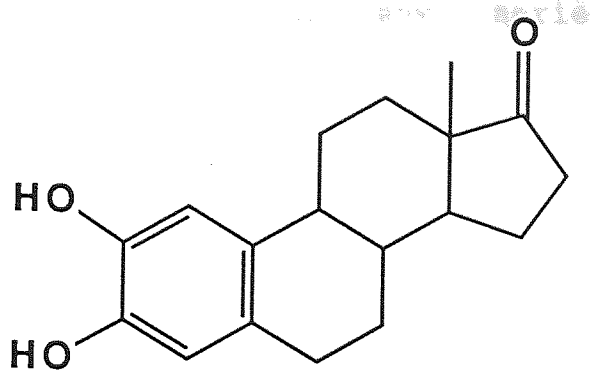

(33)

Without blockade of CMT no inhibition of growth was seen because 2-hydroxyoestrone was metabolised to the inactive 2-methoxyoestrone within one hour of its addition[54]. The growth inhibitory effect of 2-hydroxyoestrone (33) appears to be receptor mediated and irreversible as addition of oestradiol four days after 2-hydroxyoestrone did not rescue the cells. It is possible that the mechanism of growth inhibition by catechol type oestrogens is by enzymatic transformation to reactive semiquinones or quinones by enzymes such as peroxidase which are known to be found in high levels in about 30% of human breast cancer samples[55]. 2-Hydroxyoestradiol is oxidised by cytochrome P-450 leading to reactive intermediates which can irreversibly bind to cellular macromolecules. This binding is mediated by superoxide anions but is decreased only 20-35% by superoxide dismutase; another cytochrome P-450 mediated pathway is

implicated[56]. The use of catechol substitution is therefore interesting in any series of potential anticancer agents.

1.4.2 Tyrosine kinase inhibition

A further aim of this project was to investigate whether 2-phenylbenzothiazoles would be inhibitors of protein tyrosine kinases. 2-Phenylbenzothiazoles have structural similarities to the flavones and isoflavones which are kinase inhibitors (Section 1.2). These structural similarities which are discussed in detail in Section 2.3 may also be implicated in any antioestrogenic activity (Section 1.4.1).

1.5 Synthesis

Substituted 2-phenylbenzothiazoles were produced both for biological testing and to test the scope of the reaction sequence.

2-Phenylbenzothiazole derivatives were prepared by a three step synthesis (Fig. 2) beginning with preparation of substituted benzanilides from substituted anilines and acid chlorides in a Schotten-Baumann type reaction using pyridine as base. The starting materials were available with a wide range of substituents allowing various 2-phenylbenzothiazole derivatives to be synthesised.

The benzanilides were thionated using Lawesson's reagent [2,4 - bis - (4-methoxyphenyl) - 1,3 - dithia-diphosphetane-2,4-disulphide (34)]. This reagent may be used to convert a wide range of carbonyl functions to thiocarbonyls in good yield[57]. Lawesson's reagent is reported not to attack nitro groups, dealkylate ethers, or transform primary amides to nitriles. It is thought that the reaction proceeds by initial attack by the carbonyl oxygen on the phosphorus of the dithiophosphine ylide (Fig. 3). Thionation was previously carried out using phosphorous pentasulphide, but severe conditions were required and yields were variable. In reaction with Lawesson's reagent, phenols and anilines tend to form new

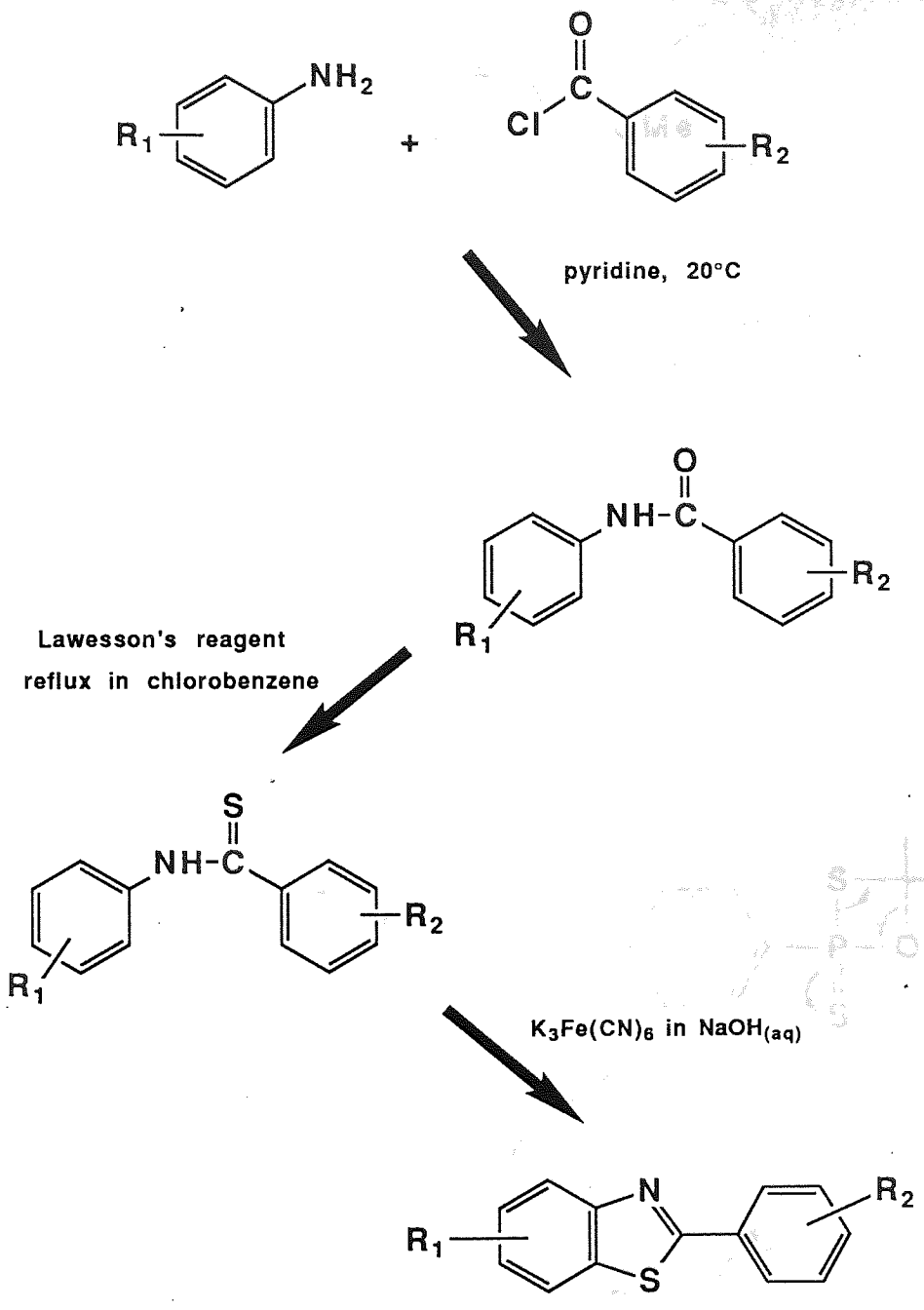

Fig 2 : Reaction scheme

for the preparation of

2-phenylbenzothiazole derivatives

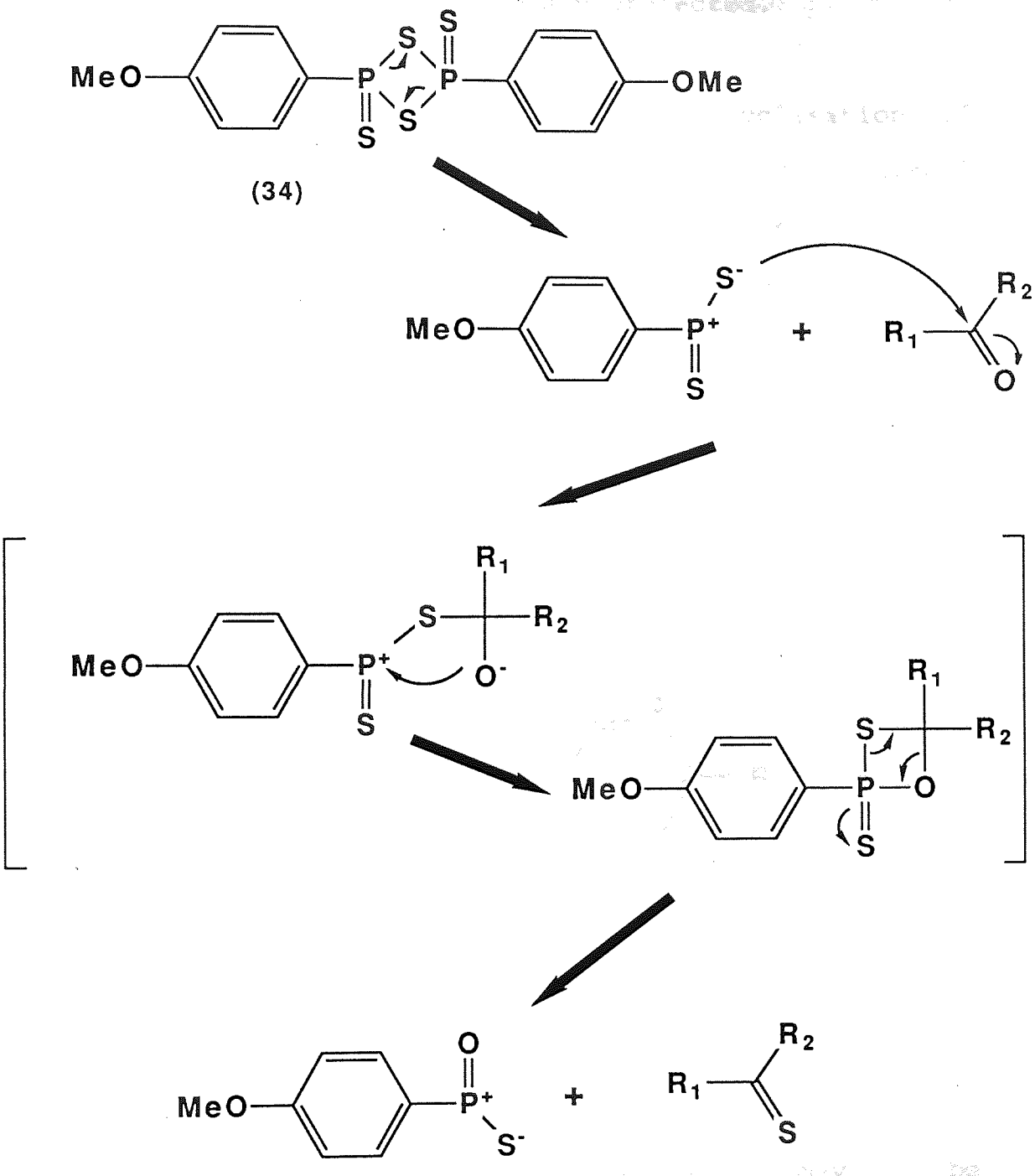

Fig. 3: Mechanism of the reaction of

Lawesson's reagent with carbonyl containing compounds

P-O and P-N bonds respectively so are not good substrates for this reaction unless previously protected.

Benzothiazoles were produced by cyclisation of thioamides using potassium ferricyanide in aqueous alkali (Jacobson synthesis)[58]. Under these conditions potassium ferricyanide acts as a complex electron-extracting ion[59]. The best results are obtained when there are electron donating groups, enhancing the electron density ortho to the nitrogen[58]. The possible mechanism of this reaction is discussed in Section 3.2.

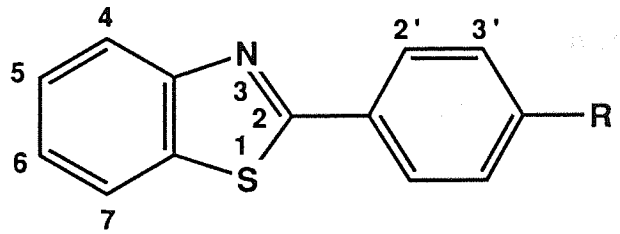

(35) R = OMe

(36) R = H

2-(Substituted-phenyl)benzothiazoles may be synthesised by the direct reaction of o-aminothiophenol with the appropriate benzoyl chloride[60]. This method was used to produce 2-(4-methoxyphenyl)benzothiazole (35) but presented no advantages over the chosen method for

preparation of compounds substituted at the benzothiazole ring. Electrophilic substitution of 2-phenylbenzothiazole (36) occurs exclusively at the 6-position[58] giving little scope for introducing substituents at the 2-phenylbenzothiazole nucleus after it has been formed.

Demethylation of the protecting methoxy groups on the 2-phenylbenzothiazoles prior to biological testing was effected using boron tribromide at -78°C in dichloromethane. This method was favoured in the demethylation of methoxy substituted 2-phenylindoles[47]. Other methods of cleaving ethers have been reviewed by Bhatt and Kulkarni[61].

The selective reduction of aromatic nitro compounds with stannous chloride in non-acidic and non-aqueous conditions has been described by Bellamy and Ou[62]. In the present work, nitro-substituted 2-phenylbenzothiazoles were reduced quickly and effectively to their amino derivatives with stannous chloride in refluxing ethanol.

Tamoxifen (1), quercetin (11), amiloride (13), DES (31), and unsubstituted 2-phenylbenzothiazole (36) were available commercially. Genistein (12) was produced by demethylation of biochanin A (37), its 4'-methyl ether.

1.6 Biological Testing

The compounds produced were subjected to initial screening as potential antioestrogenic anticancer agents and potential tyrosine kinase inhibitors.

1.6.1 Assessment of hormonal activity.

The Cancer Research Campaign have drawn up guidelines for the testing of potential antioestrogenic anticancer agents[63] which emphasise the contrast between conventional cytotoxic agents and hormonal agents. For antioestrogenic agents initial tests recommended are for oestrogen receptor binding affinity, inhibition of growth of an *in vivo* tumour model, oestrogenic and anti-oestrogenic activity in immature mice and inhibition of growth of an oestrogen dependent cell line.

1.6.1.1 Oestrogen receptor binding

The relative binding affinity of a compound to oestrogen receptor may be measured against receptors from a number of sources. The values found are specific to the receptor from that tissue type but although there are differences, values are of the same order of magnitude.

Table 4: Relative binding affinities to different oestrogen receptor types[37]

Compound	tissue type	RBA
Genistein (12)	rat uterine	1.3
	rabbit uterine	0.6
	sheep uterine	0.9
	MCF-7	2.0

The dextran-coated charcoal assay procedure for determining the ability of compounds to bind to oestrogen receptors is described in Section 6.1.

The relative binding affinity for a compound to the oestrogen receptor is an important parameter but is a physical measurement and does not give any indication of the biological consequences of such a binding interaction. Further tests are necessary to show agonist or antagonist properties.

1.6.1.2 Assay of oestrogenic or antioestrogenic activity

The assay of oestrogenic and antioestrogenic action is by the effect of the compounds on the weight of immature mouse uteri. Immature female mice are treated with test compound and the subsequent weight of the isolated uteri determined. Oestrogenic effects show as an increase in uterine weight and can be compared to the weight increase caused by a known dose of an oestrogen.

Aston University Library & Information Services
Aston Triangle Birmingham B4 7ET England

When a standard dose of an oestrogen is given along with the test compound, antioestrogenic effects can be determined by any inhibition of the increase in weight caused by the oestrogen[47]. Ideally an antioestrogen will have exclusively antioestrogenic properties but most compounds will be partial agonists.

1.6.1.3 In vivo antitumour activity

Dimethylbenz[a]anthracene (DMBA) induced tumours in Sprague-Dawley rats have commonly been used to assess the antitumour potential of antioestrogenic agents[64]. These tumours regress in response to ovariectomy and regrow with oestrogen supplementation, unfortunately regrowth does not occur if the animals are hypophysectomised indicating that this hormone dependence is primarily prolactin mediated. Human breast cancers are unlike this model in that they are directly or indirectly oestrogen dependent[65]. N-Nitrosomethylurea (NMU) can also be used to induce mammary cancer in rats; it is thought to effect a single point mutation leading to activation of H-ras-1 locus[66]. It has been reported that NMU-induced tumours have the ability to metastasise[67] and that there is a measure of direct oestrogen dependence as well as prolactin dependence[68] thereby making it a better model of human breast cancer than DMBA-induced tumours.

Transplantable tumours such as the hormone dependent MXT mammary carcinoma in BDF-1 mice may also be used to investigate antitumour effects of new compound[69]. An advantage of this in vivo model is that antitumour effect can be measured and directly related to any oestrogenic effect noted by change in uterine weight.

1.6.1.4 Cytotoxicity assays

Cytotoxicity assays are a test of the extent to which compounds are toxic to isolated cell types. The aim is to elicit cytotoxicity to transformed cells while leaving untouched cells which exhibit normal characteristics. When testing antioestrogens, cell lines which are known to be dependent on oestradiol for their growth are used. Compounds are usually tested on a similar but oestrogen independent cell line to see if growth inhibition is due to factors other than oestrogen antagonism. Compounds with partial agonist activity may increase the growth of oestrogen dependent cells.

The most commonly used oestrogen dependent cell line is MCF-7. This cell line was derived from the pleural effusion from a 69 year old patient with metastatic breast cancer[70]. MCF-7 cells synthesise α-lactalbumin which is only synthesised by functionally differentiated mammary epithelial cells thus confirming their origin. The cells

have oestrogen, progesterone, glucocorticoid and insulin receptors and show growth stimulation by oestrogen, androgen and insulin and growth inhibition by glucocorticoids[70]. The cells also have receptors for triiodothyronines, vitamin D, calcitonin, retinoids, prolactin and EGF[71].

1.6.1.5 Aromatase inhibition

Where the compound under test is a potential enzyme inhibitor, activity in the isolated enzyme system must be evaluated. Potential aromatase inhibitors should be evaluated, not only for inhibition of aromatase, but also for inhibition of related enzymes which may contribute to the side effects of a drug.

After initial tests where a compound has been shown to be a potentially useful therapeutic agent initial clinical trials should aim to find the minimum dose required to achieve the maximum endocrine effect. Patients recruited into these trials should have advanced local or metastatic disease which is progressing despite first line endocrine therapy and a predicted survival time of not less than four months. The tumour should have ER positive or unknown status. As the patient's condition is refractory to accepted hormonal treatment, the drugs which are active in these trials are likely to have a different

mode of action to those currently available. This is an advantage because it seems unlikely that an antioestrogenic drug will be produced which will provide any advantage over tamoxifen unless it has some activity in another complementary system.

1.6.2 Tyrosine kinase inhibition

Test systems for tyrosine kinase inhibition are much less well defined than those for antioestrogenic activity. Inhibition of oestrogens, by different mechanisms, is known to be an effective target in hormone dependent tumours but it is not clear what, if any, antitumour effect inhibiting tyrosine kinases will have. There are few known specific tyrosine kinase inhibitors and the function of the tyrosine kinases is not well established. Any tests used on this system are therefore much more speculative in nature and have the aim of finding specific inhibitors of tyrosine kinases which can then be used as biochemical tools to explore the biological function of these kinases.

1.6.2.1 Enzyme inhibition assays

Specific enzyme inhibition assays may be performed which give detailed information on the extent and nature of the binding interaction. Kinase enzymes will have a

number of binding sites including those for the phosphate donor in the reaction and for the substrate. It is important to know which component of the system is being mimicked by the inhibitor in order to make sense of any structure activity relationships which may become apparent.

The tyrosine kinases most often used in enzyme inhibition studies are EGFR and insulin receptor[29] and $pp60^{v\text{-}src}$[72].

1.6.2.2 Cytotoxicity assays

As tyrosine kinases are known to be involved in the transformation of cells to the malignant state, it is possible to obtain cells theoretically dependent on their expressed tyrosine kinase for their growth characteristics, for example ANN-1 cells. ANN-1 cells are derived from the 3T3 mouse fibroblast cell line transformed by the Ableson murine leukaemia virus. The Ableson gene product, which is expressed in these cells, is $pp120^{gag\text{-}abl}$ which has tyrosine kinase activity[72]. ANN-1 cells are from a clone that was deficient for virus replication and therefore do not produce virus which can infect surrounding cells[73]. These cells are grown in suspension culture and do not show density dependent growth. It may be possible to show differences in

cytotoxicity between ANN-1 cells and the parent 3T3 cells caused by inhibitors of the $pp120^{gag-abl}$ kinase.

1.6.3 Biological tests used in this project

The biological tests used to assess compounds were as follows:-

Cytotoxicity assays using MCF-7, 3T3, ANN-1, $WIDR^{74}$ cells;

Oestrogen receptor binding affinity assay;

Aromatase inhibition assay;

Assay of the inhibition of EGF stimulated EGFR tyrosine kinase inhibition.

Details are given in Section 6.1-6.4.

2 MOLECULAR MODELLING STUDIES

2.1 Introduction

2.1.1 General

Several problems suitable for investigation using molecular modelling techniques were encountered during this project. The first was simply to show the similarities between the 2-phenylbenzothiazoles and the indole antioestrogens and isoflavones. The second was to investigate why compounds inhibit tyrosine kinases by competing with ATP but are at first sight structurally unrelated to ATP.

Results obtained from both of these studies could then be used to explain biological results and to suggest further structures which might have greater oestrogen receptor binding capacity and more active and specific tyrosine kinase inhibitory activity.

2.1.2 Relationship of molecular modelling to X-ray crystallography

Molecular modelling is the logical extension of X-ray crystallography, the only physical method to give the absolute configuration of a molecule. As biological

systems are becoming better understood it has become apparent that the conformation of a molecule can have an enormous effect on the biological activity of that compound. Indenestrol A (29) has a chiral centre at C3 leading to R and S enantiomers with RBA's of 13 and 285 respectively (oestradiol = 100)[51]. There are problems with using directly the structure determined by X-ray analysis. In biological systems we are invariably dealing with compounds in aqueous solution usually at physiological pH (7.4) and temperature (37°C). X-ray data is obtained from a solid crystal and the temperature may also be manipulated in order to, for example, stop degradation of the compound under investigation or to obtain a crystal of a compound which is liquid at room temperature and pressure.

The data obtained by X-ray determination may be more representative of the biological situation when subjected to some theoretical calculations. In their simplest form such calculations will allow the removal of crystal packing distortions from the structure and at their most complex will predict the molecular conformation without any prior conformational information. Chemical calculations can therefore be used to predict the structure and properties of molecules which have not been made, or even cannot exist under "real" conditions.

2.1.3 The scope and reliability of chemical calculations

With increasing use, the commonly used calculation methods are becoming more reliable as systematic errors in results produced by these methods become known. Each of the different types of calculation has advantages for different applications and a common source of error in results is simply in using the wrong type of calculation for a specific problem. Calculations predict properties for isolated, motionless molecules *in vacuo* but these are not always applicable. When looking at differences between two reaction pathways, say, in a stereospecific reaction, marked differences between the calculated and observed activation energies of the two pathways may be seen. Solvation and other factors at work in the reaction medium may considerably enhance the stability of one transition state relative to another. Results so obtained will be valid in separating out solvent effects from the intrinsic stability of the species itself. Ionic reactions are not well treated in the gas phase.

$$A\text{—}B \longrightarrow A^{+} + B^{-}$$

This charge separation in the gas phase leads to the loss of electrostatic attraction and an increase of several hundred kilocalories in energy. In solution this increase in energy would be minimised by energy released by solvation of the ions; the true increase in energy

would be much lower, indeed charge separation may even be energetically favoured.

Specific chemical calculation programs are parameterised for different atoms; that is, treatment of different atom types is amended to take account of the experimental data available for that atom type. Details of parameterisation are found in the program manuals. Parameterisation of atoms is updated with the program so even if calculations could previously be performed on molecules containing a particular atom a new version of the same program may give different and slightly more reliable results.

The limited reliability of chemical calculations means that results obtained for a given molecular structure need to be compared with available experimental data. If this is not available then further calculations on related structures for which experimental data is available will be needed. If no experimental data is available the results obtained need to be interpreted with care bearing in mind the known limitations of the programs used.

2.1.4 Types of chemical calculations and programs

In this section, I will describe some of the important features of molecular mechanics, semi-empirical molecular orbital and ab initio calculations. This is not intended to give a full understanding of how the programs work but to point out some of the pitfalls that may be avoided by a limited understanding of the programs. Fuller details may be found in "A handbook of computational chemistry. A practical guide to chemical structure and energy calculations"[75] and in the relevant program manuals.

2.1.4.1 Molecular mechanics (MMP2, CHARMm)

Molecular mechanics (M.M.) or force field calculations are based on the simple classical mechanical model of molecular structure. Calculations are only models but are none-the-less accurate for certain types of molecules, notably alkanes.

The classical force fields used in the calculations are detailed below:-

Valence force field

Bond stretching

Angle bending

Torsion potentials

In more advanced M.M. programs, combinations of valence force field terms are used to account for experimental information, for example that bonds become

longer as the angle between them becomes less. These programs take no account of differing C-C bond lengths and are therefore not suitable for conjugated systems where bond lengths and torsion angles depend on the degree of conjugation.

Van der Waals functions

Steric interactions are included in this function but 1,3-interactions are not included but this is only important for 3- and 4- membered rings where the number of 1,3-interactions does not equal the number of atoms in the ring.

Charge density functions

Electrostatic functions

Dipole-dipole interactions

MMP2 is a molecular mechanics program which has a molecular orbital component to deal with conjugated molecules. One molecular orbital (M.O.) calculation sets a starting geometry for the conjugated parts of the molecule then M.M. calculations deal with all unconjugated parts of the molecule. Further cycles of M.O. and M.M. calculations continue until structure and energy remain constant.

Molecular mechanics calculations are very reliable for unconjugated hydrocarbons but less so for the more complicated conjugated systems. The main advantage of such programs is speed and their ability to deal with large molecules; proteins cannot be treated in any other way.

2.1.4.2 Semi-empirical molecular orbital calculations (MOPAC, CINDO, AMPAC, PM3, AM1, MINDO/3)

Semi-empirical molecular orbital calculations are based on the linear combination of atomic orbitals theory. The molecule is considered as a combination of molecular orbitals occupied by the electrons assigned to the molecule. It is assumed that nuclei remain stationary on the time scale of electron movement and therefore electronic wave functions are unaffected by nuclear motion (Born-Oppenheimer approximation). The M.O. calculation finds the self-consistent field (SCF) or the combination of atomic orbitals which has the proper symmetries and gives the lowest energy for any given conformation. Geometry optimisation similar to an M.M. calculation is performed and a new SCF obtained. This iterative process continues until optimisation is complete. M.O. calculations will however find the energy minimum nearest the starting geometry. This will not necessarily be the

conformation of lowest energy and there is no automatic way to find the global minimum.

In SCF calculations, only orbitals which contain electrons are considered as it is these which affect the energy of the molecule. For energy calculations the frozen core or valence electron approximation is used. This means that only electrons in the outer shell are used, thus simplifying the calculations needed. The effect of electronegativity is taken into account with population analysis which gives the net charge on each atom and the overall dipole moment. The chemical bond is strongest when the electrons involved are shared equally between the two atoms concerned but the electrons will also try to occupy the more stable of the two atomic orbitals. This leads to an unsymmetrical molecular orbital.

The self-consistent field is produced by taking electron-electron repulsion into account by considering the interaction between a given electron and the mean field of other electrons in the molecule (Hartree-Fock or single determinant theory). Restricted Hartree-Fock theory simplifies calculations but assumes all electrons are paired, if this is not the case other methods of treatment are available[75]. The self-consistent field (SCF) method involves an iterative process which improves

orbitals until the electronic energy reaches a constant minimum value and orbitals no longer change. SCF calculations overestimate electron-electron repulsion but this is compensated for by parameterisation in the MINDO/3 and MNDO programs.

All semi-empirical M.O. calculations use the theories set out above. Differences lie in the way they see molecular orbitals. MINDO/3 uses a modified intermediate neglect of differential overlap (INDO) approximation, while MNDO (modified neglect of diatomic differential overlap) uses the neglect of diatomic differential overlap (NDDO) approximation. These terms relate to treatment of the directionality of p-orbitals. CNDO (complete neglect of differential overlap) programs are the simplest, with NDDO being the first approximation to calculate repulsion integrals using directionality. The use of these approximations decreases the accuracy of these methods but this is compensated for by parameterisation. MNDO needs only to have parameters for each individual element whereas MINDO/3, using simpler calculations, requires parameters for combinations of elements. A major disadvantage of MINDO/3 is that it overestimates the stability of triple bonds and underestimates the stability of aromatic systems and the strength of lone pair repulsions. Although parameterised for boron, MINDO/3 is unsuitable for boron containing molecules. Hydrogen bonds

are not reproduced so where present in a molecule they must be restrained prior to optimisation. The consequence of these factors is to limit the type of problems that can be treated by this method. Comparison of molecules containing different numbers of triple bonds, including cyanides, or of aromatic ring systems with non-aromatic ring systems will give misleading results. Treatment of lone pairs by MINDO/3 means that optimisation of compounds, such as hydrazines, in which lone pairs are close together in space gives an invalid answer. The stability of highly branched alkane systems is underestimated but is systematic and can be compensated for relatively easily. MINDO/3 is superior to MNDO for carbocations as it reproduces hyperconjugative stabilisation and because MNDO underestimates the strength of three centre bonds.

All NDO approximations do not reliably predict the rotation barriers in conjugated systems or reproduce hydrogen bonds. The description of rotation barriers in trans-azobenzene and related systems have been described by Bally et al[76]. The most stable confomations of stilbene, benzylideneaniline and azobenzene were predicted by MINDO/3 as those where the phenyl ring was 90° to the double bond; this is at odds with experimental evidence.

These features may therefore need to be restrained prior to optimisation. In MNDO branching alkane systems are treated better than with MINDO/3 but underestimation of stability still occurs; the repulsive force between adjacent methyl groups is overestimated but less so than in MINDO/3. MNDO (modified neglect of diatomic differential overlap) also deals with lone pairs, unsaturated molecules and triple bonds reliably unlike MINDO/3 and its scope is further widened by the increased numbers of atoms for which it is parameterised.

The AM1 quantum mechanical molecular model was developed from MNDO by changing the core repulsion function. In doing this the tendency of MNDO to overestimate repulsions between atoms, as the distance between them approaches their van der Waals distance, is reduced; hydrogen bonds are therefore much more reliably reproduced[77].

Table 5: Atoms parametised for semi-empirical calulations with MOPAC/AMPAC△

MNDO parameters

H	Li	B	C	N	O	F	Al	Si	P	S	Cl
Cr	Zn	Ge	Br	Sn	I	Hg	Pb				

AM1 parameters

H	B	C	N	O	F	S	Cl	Br	I	Cb	Tv

Table 5: Atoms parametised for semi-empirical calulations with MOPAC/AMPAC (cont.)

MINDO/3 parameters

	H	B	C	N	O	F	Si	P	S	Cl
H	*	*	*	*	*	*	*	*	*	*
B	*	*	*	*	*	*				
C	*	*	*	*	*	*	*	*	*	*
N	*	*	*	*	*	*			*	*
O	*	*	*	*	*	*			*	*
F	*	*	*	*	*	*			*	
Si	*		*				*			
P	*		*					*		*
S	*		*	*	*	*			*	*
Cl	*		*	*	*			*	*	*

* = parameterised for this combination of atoms.

PM3 parameters

H	C	N	O	F	Al	Si	P	S	Cl	Br	I
Cb											

△ Isotopes may be specified by including the mass number of the atom to be used.

In addition to the above parameters, "sparkles" are available in both MNDO and MINDO/3. These are "elements" representing pure ionic charges with an ionic radius of 0.7 Å. They have a integer nuclear charge (i.e. +1, +2,-1, -2) and an equivalent number of electrons to maintain electroneutrality. When used in calculations the electron(s) are donated to the rest of the system. "Sparkles" can be used to introduce ionisation into a

system (eg. H_2O"+"; overall charge +1) or to mask a charge already on a system (eg. $HCOO^-$"+"; overall charge zero)*. Two sparkles of equal and opposite sign can be used to form a dipole in order to mimic solvent effects (eg. water could be surrounded by six dipoles to form a solvent cage. Sodium and potassium ions are available in MNDO and behave like sparkles.

MNDO calculations use only s- and p-orbitals so should not be used for hypervalent molecules such as sulphones and phosphates; for these compounds the recent addition of PM3[78] to the molecular modeller's armamentarium is a great advance. PM3 can use sparkles but is limited in the atoms for which it has parameters.

In conclusion MNDO is superior to MINDO/3 for most compounds the exceptions being carbocations, silanes and fluorohydrocarbons and compounds without interacting lone pairs. Both methods have limitations in their treatment of rotation barriers in conjugated systems and of hydrogen bonds. It is important to be aware of these limitations because both programs will produce a result if asked to perform this type of calculation but the result may be misleading. PM3 should be used if hypervalency is important to the calculation.

* "+" = sparkle of charge +1

2.1.4.3 Ab initio calculations

Ab initio molecular orbital theory leads to more complete calculations which are therefore more expensive in terms of computer time. Definitive results can be produced by ab initio calculations but this takes a tremendous amount of computer time and these calculations can only be performed on molecules containing only a few atoms at present. It is usual to accept a lower level of theory than is required for definitive calculations and to compensate for this in the interpretation of the results. Ab initio calculations begin with a LCAO-SCF calculation using the same assumptions as for semi-empirical M.O. calculations but use a Gaussian type orbital basis set instead of the NDO assumption. Fully occupied shell orbitals are included in the calculation unlike in semi-empirical calculations.

The basis set of molecular orbitals must be chosen to suit the calculation in hand. The number of basis functions a computer can handle is limited and the time required for the calculation is related to the fourth power of the number of basis functions; practicalities usually determine the size of basis set that can be used. A minimal basis set of molecular orbitals contains one basis function per atomic orbital but this cannot take account of positively charged species where an orbital can

contract in size as it is stabilised by the excess positive charge in the nucleus. Split-valence or double zeta basis sets are therefore used which allow the orbital size to be varied between preset limits. In split-valence basis sets this principle is only applied to valence orbitals while in double zeta basis sets, all orbitals are treated in this way. The diffuse function augmented basis set which may be used is used for anions and compounds which require very good description of non-bonding electron pairs.

The polarization basis set includes d-orbitals for all non-hydrogen atoms the purpose of which are to allow combinations of p- and d-orbitals after which the resulting orbital is deformed to one side of the atom; this is particularly important in small rings and compounds containing second row elements.

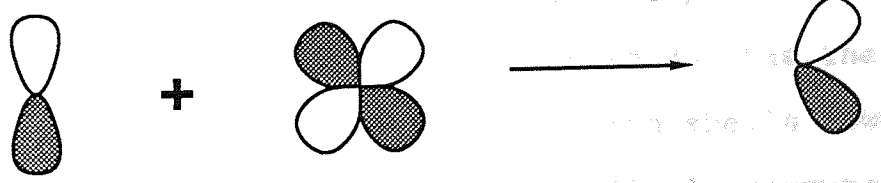

Fig. 4: Combination of a p- and a d-orbital

There are three methods of geometry optimisations, the fastest being BERNY optimisation. This uses calculated forces and a guessed force constant matrix to

predict the position of the minimum energy structure. This method will often fail for cyclic structures. The Murtagh-Sargent method is slower and more reliable than BERNY as it does not rely on a guessed force constant matrix. The Fletcher-Powell method is extremely slow and should only be used where no analytical atomic forces are available. Population analysis is carried out for the optimised geometry and the calculated SCF is amended using perturbation theory.

SCF does not allow electrons to avoid each other as it assumes their instantaneous positions are independent of the other electrons in the molecule. A better model of the position of electrons is obtained with electron correlation; that is electrons like to be as far away from each other as possible.

Due to the complexity of the problems to be solved, ab initio calculations can only be performed on small molecules of about 20 atoms. Gaussian 80 has theoretical limits of 50 atoms or 120 electron shells however the practical limits are less due to available computer space.

2.1.5 Programs for manipulating and displaying molecules

2.1.5.1 CHEM-X

CHEM-X is a suite of programs produced by Chemical Design, Oxford[79] which allows the user to build and amend existing structures, compare molecular conformations and perform a variety of chemical calculations. Molecules are displayed in a variety of formats including ball and stick and space filling. Dot surfaces can be produced and colour coded according to set parameters. Simple molecular mechanics calculations can define energy contour maps with respect to a given parameter allowing simple conformational analysis.

The strength of CHEM-X is the ease of changing and building structures and its simple calculations but the visualisation of the resulting molecules is static giving some difficulty in interpreting 3-D structural features. MOPAC 4.0 can be run from within CHEM-X. MOPAC 5.0[80] which is run external to CHEM-X and gives output which must be transposed to make it readable was also available in the present work.

In this study CHEM-X was used to build and alter structures which were then optimised and re-examined within CHEM-X. Further visualisation and the complex manipulations required to build the model of ATP were done using QUANTA. CHEM-X manipulations and calculations were performed on a cluster of two VAX 11/8650 computers.

2.1.5.2 QUANTA

QUANTA is a program produced by Polygen Corporation[81] and is run on an IRIS 3130 UNIX workstation produced by Silicon Graphics Inc. QUANTA is a flexible program allowing the user to either build or import structures, optimise these using CINDO, AMPAC or CHARMm. The display capabilities of the program are impressive, allowing independent manipulation of an unlimited number of independent molecules or fragments. The display is dynamic and makes appreciation of 3-dimensional (3-D) structures far easier than with the equivalent still pictures produced by repeated move and display commands within CHEM-X. Docking experiments are aided greatly by production, in real-time, of interaction energies between fragments. Up to 4500 atoms can be displayed at once; thus protein molecules may be visualised and receptor-substrate interactions modelled. Proteins may be displayed with a ribbon representing the peptide backbone or with a van der Waals surface coloured by various parameters such as atom type, electrostatic potential or by user specification. When displayed, a 3-D image is created as parts of the molecule further away from the plane of the screen are less intense.

Electrostatic potentials are calculated from partial charges obtained from semi-empirical M.O. calculations.

Electrostatic potential is related to the force exerted on a point positive charge by the partial charges on nearby atoms and is inversely proportional to the distance from source of the partial charge. The electrostatic potential at the molecular surface is obtained by calculating the position of the molecular surface and then moving a point charge around on the surface, calculating the force on that charge at each point. Positive regions of potential will repel other positive areas of potential and attract negative ones and vice versa. When comparing substrates of a particular enzyme it is therefore possible to compare both steric differences which may affect receptor binding and show similar areas of potential which may be active in the binding site. If the structure of the binding site is available such binding forces can be examined by direct docking experiments.

The IRIS workstation is self contained and therefore does not have the computational power of a mainframe computer. The optimisation programs which can be run are consequently limited. CINDO is a relatively crude program which can take up to 200 atoms, MOPAC (using AM1 parameter set) on the IRIS can use up to 35 non-hydrogen atoms but is also available on the VAX cluster which has much greater power. Calculations were therefore performed on the mainframe computer and the output transferred to the IRIS workstation for visualisation and interpretation.

2.1.6 Techniques used for this project

In order to decide which techniques to use for a particular set of problems, it is necessary to define those problems.

The 3-D structures of the oestrogen receptor and of tyrosine kinases or their binding sites are not known so it is not possible to examine the interaction between the substrates and their binding site. This study therefore relied on comparison of compounds using the assumption that features common to competitive agonists will be necessary in potential agonists to be developed. This assumption is not necessarily true, the presence of comparable molecular features does not mean that these specific features are necessary to the binding interaction; experimental evidence will therefore be required to back up any conclusions drawn.

To complete this study it is necessary to have reliable molecular geometries and partial charges for the molecules involved. Molecular mechanics calculations are not suitable for complicated conjugated systems and also do not give partial charge information. Ab initio calculations would give the most accurate results but would not be possible for the larger molecules and even for the smaller ones, would take an enormous amount of

computer time which is not justified for this project. Semi-empirical calculations were therefore used. The specific programs and sources of starting coordinates will be given later.

2.1.7 Information available from semi-empirical M.O. calculations.

The output from a calculations gives:-

- Heat of Formation
- Electronic energy
- Core-core repulsion
- Ionisation potential
- Final geometry
- Net atomic charges
- Interatomic distances
- Dipole moment

The heat of formation gives a measure of the stability of the isolated molecule. This figure can be used to compare the stabilities of like compounds but only relates to the gas phase. Some molecules, particularly charged species, may be predicted to be unstable but in solution, solvation effects may outweigh a positive heat of formation.

The final geometry is calculated using the iterated self-consistent field (S.C.F.) of the molecule. This is related to the positions of all electrons associated with the molecule and allows calculation of the partial charges on each atom. This information can be used by QUANTA to generate electrostatic potential maps associated with the molecules. Areas of positive and negative potential may be important in drug receptor interactions as attraction will occur between areas of opposite sign. The potential to form hydrogen bonds and hydrophobic interactions between drug and receptor are also important as is the molecular shape. A molecule containing all the required features, such as, areas of potential and hydrogen bonds will not be an agonist if somewhere else on the molecule is a group which sterically will not fit into the binding site.

2.2 Modelling Methods

2.2.1 Materials

The raw data for the modelling studies undertaken was obtained from published crystal structures, coordinates being obtained from the Cambridge Crystallographic Database (CCDB)[82], the Brookhaven Protein Databank (BPDB)[83] and from our own data (see Appendix 1). Where crystal structures of the compound were unavailable, the nearest available structure was modified with the CHEM-X programme[79] using standard bond lengths and angles. The crystal structures of amiloride (13) and zindoxifene (22) have been determined but the coordinates were not available. These structures were built in CHEM-X as close as possible to the X-ray crystal structure using the data available. Only simple modifications were made to molecules except ATP which required a more complex treatment and will be described later.

Where the crystal structure was available, coordinates were unchanged and MNDO within MOPAC used to calculate SCF partial charges.

Table 6: Source of atomic coodinates for modelling studies

Compound	Source or reference
tamoxifen (1)	Ref. 84
oestradiol (4)	Ref. 85
ATP (10)	Refs. 86, 87
ATP (kinase bound) (10)	Ref. 88
quercetin (11)	Ref. 89
genistein (12)	Ref. 90
Amiloride (13)	Ref. 91
D15414 (23)	Built from 2-(4-bromophenyl)-4,6-dimethoxyindole (38) (Ref.92) Modified using ref. 93
DES (31)	Ref. 94
2-(4-methoxyphenyl)-5,6-dimethoxybenzothiazole (39)	see Appendix 1
2-(4-hydroxyphenyl)-6-hydroxybenzothiazole (40)	modified from (39)
2-(3-hydroxyphenyl)-6-hydroxybenzothiazole (41)	modified from (39)
2-(4-hydroxyphenyl)-5-hydroxybenzothiazole (42)	modified from (39)
2-(2-cyano-4-hydroxyphenyl)-6-hydroxybenzothiazole (43)	modified from (39)
2-(2-chloro-4-hydroxyphenyl)-6-hydroxybenzothiazole (44)	modified from (39)
2-(2,4-dihydroxyphenyl)-6-hydroxybenzothiazole (45)	modified from (39)
2,4,4'-trihydroxyazobenzene	modified from trans azobenzene (Ref. 95)

For a number of structures this simple approach was not suitable due to the unavailability of X-ray data. Amiloride (13) was constructed in CHEM-X using standard bond lengths and angles. This structure was then modified to take account of the solid state data[91]. As semi-empirical molecular orbital calculations underestimate the stabilising effect of hydrogen bonds on the conformation of the lowest energy state, hydrogen bonds were fixed (as shown in Fig. 5) prior to the starting coordinates being subjected to a selective optimisation using MNDO within MOPAC.

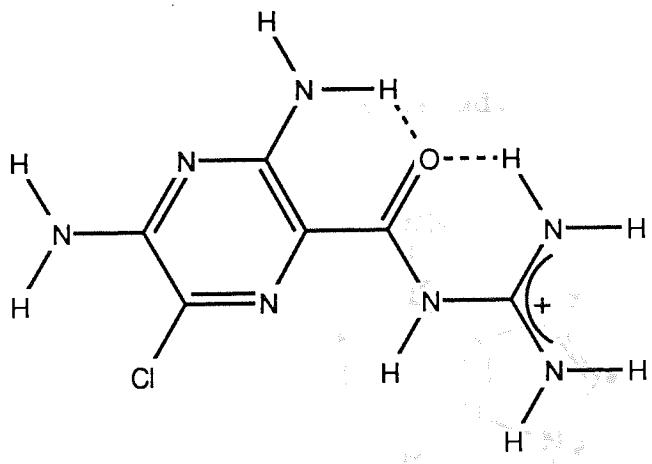

Fig. 5: Amiloride (13) in planar conformation as determined by Hirshfield et al[91]

The starting coordinates for D15414 (23) were derived from those of 2-(4-bromophenyl)-4,6-dimethoxyindole (38)[92] which was the only X-ray structure of an indole available from CCDB. The substituents were altered using CHEM-X

with standard bond lengths and angles and this structure was optimised using MNDO within MOPAC. The ring twist angle has been determined by X-ray crystallography to be 56.5° and this was incorporated into the structure and fixed. The actual coordinates from the crystal structure are unavailable[96] but from a diagrammatic representation, the ethyl and methyl side chains were oriented as close as possible to the X-ray data. The structure produced was selectively optimised using MNDO within MOPAC.

The above descriptions are of the relatively simple manipulations we used to produce the structures and data for comparison. The production of the model of ATP (10) in the conformation that it would take up if bound to a tyrosine kinase was far more complicated.

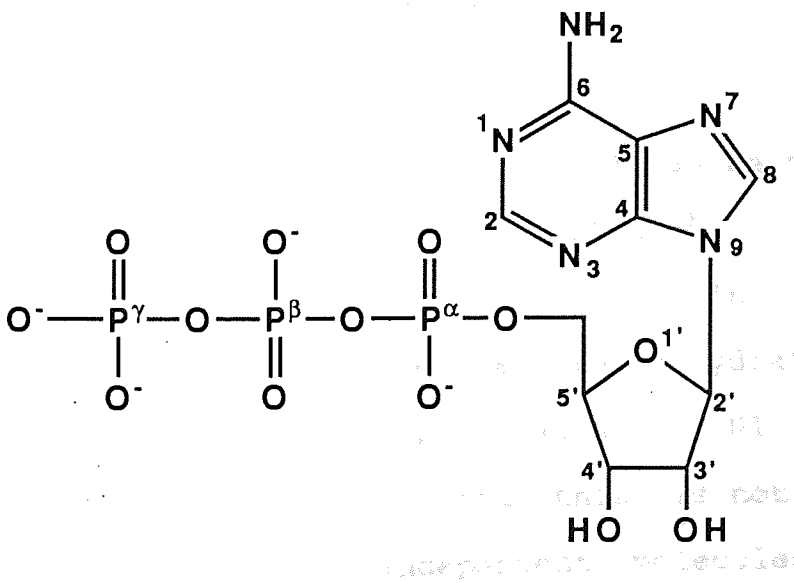

(10)

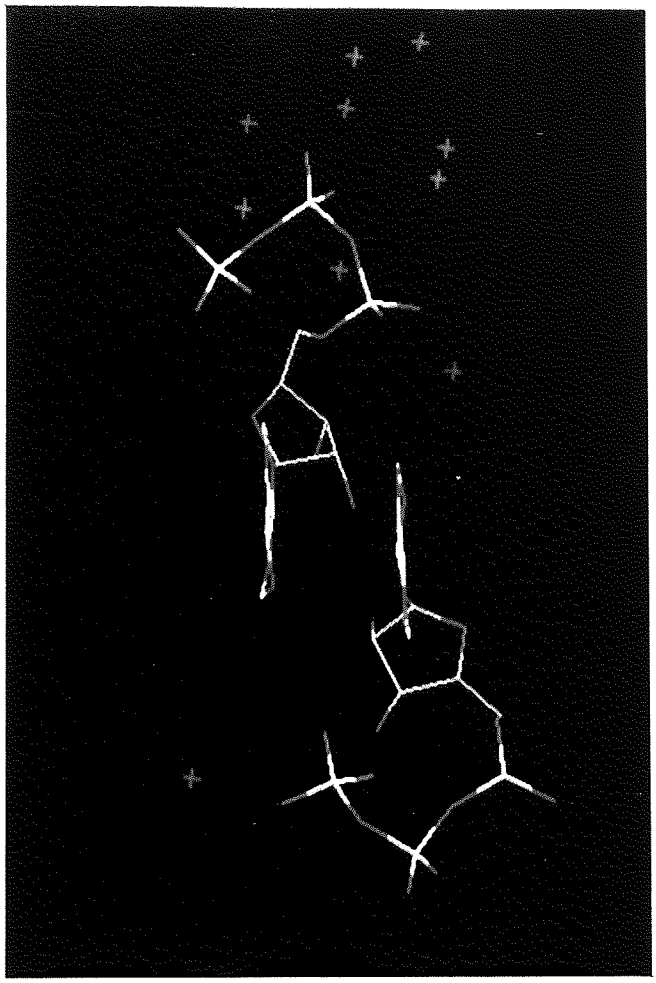

Plate 1: The crystal structure of disodium ATP trihydrate , showing the two conformations of ATP in the solid state.

The crystal structure of ATP (10) has been determined by Kennard[86] and rerefined by Larson[87]. We began by looking in detail at this structure. In this crystal structure the ATP is present as the dihydrated disodium salt (Plate 1) and is protonated on N1 although as hydrogens were not identified this is not immediately apparent. There are two independent molecules of ATP in the asymmetric unit (Plates 2 and 3).

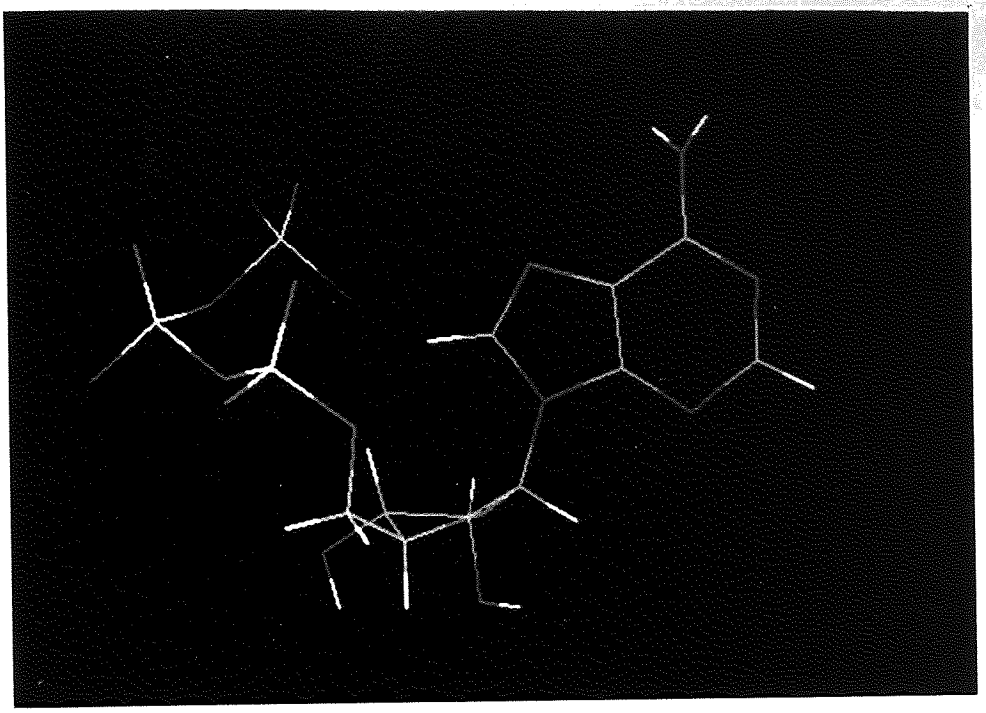

Plate 2: The conformation of molecule A from the crystal structure of isolated ATP.

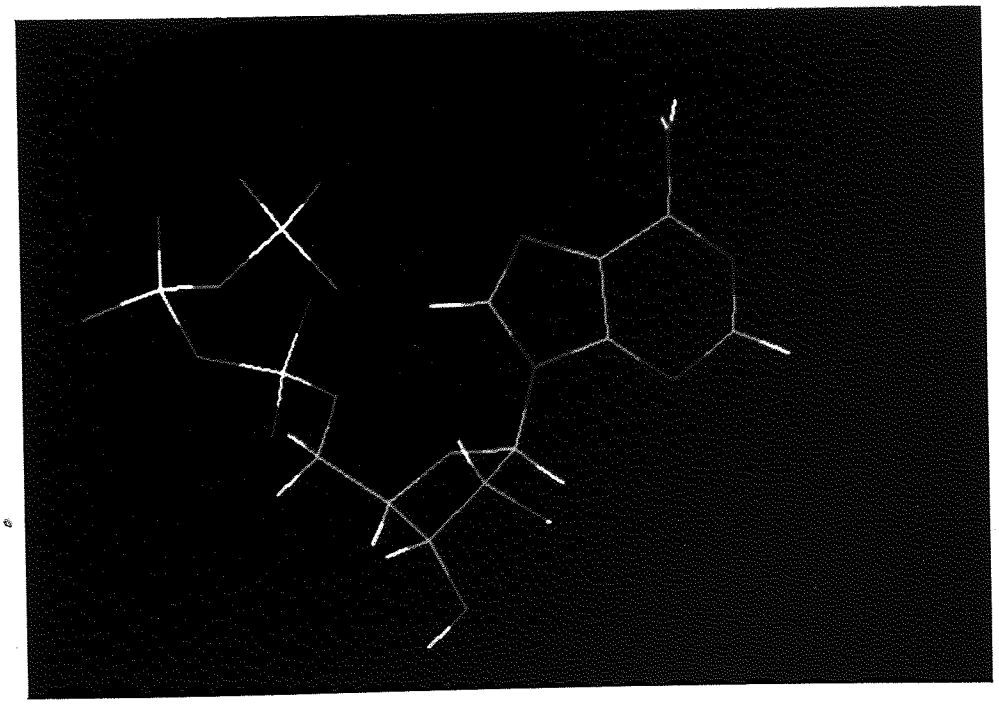

Plate 3: The conformation of molecule B from the crystal structure of isolated ATP.

In both molecules the phosphate chain is folded back towards the adenine base, stabilised by the sodium ions which form a bridge between N7 and the phosphate chain. The difference between the two molecules is that the phosphate chains form left and right handed helices in molecules A and B respectively. Ribose ring conformations are C3'-endo and C2'-endo and the glycosidic torsion angles are 111.8° and 150.6° (C4, N9, C2', O1) in molecules A and B respectively.

This structure of ATP did not seem very satisfactory as a model for the biologically active conformation of ATP, so we undertook a search of the Brookhaven database to see if there was a X-ray structure of ATP bound to an enzyme. There was one kinase crystal structure with ATP bound to it[88] (Plate 4). Phosphoglycerate kinase is involved in the production of ATP from ADP. The reaction we are interested in is the transfer of the terminal phosphate from ATP to a substrate tyrosine; as such this enzyme is not the best model.

Little structural information on the ATP binding site of protein tyrosine kinases is available despite the fact that a number of these enzymes have been sequenced. It is clear, however, that there is a conserved lysine and a series of glycine residues in the form Gly-X-Gly-X-X-Gly in the ATP binding site[97]. These features are not

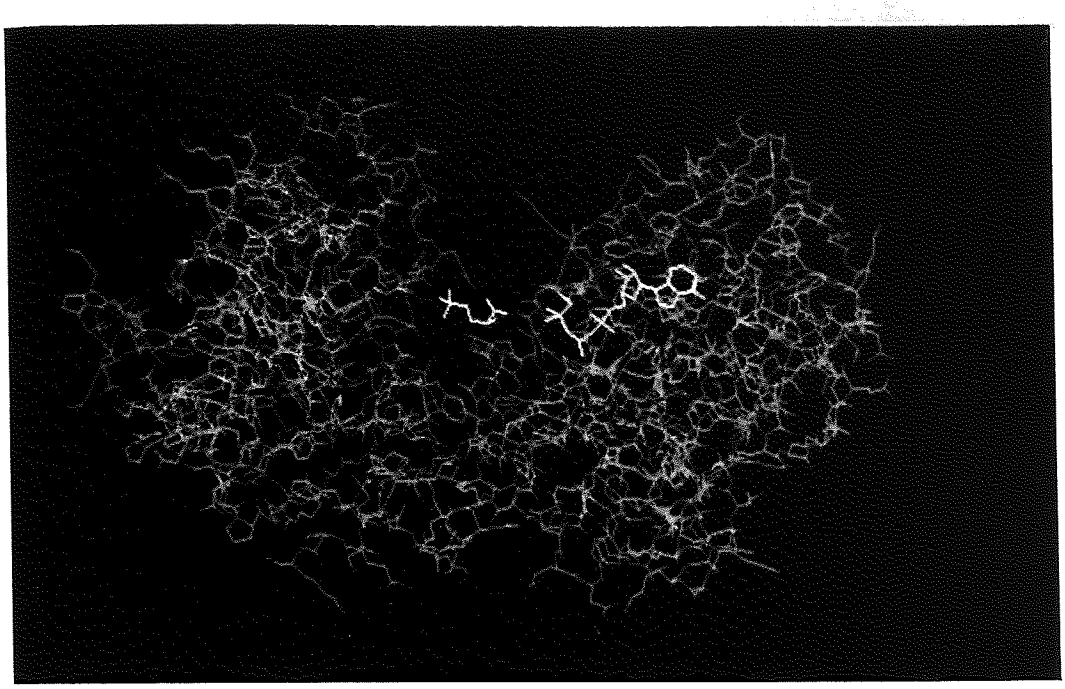

Plate 4: The crystal structure of phosphoglycerate kinase with ATP and phosphoglycerate highlighted in white.

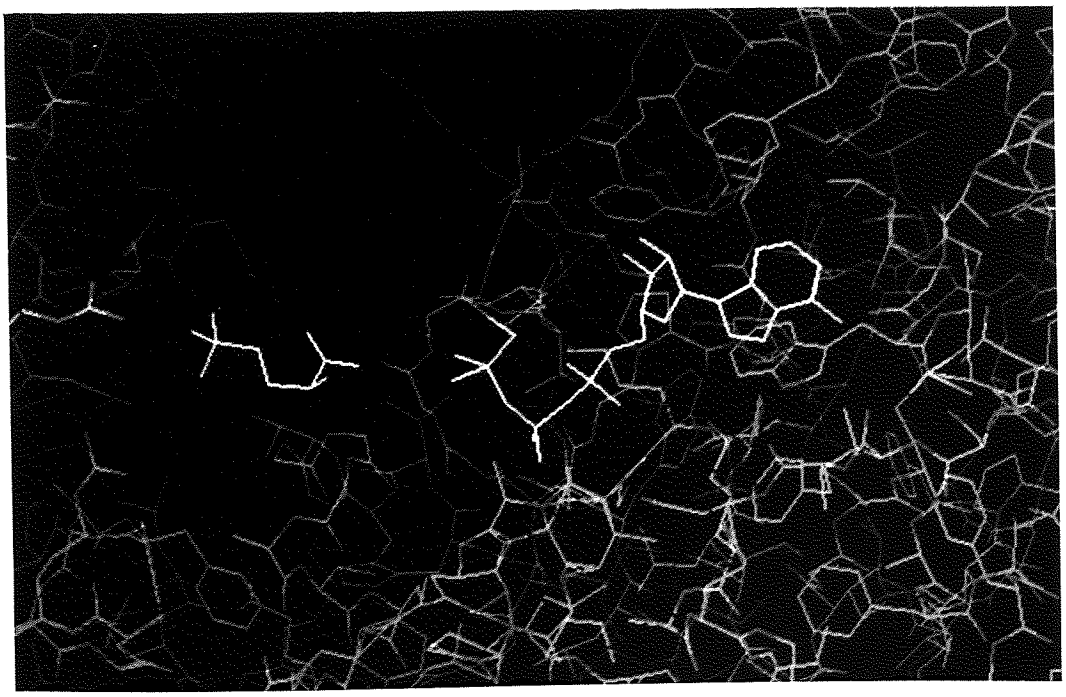

Plate 5: The con formation of ATP and phosphoglycerate (shown in white) bound to phosphoglycerate kinase.

immediately apparent in the sequence of phosphoglycerate kinase but there are two lysine residues within the ATP binding site and the X-ray structure shows that glycines 210, 211 and 274 are brought close together and adjacent to the bound ATP[88].

As with most protein crystal structures the resolution is not very good due to the difficulty of collecting and refining the data on such a large structure. The resolution was 2.5Å[88] which means that no hydrogen atoms could be found (radius of a hydrogen atom is 1.0Å[79]) and that the bond lengths and angles determined were not accurate enough for the in depth study we wished to execute. ATP had been introduced into the crystal matrix by soaking the crystal in a solution of 10nM Mg-ATP as crystals could not be grown in the presence of either ATP or ADP.

The conformation of ATP bound to phosphoglycerate kinase (Plate 5) was totally different to that of ATP alone which was not very surprising in view of the strains put on the isolated molecules by its coordination with sodium, charge and the local packing forces. The final model used was a combination of these two crystal structures.

By using the defined bond lengths from the Larson refined structure (molecule B) but altering ATP's gross conformation to that seen in the phosphoglycerate kinase crystal structure we were able to produce a reasonable model of kinase bound ATP. The manipulations involved in the transformation were quite complex. Using CHEM-X the first step was to change the glycosidic torsion angle from 150.6° to 174.9° (C4, N9, C2', O1') to give the anti-configuration. The next step was to change the ribose sugar pucker to C2'-endo. This was achieved by swapping over the substituents on 2',3' and 4' while keeping the same bond angles both within the ribose ring and those of the substituents. The phosphate chain was then manipulated to mimic that of the bound ATP using QUANTA.

The next problem we encountered was how to deal with the four negative charges that ATP carries at physiological pH. In a biological system the ATP would be in aqueous solution and would no doubt be surrounded by positive ions. Therefore the four negative charges on the phosphate chain would not contribute greatly to the electronic structure of the adenosine. In the isolated crystal structure, sodium ions were present[87] while in the bound crystal structure magnesium-ATP complex was used for the binding studies[88]. The magnesium-ATP complex is often the phosphate donor for reactions rather than ATP itself[98]. The magnesium ion binds between the β- and γ-

phosphate groups and is proposed to weaken the bond between these groups[98].

The four negative charges on the phosphate chain of ATP were masked using magnesium-like sparkles. One magnesium was located in the crystal structure of ATP bound to phosphoglycerate kinase so one sparkle was placed in an analogous position in our ATP model. The second sparkle was not used to mimic any biological state but purely to mask the remaining two negative charges. In vivo the charges would be surrounded by solvent and counterions but it is not possible to produce this effect in chemical calculations at present.
The second sparkle was placed on the perpendicular bisector of the line joining the two α- and β-oxygen atoms which were closest together. The sparkle oxygen distance was consistent throughout.

2.2.2 Methods

Having produced our best guess at the kinase-bound ATP conformation this was fully optimised using the MNDO parameter set within MOPAC 5.0. The resulting structure (plate 6) was used to look for structure activity relationships between the known ATP competitive kinase inhibitors, quercetin (11), genistein (12) and amiloride

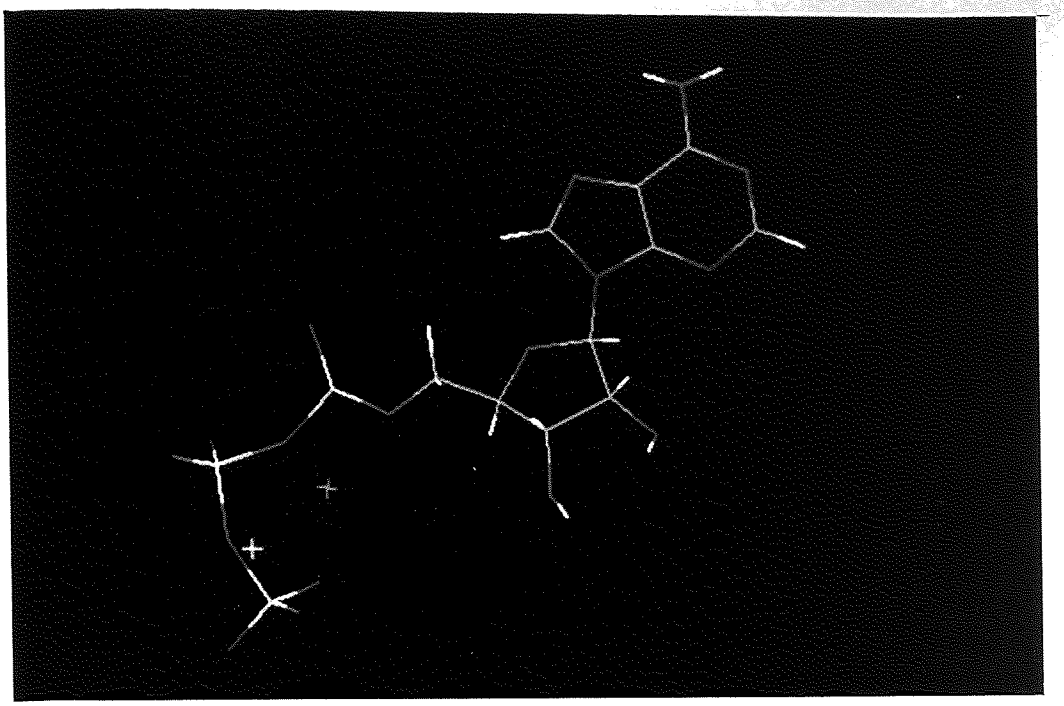

Plate 6: The optimised conformation of ATP with magnesium-like sparkles used in molecular modelling studies.

(13) and ATP (10). The partial charges obtained from MNDO calculations were used to produce molecular surfaces coloured on electrostatic potential. The molecules were visualised using QUANTA and superimposed where possible. In order to allow direct comparison, the electrostatic potentials were ramped from -10eV to 10eV except for amiloride which was ramped from 0eV to 20eV because at physiological pH amiloride carries a positive charge which we had made no attempt to mask. The molecular surface is shown where the electrostatic potential is close to the limits set; therefore no surface is shown around the sparkles and negatively charged areas of the phosphate chain, where the electrostatic potential approaches the extremes of -27eV to 123eV.

2.3 Modelling Results

2.3.1 Factors affecting oestrogenicity

The aim of this section of work was to show the similarities between the 2-phenylbenzothiazoles and known oestrogens and antioestrogens in order to provide a rationale for the preparation of 2-phenylbenzothiazole derivatives.

The two lead compounds for this research were genistein (12) and zindoxifene (22). Plate 7 shows oestradiol (4) in comparison with the hydroxy derivative of zindoxifene (D15414) (23).

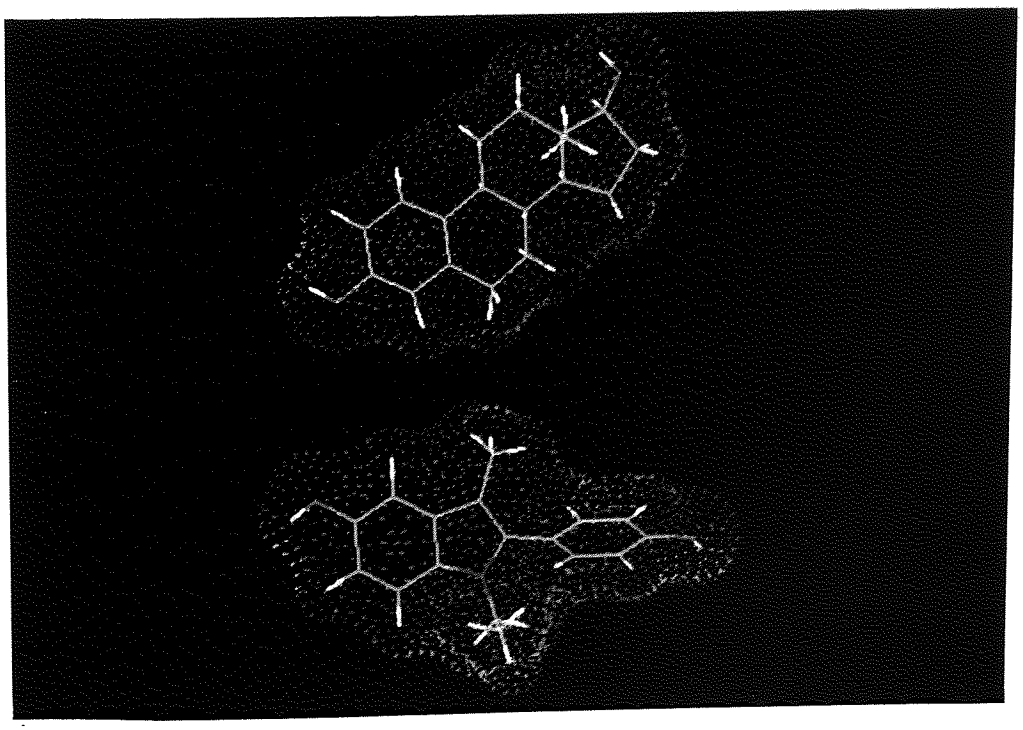

Plate 7: Oestradiol (4) and D15414 (23) shown with molecular surface ramped on electrostatic potential from -10 eV (blue) to 10eV (red).

Correlations between molecules which bind to oestrogen receptors are few, some factors have been defined within groups of active agents[47], but the most common features are the presence of two hydroxyl groups at either end of the molecule and a relatively hydrophobic region in between. The similarities between 2-(4-hydroxyphenyl)-6-hydroxybenzothiazole (40) and D15414 (23) are shown in Plate 8 and that between 2-(4-hydroxyphenyl)-6-hydroxybenzothiazole (40) and genistein (12) in Plate 9. The 2-phenylbenzothiazoles are structurally similar to D15414 (23) varying by the substitution of C3 with a heterocyclic sulphur and loss of the ethyl and methyl groups. Due to the nature of the thiazole ring, substitution is difficult as discussed in Section 3.4. The bulk of the thiazole sulphur leads to steric displacement of the 2-phenyl ring towards the heterocyclic nitrogen allowing the 2-phenylbenzothiazole to adopt a conformation closer to that of the isoflavones.

2,4,4'-Trihydroxyazobenzene (46) was prepared to give a multiply hydroxylated simple diaromatic compound. Plates 10 and 11 show the similarities between this compound and the synthetic oestrogen, DES (31); the difference in inter-oxygen distance is 0.2Å.

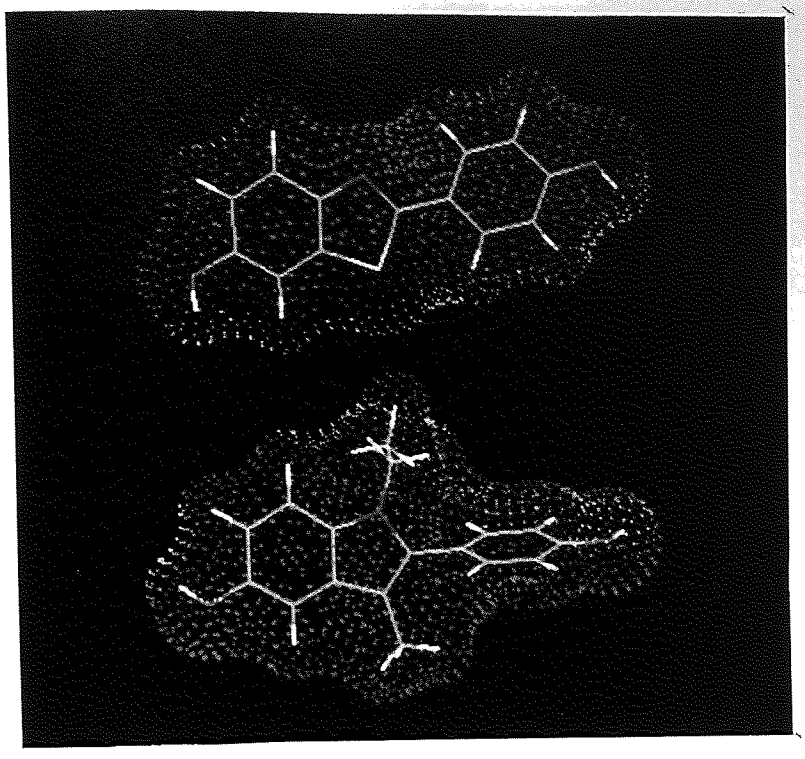

Plate 8: 2-(4-hydroxyphenyl)-6-hydroxybenzothiazole (40d) and D15414 (23) shown with molecular surface ramped on electrostatic potential from -10 eV (blue) to 10eV (red).

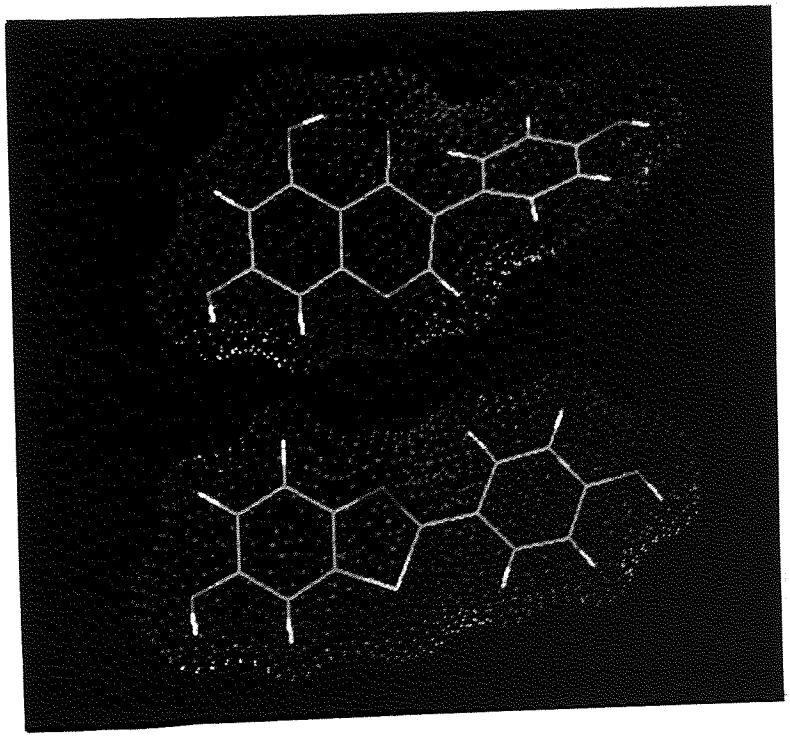

Plate 9: Genistein (23) and 2-(4-hydroxyphenyl)-6-hydroxybenzothiazole (40d) shown with molecular surface ramped on electrostatic potential from -10 eV (blue) to 10eV (red).

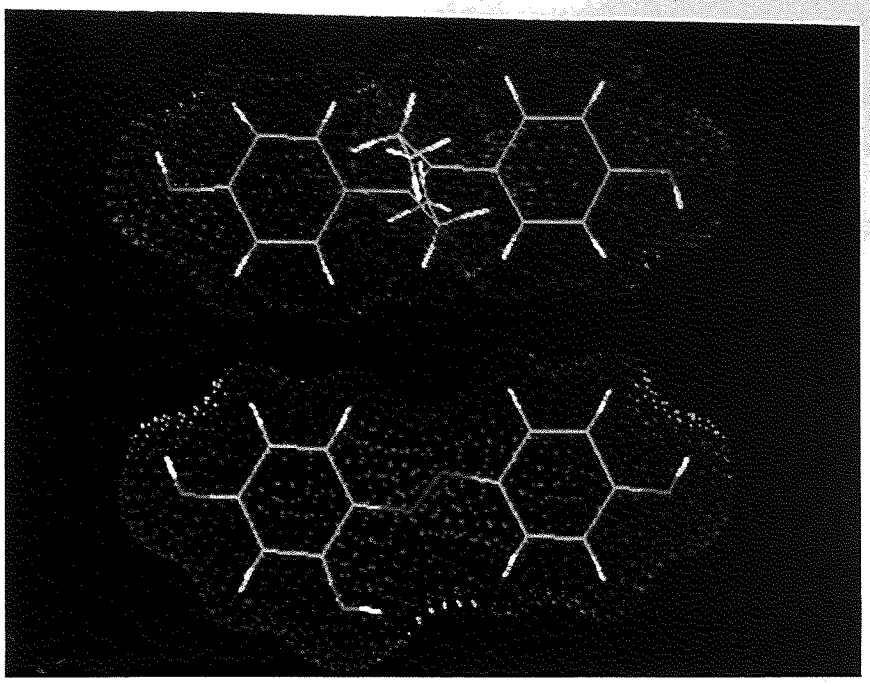

Plate 10: Diethylstilbestrol (31) and 2,4,4'-trihydroxyazobenzene (46) shown with molecular surface ramped on electrostatic potential from -10 eV (blue) to 10eV (red).

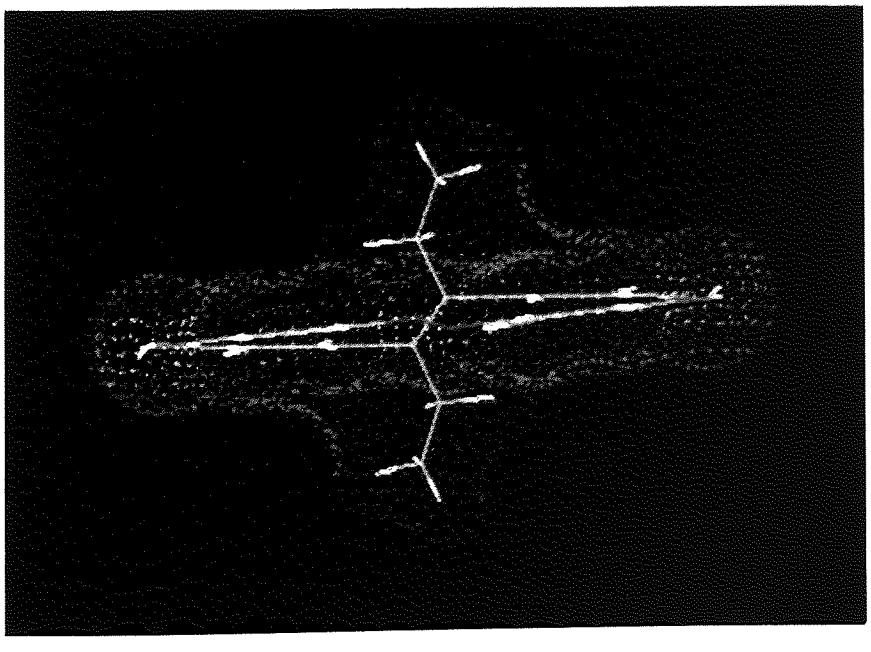

Plate 11: Diethylstilbestrol (31) and 2,4,4'-trihydroxyazobenzene (46) superimposed and shown with molecular surfaces ramped on electrostatic potential from -10 eV (blue) to 10eV (red).

Chemical calculations gave the inter-oxygen distances and dipole moments of the oestrogen agonists and antagonists and compounds under test; the result of these are presented in Table 7.

Table 7: Results of chemical calculations on oestrogens, antioestrogens and test compounds

Comp. no.	ΔH_f (kcal mol^{-1})	μ (D)	τ_x (°)	O-O (Å)	Electrostatic potential min. (eV)	Electrostatic potential max. (eV)
(12)	8.8	4.58	23.1	11.97 8.86	-8.26	6.02
(23)	-38.8	3.35	61.4	11.56	-7.91	6.56
(31)	166.1	0.00	-	12.13	-3.40	5.00
(4)	185.4	1.96	-	10.92	-4.62	5.27
(46)	-64.2	3.03	-	11.93	-6.87	6.69
(40)	-31.3	2.78	21.3	11.74	-8.42	6.95
(41)	-30.4	1.71	21.3	10.78	-8.42	7.01
(42)	-31.1	2.98	21.3	11.33	-8.08	7.12

KEY

ΔHf = heat of formation

μ = dipole moment

τ = angle between the two ring systems

O-O = distance between oxygen atoms

From the results for compounds 12, 23 and 31, it would appear that an inter-oxygen distance of 11.5Å to

12.2Å is optimal for oestrogenicity. Using this parameter, compounds 40 and 46 would be predicted to have the best oestrogen receptor binding affinities and this is in fact the case (Section 4.1). The inter-oxygen distance in oestradiol (4) is however 10.92Å so it would seem that this parameter only applies to non-steroidal oestrogens.

There is no correlation with the overall dipole moment and oestrogen receptor binding, however a local dipole might be important.

2.3.2 Tyrosine kinase inhibition

The aim of this section of the work was to show the similarities between known ATP-competitive kinase inhibitors, potential ATP-competitive kinase inhibitors and ATP itself. The final conformation of ATP with associated sparkles used in comparative work is shown in Plate 6 and detailed in Appendix 2.

As can be seen from Plate 12, the adenine group of ATP and the bicyclic portion of the flavones have a remarkably similar molecular surface in three dimensions. This would be in keeping with a hypothesis that when ATP binds to kinases, the adenine fits snugly into a pocket in the enzyme. There are several possible hydrogen bond interactions from N6-amino group and from N1, N3, and N7.

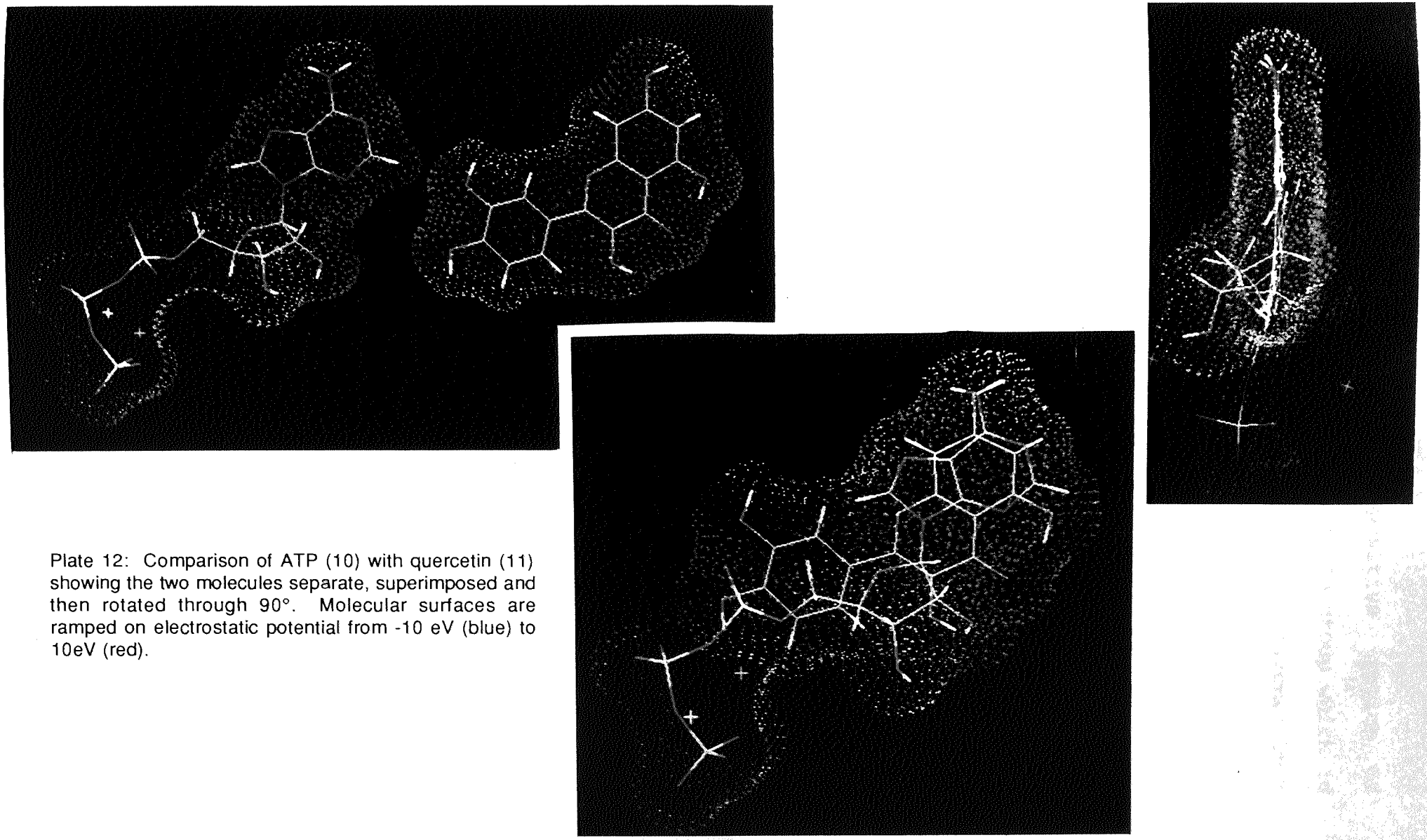

Plate 12: Comparison of ATP (10) with quercetin (11) showing the two molecules separate, superimposed and then rotated through 90°. Molecular surfaces are ramped on electrostatic potential from -10 eV (blue) to 10eV (red).

In adenine there is a positive region of electrostatic potential about the N6-amino group which is mimicked by the 7-hydroxyl group on the flavones both corresponding to potential hydrogen bond donors. The flavone carbonyl region gives a region of negative electrostatic potential which is in the same position as one on the adenosine moiety caused by N3 of adenine and the 3-hydroxyl oxygen of the ribose ring. The fit of molecular surface in this region does not appear to be critical. As previously discussed we feel that the phosphate chain region of ATP is not important in the initial binding interaction between ATP and kinase enzymes, therefore possible interactions from the 2- and 3- phenyl rings in quercetin (11) and genistein (12) respectively were not considered. Plate 13 shows the analogous similarities between genistein (12) and ATP (10).

These conclusions would apply to any flavone with a 7-hydroxyl group. Although not directly comparable, Ferrell et al[99] performed an extensive study of flavonoid inhibitors of phosphodiesterase which compete with its substrate, c-AMP. Quercetin was the most active flavone inhibiting phosphodiesterase by 90% at less than 25μM. Other compounds giving more than 70% inhibition at <25μM all had 7-hydroxy groups except 3-amino flavone, flavone itself and two compounds which had 7-methoxy groups.

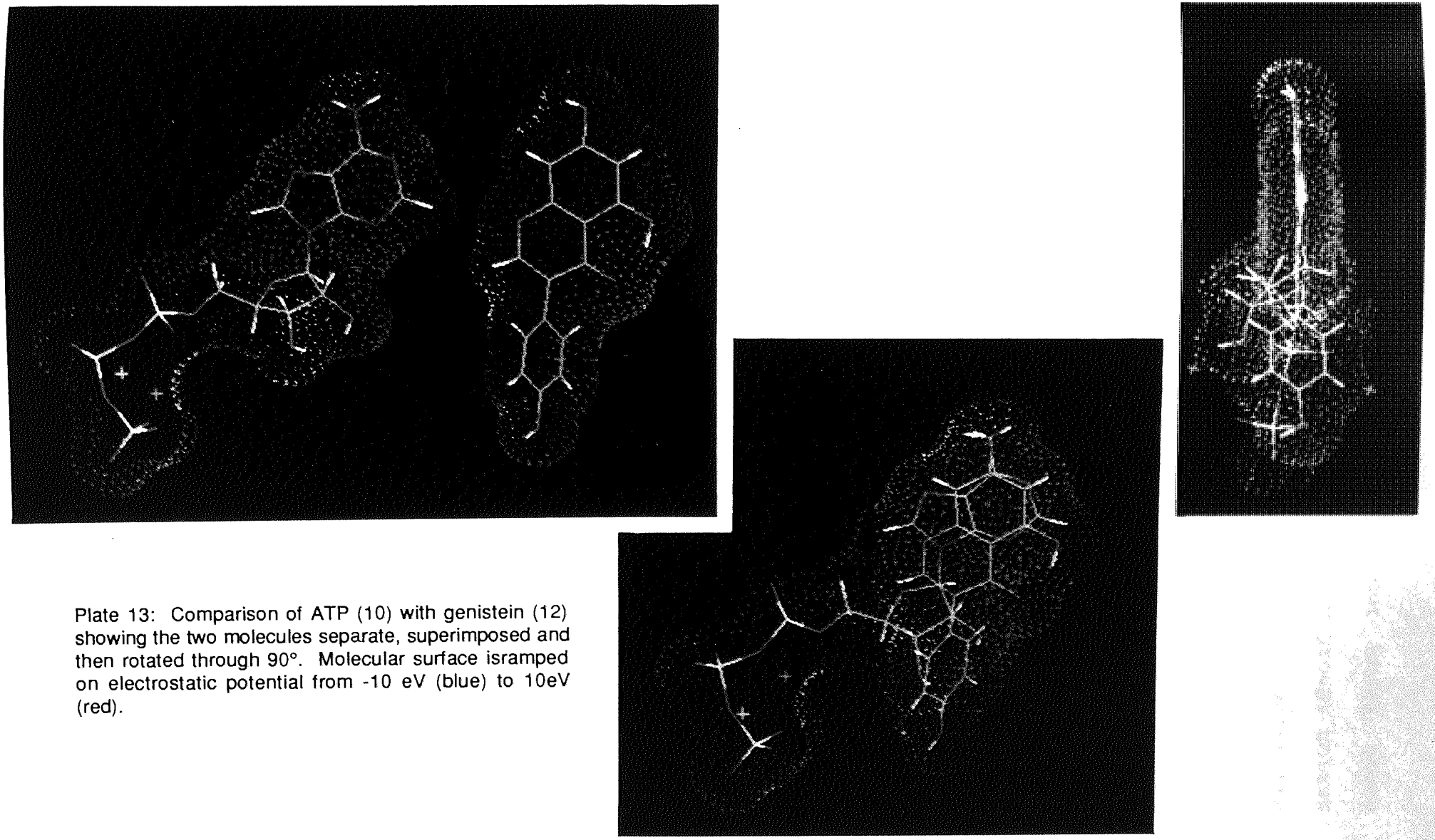

Plate 13: Comparison of ATP (10) with genistein (12) showing the two molecules separate, superimposed and then rotated through 90°. Molecular surface isramped on electrostatic potential from -10 eV (blue) to 10eV (red).

These data cannot be explained by our model above especially in the case of the 7-methoxy groups unless these are demethylated to the free hydroxyl under the assay conditions used but this is unlikely. One of the conclusions of this study was that adding exocyclic substituents only slightly affected activity while changes that resulted in loss of planarity of the heterocyclic ring decreased activity greatly. In 1979, an attempt was made to correlate activity against phosphodiesterase with electronic structures of c-AMP, the substrate, and a number of flavonoid inhibitors. The study used CNDO/2, a relatively crude program, with calculations performed on c-AMP in its zwitterionic form, protonated on N1. As previously explained we did not use the protonated form of adenine in our model of kinase bound ATP.

Amiloride (13) is known to inhibit EGFR with respect to ATP[34], the results of our molecular comparison are shown in Plates 13. The treatment of amiloride was different to those of the flavones as amiloride has a pKa of 8.7 and is therefore predominantly positively charged as physiological pH. We used the conformation of amiloride in its charged state as suggested by Hirshfield et al[91] which gave electrostatic potentials from 1.2eV to 27.3eV. It seemed reasonable to display the electrostatic potential surface ramped from 0eV to 20eV under these circumstances although this undoubtedly means that the

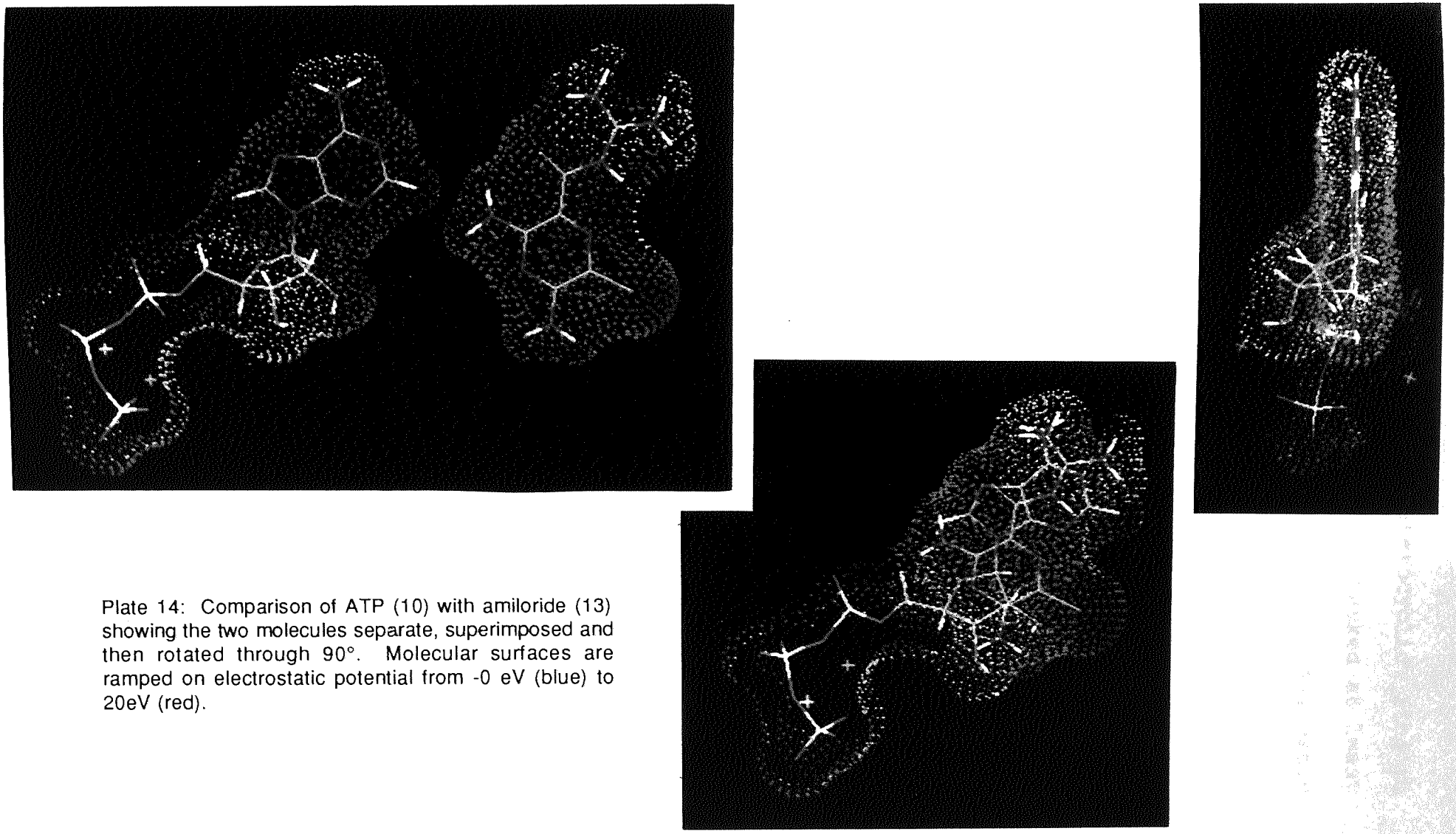

Plate 14: Comparison of ATP (10) with amiloride (13) showing the two molecules separate, superimposed and then rotated through 90°. Molecular surfaces are ramped on electrostatic potential from -0 eV (blue) to 20eV (red).

"negative" (blue) region over the heterocyclic ring is extended. The charge would probably be masked at least to some extent in biological fluids so we felt reasonably justified in this action. Like the flavones, amiloride has similarities between the adenine ring of ATP and the acylguanidinium moiety of amiloride. In addition the aromatic chloro group gives an area of negative potential corresponding to that produced by N3 and the 3-hydroxyl oxygen of the ribose ring. The fit of molecular surfaces is not so good in the region of N1 of adenine but the negative potential surface about N7 is well mimicked by the carbonyl group of amiloride.

Having established a hypothesis for the required features of ATP-competitive kinase inhibitors, we proceeded to apply this to the benzothiazole derivatives which are the subject of this project.

The results of fitting experiments using 2-(4-hydroxyphenyl)-6-hydroxybenzothiazole (40) to ATP (10) are shown in Plate 15. This plate shows that there is an interesting potential for 2-phenylbenzothiazole derivatives to fulfil the criteria we have set out in relation to known ATP competitive kinase inhibitors. The N6-amino group of adenine may be mimicked by a 6-hydroxyl on the benzothiazole. The thiazole nitrogen occurs in between N3 and N9 of adenine and there is an interesting

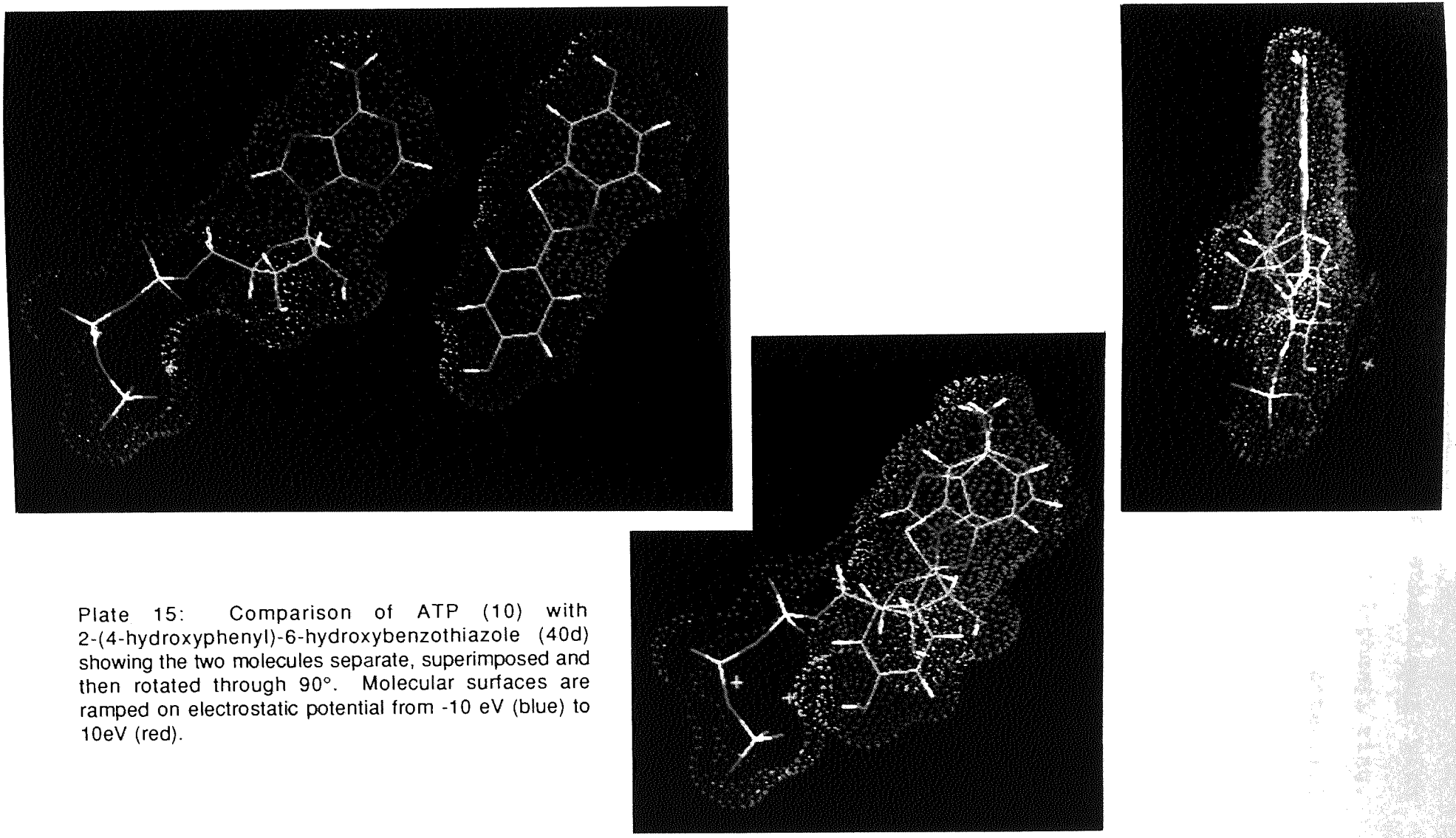

Plate 15: Comparison of ATP (10) with 2-(4-hydroxyphenyl)-6-hydroxybenzothiazole (40d) showing the two molecules separate, superimposed and then rotated through 90°. Molecular surfaces are ramped on electrostatic potential from -10 eV (blue) to 10eV (red).

possibility to introduce a further substituent with negative potential surface ortho on the 2-phenyl ring, thus increasing the coincidence of electrostatic potential between the thiazoles and ATP.

Theoretical studies have shown the probable effect of introducing cyano, chloro or hydroxyl substituents on to the 2-position of the 2-phenyl ring of the benzothiazoles. After building these structures by modifying the crystal structure of 2-(4-methoxyphenyl)-5,6-dimethoxybenzothiazole (38c), it was thought necessary to fully optimise the structures using MNDO within MOPAC as the introduction of a bulky ortho-substituent could have a profound effect on the orientation of the 2-phenyl ring. Plates 16,17 and 18 show the comparison of 2-(2-cyano-4-hydroxyphenyl)-6-hydroxybenzothiazole (43), 2-(2-chloro-4-hydroxyphenyl)-6-hydroxybenzothiazole (44) and 2-(2,4-dihydroxyphenyl)-6-hydroxybenzothiazole (45) respectively with ATP (10). In interpreting the results it must however be remembered that the chemical calculations used underestimate the stabilising effect of conjugation throughout conjugated systems and of hydrogen bonds, therefore the angles between the benzothiazole moiety and the 2-phenyl ring are not reliable but indicative of a possible conformation. Crystal structure analysis of these compounds would allow a better prediction.

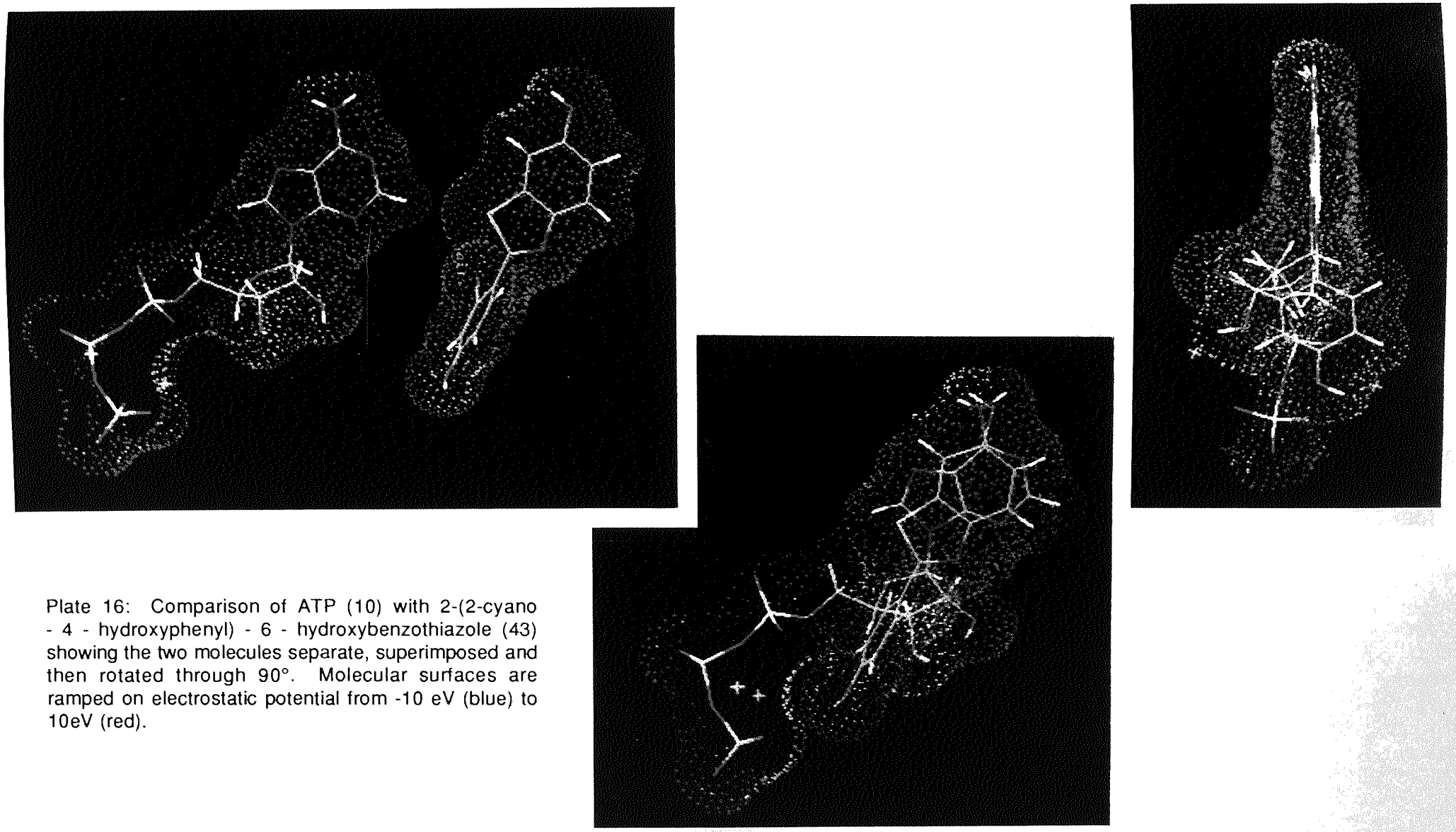

Plate 16: Comparison of ATP (10) with 2-(2-cyano - 4 - hydroxyphenyl) - 6 - hydroxybenzothiazole (43) showing the two molecules separate, superimposed and then rotated through 90°. Molecular surfaces are ramped on electrostatic potential from -10 eV (blue) to 10eV (red).

INFORMATION SERVICES

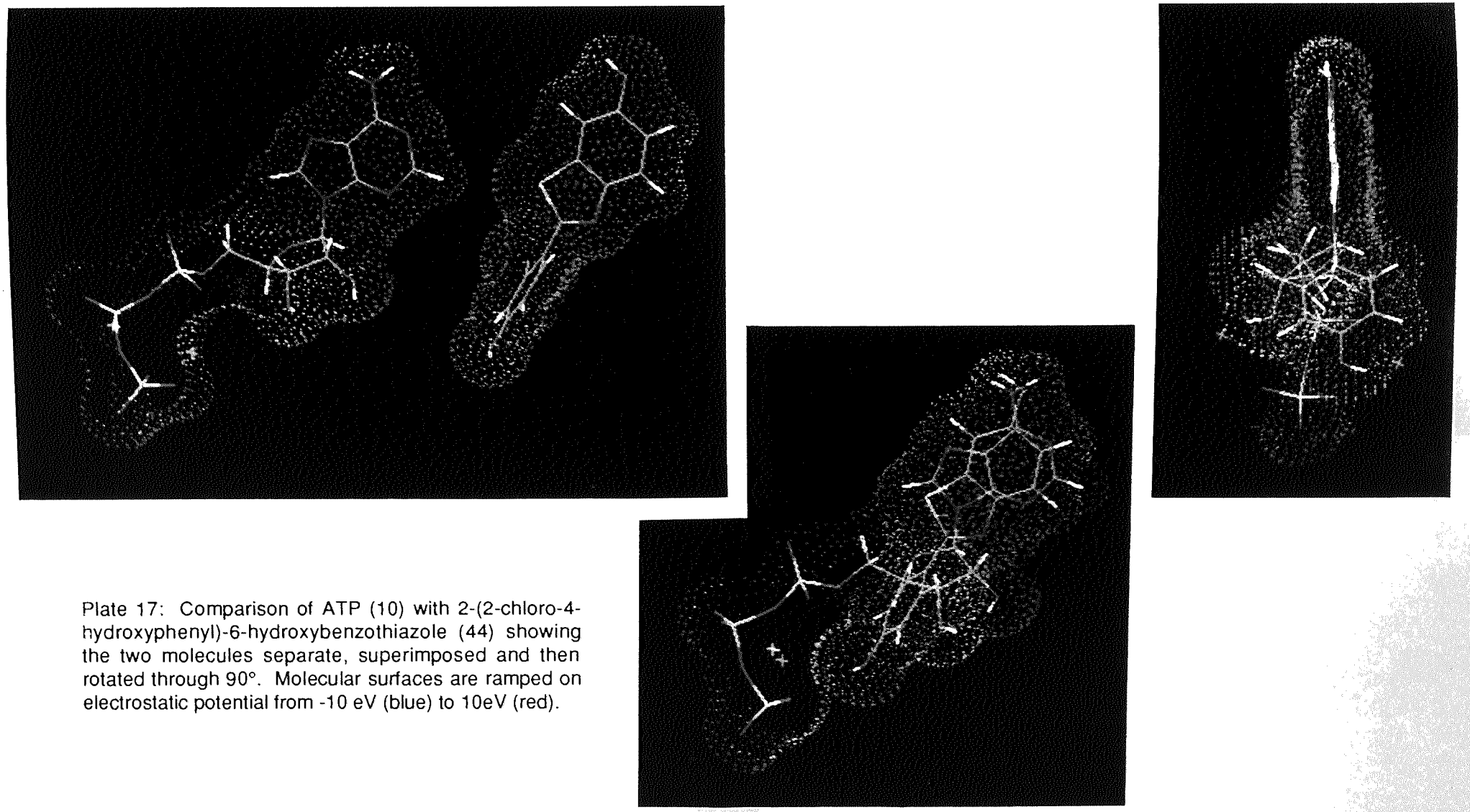

Plate 17: Comparison of ATP (10) with 2-(2-chloro-4-hydroxyphenyl)-6-hydroxybenzothiazole (44) showing the two molecules separate, superimposed and then rotated through 90°. Molecular surfaces are ramped on electrostatic potential from -10 eV (blue) to 10eV (red).

INFORMATION SERVICES

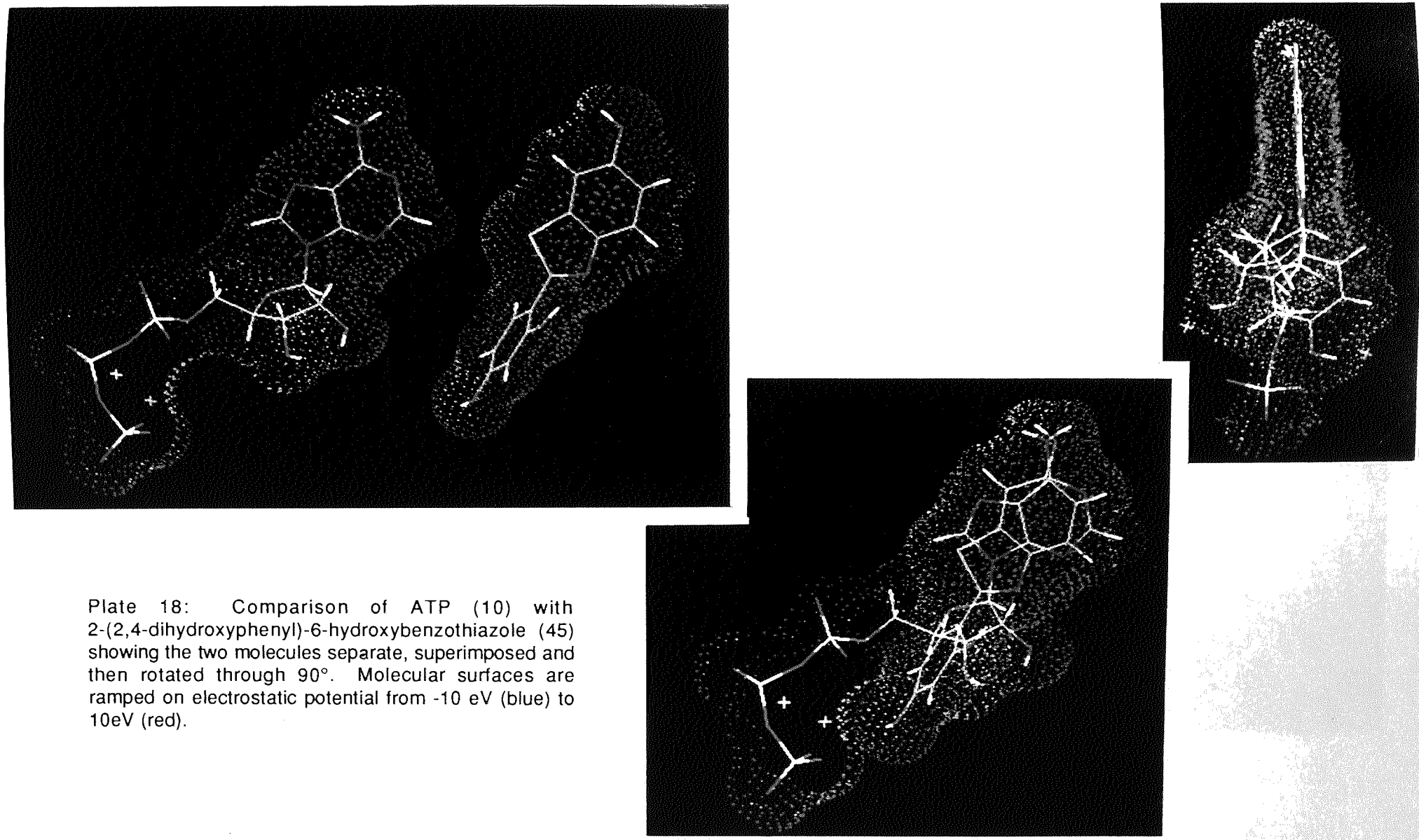

Plate 18: Comparison of ATP (10) with 2-(2,4-dihydroxyphenyl)-6-hydroxybenzothiazole (45) showing the two molecules separate, superimposed and then rotated through 90°. Molecular surfaces are ramped on electrostatic potential from -10 eV (blue) to 10eV (red).

INFORMATION SERVICES

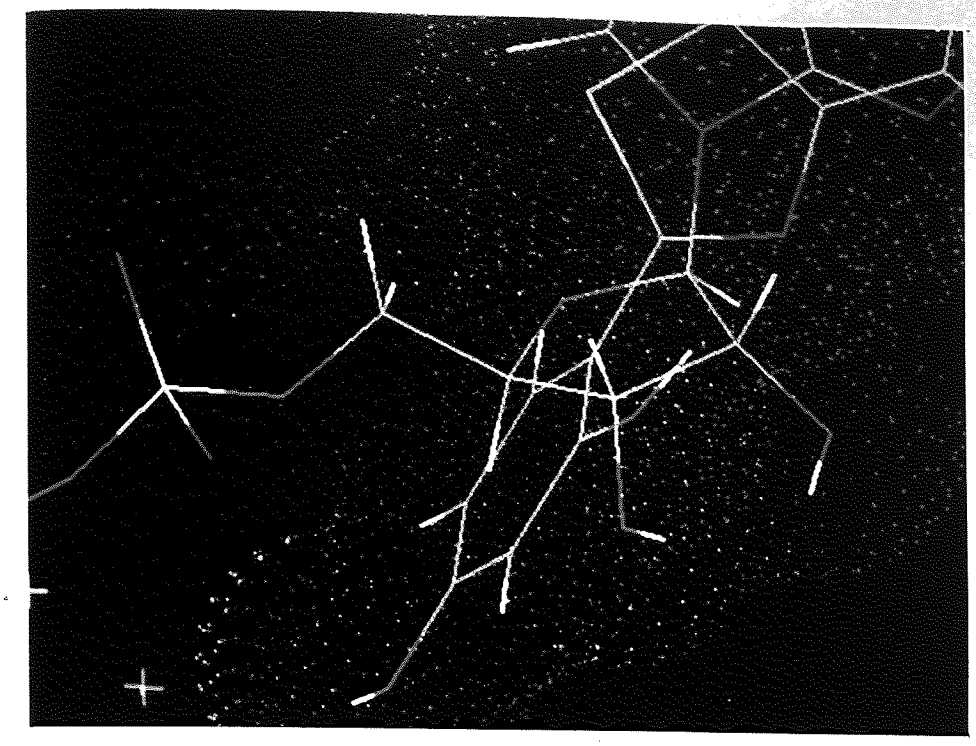

Plate 19: Detail of the possible similarity between the 2-hydroxy of 2-(2,4-dihydroxyphenyl)-6-hydroxybenzothiazole (45) and the 3-hydroxy of the adenosine ribose of ATP (10). Molecular surfaces are ramped on electrostatic potential from -10 eV (blue) to 10eV (red).

Of the three structures shown, 2-(2,4-dihydroxyphenyl)-6-hydroxybenzothiazole (45) has the most interesting prospects. Plate 18 shows the features set out above with Plate 19 show a enlarged view of the 2-phenyl ring of the benzothiazole and the ribose portion of ATP. It is easy to envisage the 2-hydroxy hydrogen of the thiazole being able to mimic the 3-hydroxyl of the ribose after a slight change in the inter-ring twist angle. As mentioned before this is quite possible as ring twist predictions are not precise using semi-empirical M.O. calculations. The most stable conformation of this benzothiazole may be planar as there is a possible hydrogen bond between the 2'-hydroxy group and N3.

Table 8: Predicted angle between the 2-phenyl group and the bicylic heterocycle for 2-phenylbenzothiazolederivatives

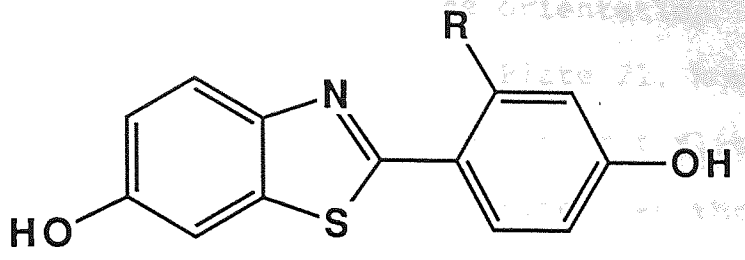

Comp. no.	R	Initial angle from X-ray data (°)	predicted angle (°)
43	CN	21.3	90.7
44	Cl	21.3	86.6
45	OH	21.3	75.9

A study of the rotation barrier about C2-C1' of the 2-phenylbenzothiazoles has not been performed but it is unlikely that, in solution, the barrier will be sufficient to stop the molecule taking up any conformation required for fitting into the binding site. As previously pointed out, X-ray data appertains to the solid state and chemical calculation results to isolated gas phase molecules, neither of which are particularly good representations of molecules in solution.

Tamoxifen (1) was shown to be an inhibitor of EGFR tyrosine kinase in our system (see Section 4.4) but we have no information on the nature of the inhibition. The

same method of analysis was applied to fitting tamoxifen to our ATP model and as can be seen in Plate 20 there is a possibility that tamoxifen in the orientation shown could mimic ATP in two dimensions. Plate 21, however, shows that in three dimensions tamoxifen is not flat enough to fit into our postulated binding site. We therefore feel it is unlikely that the biological activity of tamoxifen are a result of competition with ATP.

In conclusion we have put forward a possible group of interactions necessary for a molecule to compete with ATP in binding to kinase enzymes. Within this hypothesis we have shown gross interactions involved in recognition of potential ATP competitive antagonists, but cannot at this stage show any reasons for specificity of molecules towards different kinases. Despite the fact the ATP is cofactor in many biological reactions it is possible to produce molecules which will inhibit one tyrosine kinase and not another[35]. ATP is a flexible molecule which is likely to take up different conformations to fit into different enzyme binding sites; therefore a single model cannot show reasons for this selective inhibition. It will be possible to apply the same techniques to new crystal structures of ATP bound to different tyrosine kinases and allow the rational design of specific tyrosine kinase inhibitors.

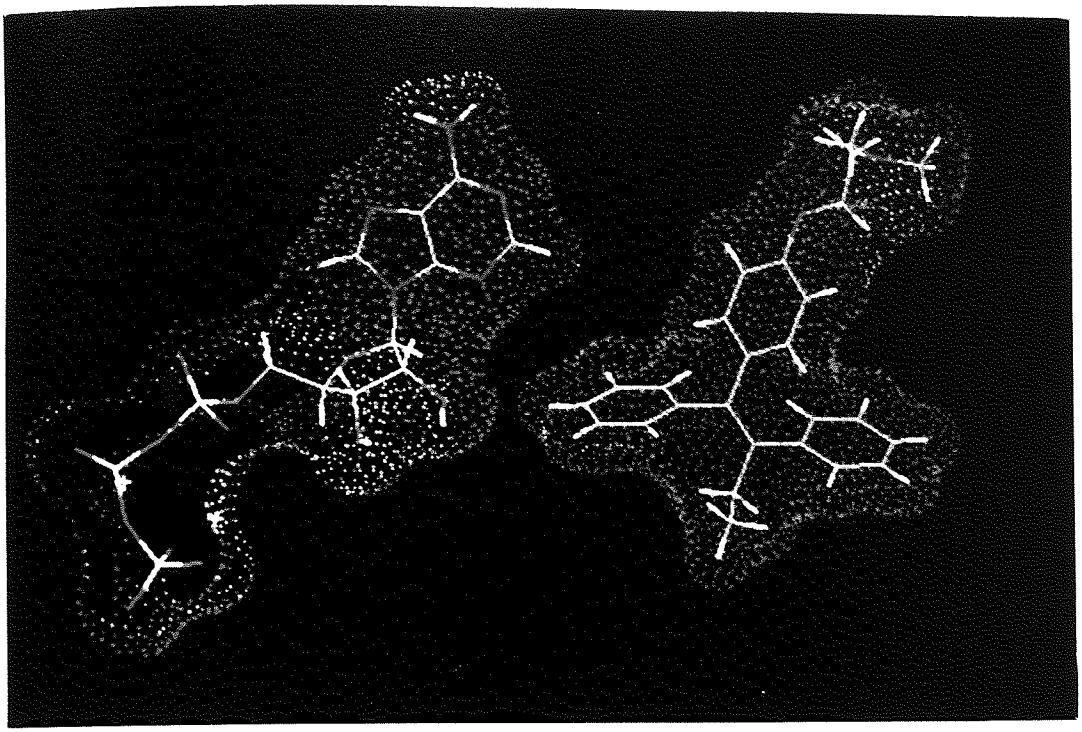

Plate 20: Comparison of ATP (10) with tamoxifen (1) with molecular surfaces ramped on electrostatic potential from -10 eV (blue) to 10eV (red).

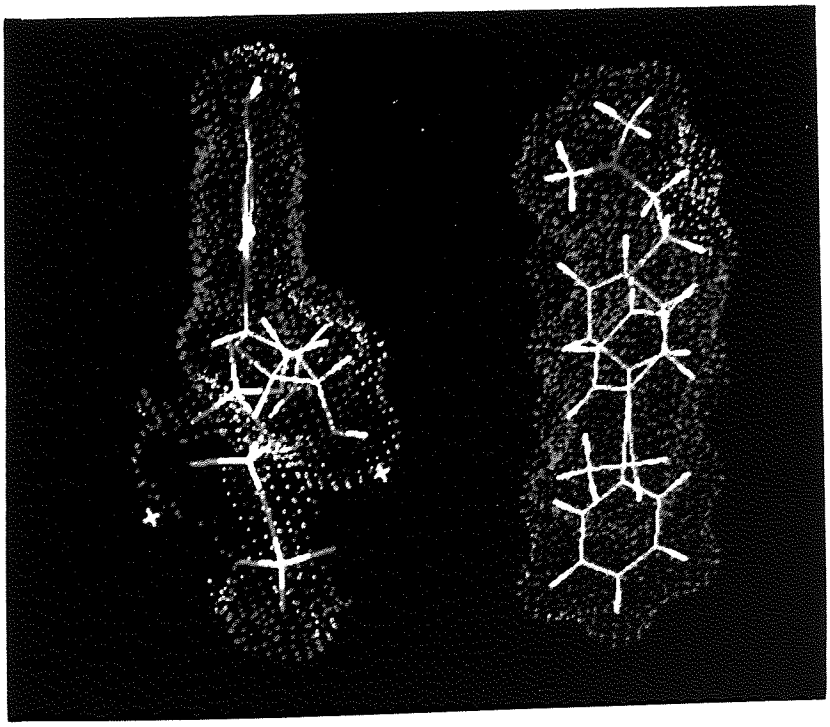

Plate 21: Comparision of ATP (10) with tamoxifen (1) as plate 20 but with each molecule rotated though 90°.

Table 9: Result of chemical calculations on tyrosine kinase inhibitors and potential inhibitors

Comp. no.	ΔHf (kcal mol^{-1})	μ (D)	Electrostatic Potential Min. (eV)	Max. (eV)
Tamoxifen (1)	194.3	1.61	-4.64	5.63
ATP (10)	-1163.7	8.89	-27.89	122.70
Quercetin (11)	-179.3	1.77	-7.70	7.83
Genistein (12)	8.8	4.58	-8.26	6.02
Amiloride (13)	155.9	9.65	1.17	27.26
(40d)	-31.3	2.78	-8.42	6.95
(41d)	-30.4	1.71	-8.42	7.01
(42d)	-31.1	2.98	-8.08	7.12
(43)	0.8	4.41	-11.13	8.29
(44)	-34.1	3.21	-8.53	5.00
(45)	-79.5	2.93	-8.08	6.99

KEY

ΔHf = Heat of formation

μ = dipole moment

3 Chemistry Results and Discussion

3.1 Synthesis of benzanilides and thiobenzanilides

Benzanilides were prepared, in good yield, from commercially available anilines and benzoyl chlorides. 3,4-Dimethoxybenzoyl chloride (47) and 2-chloro-4-nitrobenzoyl chloride (48) were prepared by reaction of thionyl chloride with the appropriate acid. Schotten-Baumann reactions using pyridine as base gave an average yield of 80% (range 57-95%).

Thionation of benzanilides was effected by treatment with Lawesson's reagent (34) in refluxing chlorobenzene (Tables 10 and 11). In the majority of cases the product crystallized out of the reaction mixture on cooling and was filtered off. When this was not the case various extraction methods were attempted. Removal, by evaporation under reduced pressure, of most of the chlorobenzene followed by recrystallization was useful in many cases. In other cases extraction into sodium hydroxide was possible either directly from the chlorobenzene or after removal of the chlorobenzene and redissolution in another organic solvent such as ethyl acetate. Yields were therefore heavily dependent on the solubility of the product in chlorobenzene but were generally greater than 70%.

Table 10: Synthesis of Thiobenzanilides

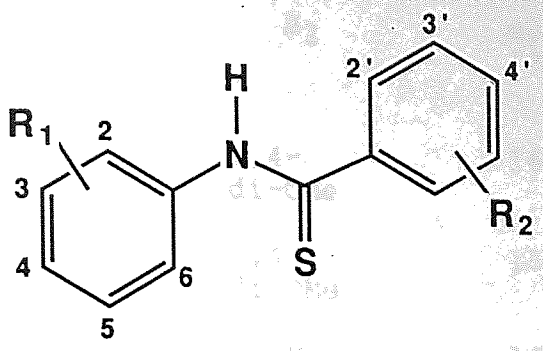

Cmp No	R_1	R_2	m.p. (°C)	Yield %
(38b)	3,4-di-OMe	4-OMe	149-151	83
(40b)	4-OMe	4-OMe	151-152	89
(41b)	4-OMe	3-OMe	75-76	47
(42b)	3-OMe	4-OMe	98-99	24
(49b)	2-OMe	H	121-122	76
(50b)	3-OMe	H	81-82	70
(51b)	4-OMe	H	131-133	79
(52b)	H	3-OMe	91-93	74
(53b)	2-OMe	4-OMe	69-71	25
(54b)	3,4-di-OMe	H	154	75
(55b)	3,5-di-OMe	H	135-136	73
(56b)	2,4-di-OMe	4-OMe	103-104	43
(57b)	4-OMe	3,4-di-OMe	154-155	87
(58b)	2,4-di-OMe	3,4-di-OMe	128-129	84

Table 10: Synthesis of Thiobenzanilides (cont.)

Cmp No	R_1	R_2	m.p. (°C)	Yield %
(59b)	3,4-di-OMe	3,4-di-OMe	165-166	86
(60b)	3,5-di-OMe	3,4-di-OMe	155-156	75
(61b)	4-NO_2	4-OMe	187-188	86
(62b)	4-OMe	4-NO_2	164-166	64
(63b)	4-OMe	2-Cl 4-NO_2	176	60
(64b)	H	3-NO_2	124-126	63
(65b)	H	4-NO_2	149-150	32
(66b)	4-Cl	4-OMe	180-183	91
(67b)	2-Me	4-OMe	119-120	65
(68b)	2,6-di-Me	4-OMe	150-160	87

For details of purification, crystallization, solvents, and melting points, see Section 6.5.

Table 11: Synthesis of other thioamides

Comp no.	Compound name	m.p. (°C)	Yield (%)
(69b)	N-Methyl-4'-methoxy-thiobenzanilide	100-101	50
(70b)	N-(4-methoxythio-benzoyl)-1,2,3,4-tetrahydroquinoline	146-147	58
(71b)	N-(4-methoxythio-benzoyl)indoline	120-122	42

3.2 Scope of the cyclisation reaction

2-Phenylbenzothiazoles were prepared by cyclisation of thiobenzanilides by potassium ferricyanide in aqueous alkali (Table 11). Yields were good, in the majority of cases being 70-90%.

The cyclisation of 3,4,4'-trimethoxythiobenzanilide (38b), 3,4-dimethoxythiobenzanilide (54b) and 3,3',4,4'-tetramethoxythiobenzanilide (59b) gave exclusively 5,6-disubsitution on the benzothiazole nucleus (Table 12). 6,7-Methoxy substituted benzothiazoles were not seen presumably due to steric influences on the cyclisation reaction.

5-Methoxy-2-(4-methoxyphenyl)benzothiazole (42c) and 7-methoxy-2-(4-methoxyphenyl)benzothiazole ($42c^{i}$) were produced in 23 and 29% yields respectively from the cyclisation of 3,4'-dimethoxythiobenzanilide (42b). The overall lower yield of this reaction may be due to decreased electron density ortho to the anilide nitrogen[59] in 3-methoxythiobenzanilides compared to that in 4- and 6-methoxythiobenzanilides. Where the thioamide had 3- and 5-methoxy substituents (compound 60b) the yield of cyclised product was reduced still further to 27%. This low yield may also have been due to the presence of 3,4-dimethoxy substitution in the 2-phenyl ring as in 3 out of

4 cases this resulted in a yield of cyclised product of less than 50% (compounds 57c, 58c, 59c, 60c).

Table 12: Synthesis of Benzothiazoles

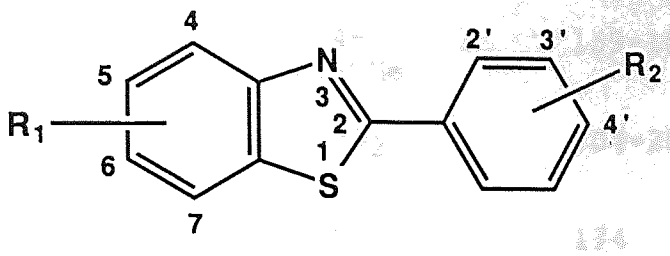

Cmp No	R_1	R_2	m.p. (°C)	Yield %
(35c)	H	4-OMe	122	90
(38c)	5,6-di-OMe	4-OMe	159-160	91
(40c)	6-OMe	4-OMe	156-158	71
(41c)	6-OMe	3-OMe	98-99	71
(42c)	5-OMe	4-OMe	120-121	23
(42c^{i})	7-OMe	4-OMe	140-141	29
(49c)	4-OMe	H	103-104	76
(51c)	6-OMe	H	111	73
(52c)	H	3-OMe	74-75	80
(54c)	5,6-di-OMe	H	142-144	91
(56c)	4,6-di-OMe	4-OMe	123-124	66
(57c)	6-OMe	3,4-di-OMe	123-124	86
(58c)	4,6-di-OMe	3,4-di-OMe	148-149	48

Table 12: Synthesis of Benzothiazoles (cont.)

Cmp No	R_1	R_2	m.p. (°C)	Yield %
(59c)	5,6-di-OMe	3,4-di-OMe	176-177	47
(60c)	5,7-di-OMe	3,4-di-OMe	159-160	27
(62c)	6-OMe	4-NO_2	204-205	68
(63c)	6-OMe	2-Cl 4-NO_2	174	55
(64c)	H	3-NO_2	144-145	94
(65c)	H	4-NO_2	225-226	28
(66c)	6-Cl	4-OMe	145-146	90
(67c)	4-Me	4-OMe	87-88	90

For details of purification, crystallization, solvents, yields and melting points, see Section 6.5.

Where R_1 was a 4-nitro group, no product was isolated and further investigation showed 4-nitro-4'-methoxythiobenzanilide (61b) to be unstable in aqueous alkali at room temperature. It is also possible that some of the benzothiazoles formed could have further reacted with the alkali present. Benzothiazoles substituted with nitro groups in the 5- or 6-position are prone to attack at C2 in alkaline solutions leading to ring opening[58]. Purification of compounds with nitro substituents in the 2-phenyl ring was hampered by the low solubility of these compounds. 2-(3-Nitrophenyl)benzothiazole (64c) and 2-(4-

nitrophenyl)benzothiazole (65c) were only slightly soluble in chloroform and insoluble in other organic solvents. Purification was effected by flash column chromatography on small amounts of the compounds. Recrystallization from methanol was possible for 2-(2-chloro-4-nitrophenyl)-6-methoxybenzothiazole (63c) due to its increased solubility.

The effect of N-substitution on the cyclisation of thiobenzanilides to 2-phenylbenzothiazoles was investigated using standard reaction conditions (see Section 6.5). Under these conditions no cyclised product was formed from N-methyl-4'-methoxythiobenzanilide (69b), N-(4-methoxythiobenzoyl)-1,2,3,4-tetrahydroquinoline (70b) or N-(4-methoxythiobenzoyl)-indoline (71b) in all cases starting material was recovered unaltered. This suggests that the mechanism of cyclisation involves initial formation of the thioenol tautomer.

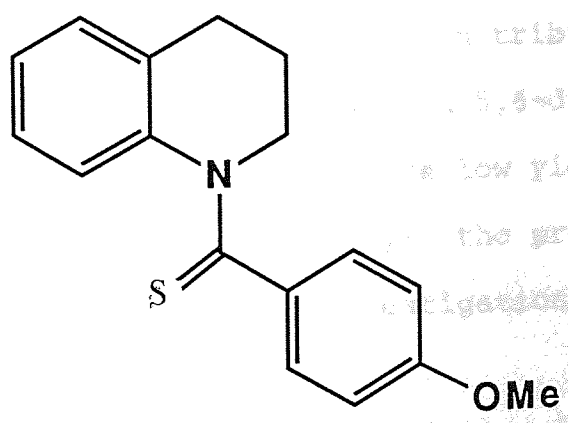

(70b)

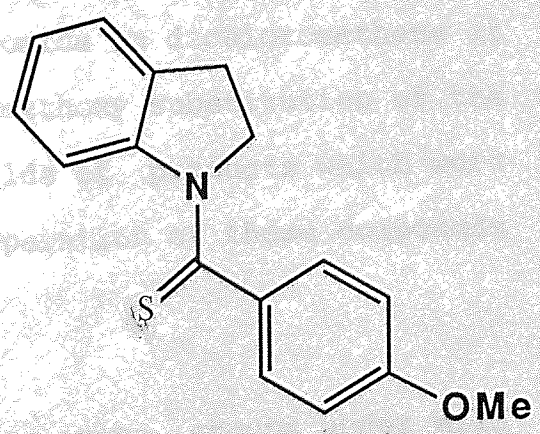

(71b)

One electron oxidation of thiolate anion by the ferricyanide anion gives a sulphur radical which can then directly attack the aromatic carbon ortho to the imine nitrogen (Fig. 6) or, less likely, can form a spiro intermediate (Fig. 7). In both cases rearangement and elimiation of a hydrogen radical would lead to the 2-phenylbenzothiazole product. The existence of a spiro intermediate is unlikely as 2,6-dimethyl-4'-methoxythiobenzanilide (68b) does not cyclise under the standard conditions used. The cyclisation of thiobenzanilides to 2-phenylbenzothiazoles probably proceeds via direct attack of a sulphur radical on the unsubstituted ortho carbon as shown in Fig. 6.

3.3 Manipulation of substituents

The hydroxy-substituted 2-phenylbenzothiazole compounds prepared for biological testing are shown in Table 13. Demethylation proceded cleanly and effectively in most cases using boron tribromide in dichloromethane at -70°C. Compounds with 5,6-dimethoxy substitution of the benzothiazole ring gave low yields of products which were difficult to purify; the preparation of these compounds requires further investigation.

Nitro groups were reduced to amino groups under mild conditions by reaction with tin (II) chloride in

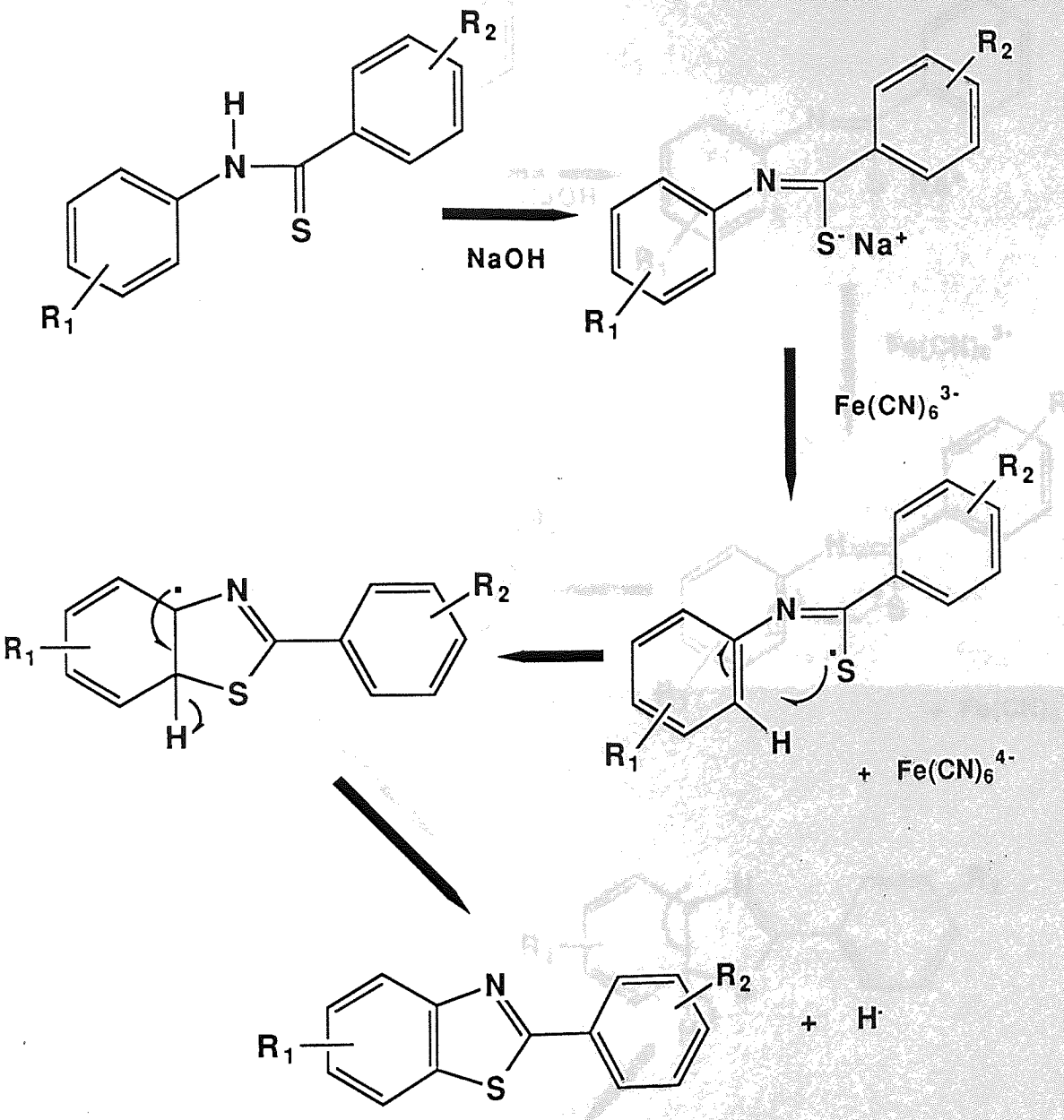

Fig 6: Proposed mechanism of cyclisation

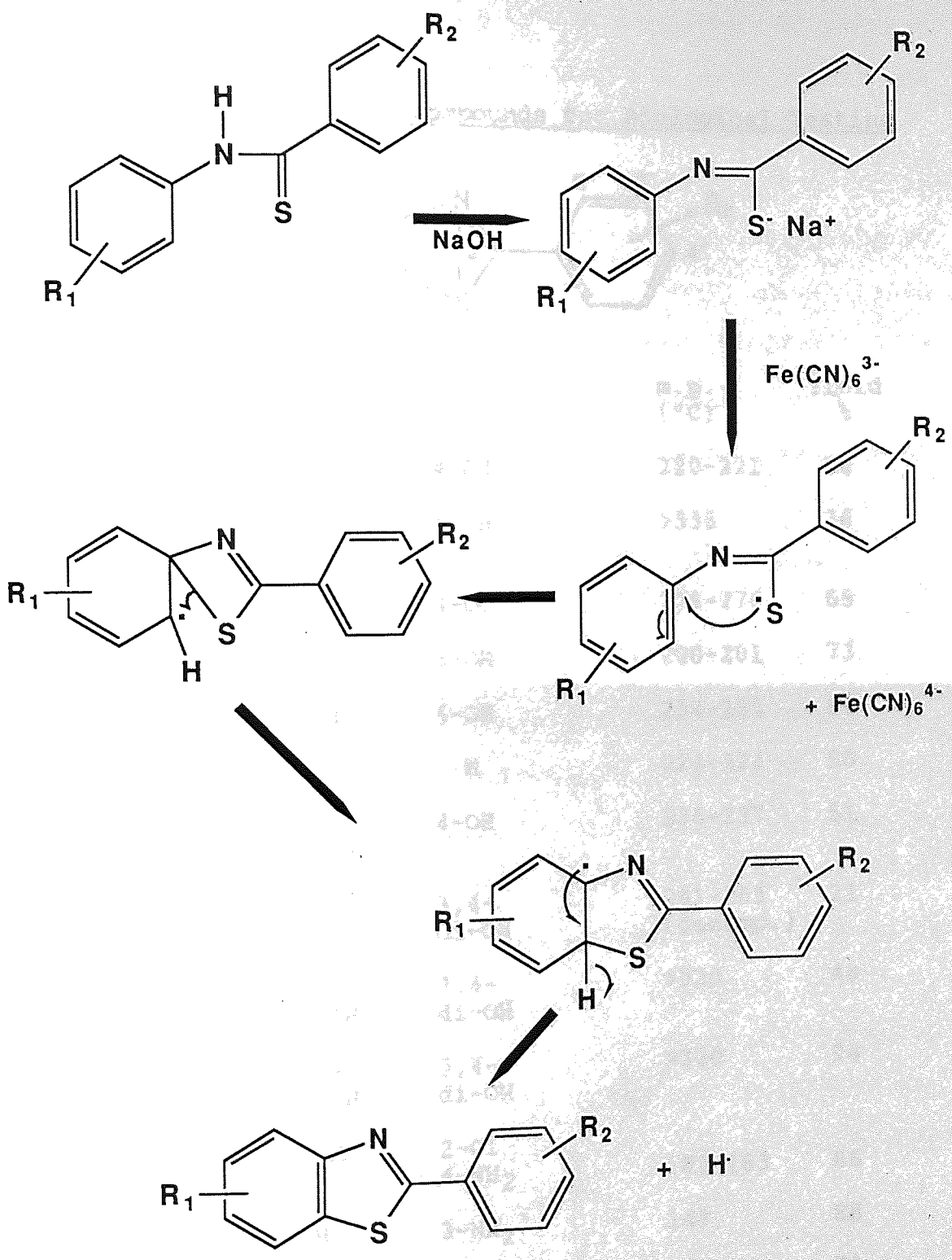

Fig. 7: Alternative mechanism of cyclisation

ethanol[62]. Yields attained by this method were greater than 70%.

Table 13: Synthesis of Compounds for Biological Testing

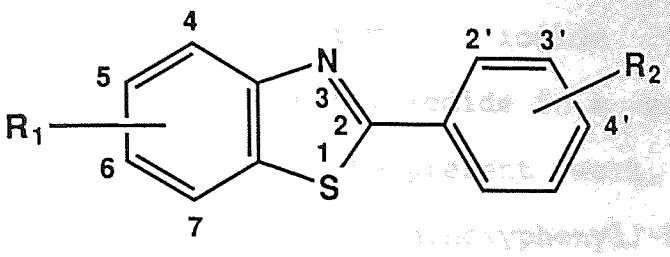

Cmp No	R_1	R_2	m.p. (°C)	Yield %
(35d)	H	4-OH	220-221	56
(38d)	5,6-di-OH	4-OH	>335	36
(40d)	6-OH	4-OH	275-276	65
(41d)	6-OH	3-OH	200-201	73
(42d)	5-OH	4-OH	234-235	80
(51d)	6-OH	H	223-224	50
(56d)	4,6-di-OH	4-OH	236-237	51
(57d)	6-OH	3,4-di-OH	261-265 (decomp.)	21
(58d)	4,6-di-OH	3,4-di-OH	>330	48
(60d)	5,7-di-OH	3,4-di-OH	>320	94
(63d)	6-OMe	2-Cl 4-NH_2	182-183	86
(64d)	H	3-NH_2	143	88
(65d)	H	4-NH_2	155-156	73

For details of purification, crystallisation, solvents, Yields and melting points, see Section 6.5.

3.4 Oxidation and alkylation of the heterocyclic ring

In the present work, attempts were made to oxidise and alkylate 2-(4-methoxyphenyl)benzothiazole (35c) on nitrogen. Akiba et al[100], reported the preparation of 2-phenyl-3-methylbenzothiazolium iodide from 2-phenylbenzothiazole and methyl iodide in a sealed tube at 100°C for 20 hours. In the present work, no alkylated product was formed from 2-(4-methoxyphenyl)-benzothiazole (35c) with methyl iodide or methyl tosylate in boiling dichloromethane for 2 hours; or with methyl tosylate in dichloromethane at room temperature for 72 hours; or refluxing in ethyl iodide for 4 hours. Clearly more vigorous conditions are required.

Oxidation of 2-phenylbenzothiazole (36) to the N-oxide has been described by Takahashi & Kano[101]. Under the conditions used, oxidation of 2-(4-methoxyphenyl)-benzothiazole (35c) was not seen. Formation of 2-methylbenzothiazole-N-oxide occurs readily but no N-oxide is formed when the 2-position is substituted by thiol, thioether or alkoxy group[102]. The mesomeric electron-donating effects of these groups is similar to that of the 4-methoxyphenyl group which would explain the failure of the oxidation reaction.

3.5 Preparation of other compounds

2,4,4'-Trihydroxyazobenzene (46) was prepared by coupling between diazotised 4-hydroxyaniline and resorcinol (see Section 6.5).

Genistein (12) was prepared by the demethylation of its 4-methyl ether (37) by boron tribromide in dichloromethane (see Section 6.5).

3.6 Compounds not previously described

(38a) 3,4,4'-trimethoxybenzanilide

(38b) 3,4,4'-trimethoxythiobenzanilide

(38c) 2-(4-methoxyphenyl)-5,6,-dimethoxybenzothiazole

(38d) 2-(4-hydroxyphenyl)-5,6,-dihydroxybenzothiazole

(40d) 2-(4-hydroxyphenyl)-6-hydroxybenzothiazole

(41b) 4,3'-dimethoxythiobenzanilide

(41c) 2-(3-methoxyphenyl)-6-methoxybenzothiazole

(41d) 2-(3-hydroxyphenyl)-6-hydroxybenzothiazole

(42b) 3,4'-dimethoxythiobenzanilide

(42c) 2-(4-methoxyphenyl)-5-methoxybenzothiazole

($42c^{i}$) 2-(4-methoxyphenyl)-7-methoxybenzothiazole

(42d) 2-(4-hydroxyphenyl)-5-hydroxybenzothiazole

(49c) 2-phenyl-4-methoxybenzothiazole

(50b) 3-methoxythiobenzanilide

(51d) 2-phenyl-6-hydroxybenzothiazole

(53b) 2,4'-dimethoxythiobenzanilide

(54a) 3,4-dimethoxybenzanilide

(54b) 3,4-dimethoxythiobenzanilide

(55a) 3,5-dimethoxybenzanilide

(55b) 3,5-dimethoxythiobenzanilide

(56a) 2,4,4'-trimethoxybenzanilide

(56b) 2,4,4'-trimethoxythiobenzanilide

(56c) 2-(4-methoxyphenyl)-4,6-dimethoxybenzothiazole

(56d) 2-(4-hydroxyphenyl)-4,6-dihydroxybenzothiazole

(57a) 4,3',4'-trimethoxybenzanilide

(57b) 4,3',4'-trimethoxythiobenzanilide

(57c) 2-(3,4-dimethoxyphenyl)-6-methoxybenzothiazole

(57d) 2-(3,4-dihydroxyphenyl)-6-hydroxybenzothiazole

(58a) 2,4,3',4'-tetramethoxybenzanilide

(58b) 2,4,3',4'-tetramethoxythiobenzanilide

(58c) 2-(3,4-dimethoxyphenyl)-4,6-dimethoxy-benzothiazole

(58d) 2-(3,4-dihydroxyphenyl)-4,6-dihydroxy-benzothiazole

(59a) 3,4,3',4'-tetramethoxybenzanilide

(59b) 3,4,3',4'-tetramethoxythiobenzanilide

(59c) 2-(3,4-dimethoxyphenyl)-5,6-benzothiazole

(60a) 3,5,3',4'-tetramethoxybenzanilide

(60b) 3,5,3',4'-tetramethoxythiobenzanilide

(60c) 2-(3,4-dimethoxyphenyl)-4,6-dimethoxy-benzothiazole

(60d) 2-(3,4-dihydroxyphenyl)-4,6-dihydroxy-benzothiazole

(62c) 2-(4-nitrophenyl)-6-methoxybenzothiazole

(63a) 2'-chloro-4-methoxy-4'-nitrobenzanilide

(63b) 2'-chloro-4-methoxy-4'-nitrothiobenzanilide

(63c) 2-(2-chloro-4-nitrophenyl)-6-methoxy-benzothiazole

(63d) 2-(2-chloro-4-aminophenyl)-6-methoxy-benzothiazole

(66a) 4-chloro-4'-methoxybenzanilide

(66b) 4-chloro-4'-methoxythiobenzanilide

(66c) 2-(4-methoxyphenyl)-6-chlorobenzothiazole

(67b) 2-methyl-4-methoxythiobenzanilide

(67c) 2-(4-methoxyphenyl)-4-methylbenzothiazole

(68b) 2,6-dimethyl-4'-methoxythiobenzanilide

(70a) N-(4-methoxybenzoyl)-1,2,3,4-tetrahydroquinoline

(70b) N-(4-methoxythiobenzoyl)-1,2,3,4-tetrahydro-quinoline

(71a) N-(4-methoxybenzoyl)indoline

(71b) N-(4-methoxythiobenzoyl)indoline

4 BIOLOGICAL RESULTS AND DISCUSSION

4.1 Oestrogen Receptor Binding Assay

The values for oestrogen receptor binding affinity of eight 2-phenylbenzothiazole derivatives are shown in Fig. 8. As expected compounds 35d and 51d showed no binding activity. Of the dihydroxy-substituted 2-phenylbenzothiazoles some interesting differences in RBAs are seen. 6,4'-Substitution (compound 40d) gives the strongest ER binding of the 2-phenylbenzothiazole analogues tested. Changing the substituent on the 2-phenyl ring to the 3'-position, (compound 41d), reduces binding by half; alternatively moving the benzothiazole hydroxy from the 6- to the 5-position (compound 42d) abolishes binding altogether.

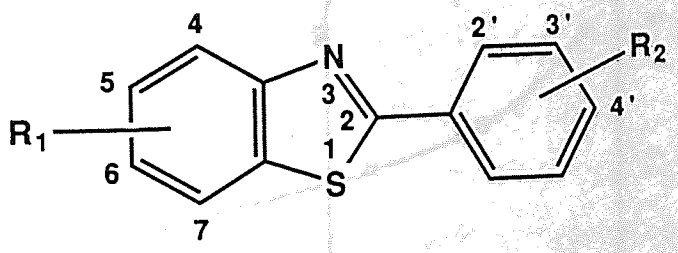

The addition of a third hydroxyl group in the 4-position of 2-(4-hydroxphenyl)-6-hydroxybenzothiazole (40d) gives compound (56d) and decreases the RBA greatly despite this being the substitution pattern which would most closely resemble genistein (12) (Fig. 9).

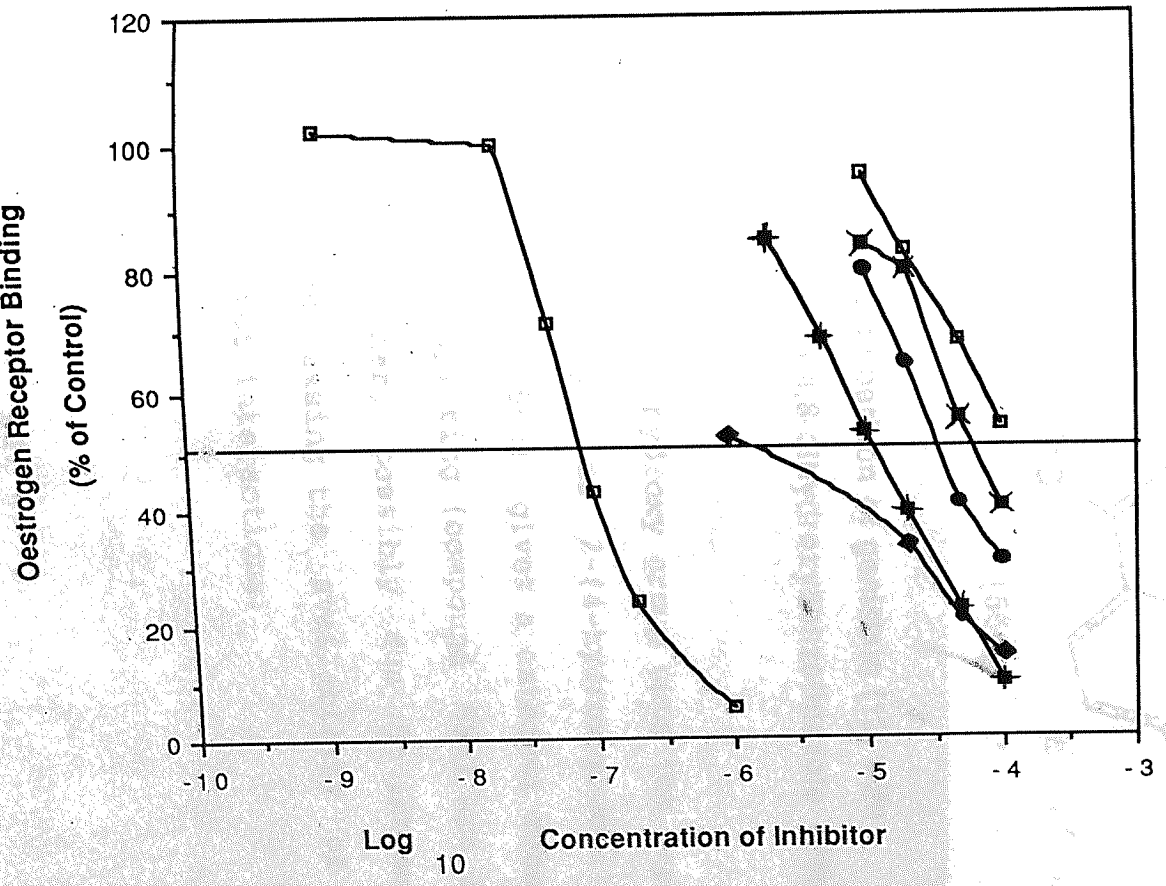

Compound	RBA
Oestradiol (4)	100
46	0.78
40d	0.70
41d	0.24
56d	0.13
58d	0.06
51d	<0.01
35d	<0.01
42d	<0.01
60d	<0.01

Fig. 8 Oestrogen receptor binding affinities of test compounds

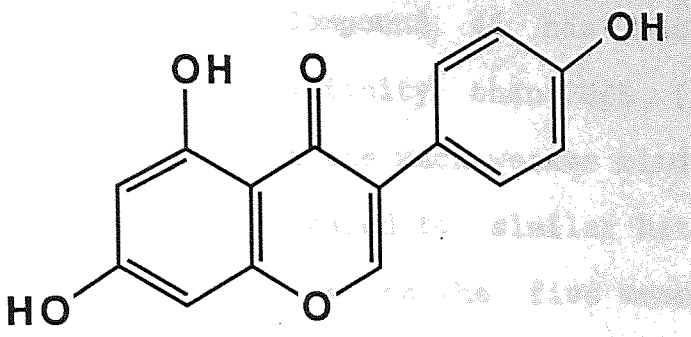

(12)

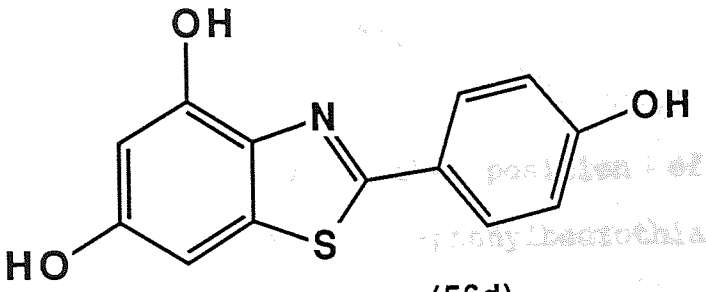

(56d)

Fig. 9 Comparison of genistein (12) with 2-(4-hydroxyphenyl)-4,6-dihydroxybenzothiazole (56d)

The addition of a hydroxy group onto the 3-position, of the 2-phenyl ring, of 2-(4-hydroxyphenyl)-4,6-dihydroxybenzothiazole (56d) gives a catechol substitution pattern on the 2-phenyl ring (compound 58d) and decreases binding still further, possibly due to intramolecular hydrogen bonding decreasing the availability of the 4'-hydroxyl for receptor interactions.

The most active compound tested was 2,4,4'-trihydroxyazobenzene (46) which structurally resembles DES (31) (Section 2.3.1). Compound 46 has much weaker oestrogen receptor binding affinity than DES (31)(RBA = 286)[51]. This coupled with the much weaker binding of 2-phenybenzothiazoles when compared to similar heterocycles which have alkyl substituents on the five membered ring (Table 14), reinforces the conclusion that hydrophobic groups in the centre portion of the molecule are important for oestrogen receptor binding[47].

The effect of changing the position of hydroxyl substituents on the RBA of 2-phenylbenzothiazoles, 2-phenylindoles, 2-phenylbenzothiophenes, 2-phenylbenzofurans and 2-phenylbenzimidazoles is shown in Table 14. Indoles and thiazoles must bind to the oestrogen receptor so that ring nitrogens are in the same orientation, despite them being in different hybridization states. Data from the 2-phenylbenzothiophene series shows a similar pattern but binding must occur with the molecule flipped over so that the heterocyclic sulphur is in the same orienation as the hetercyclic nitrogen in the benzothiazole. Had the oppposite been true, the positions of the two heterocyclic atoms in the benzothiazole would have reinforced the positive effects on oestrogen receptor binding of the thiophene and indole heteroatoms.

Table 14: Comparison of oestrogen receptor binding affinity in some heterocyclic compounds[47,52]

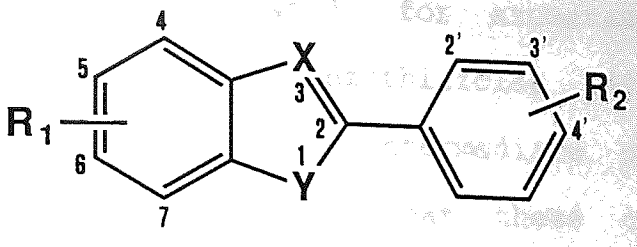

Cmp No.	R_1	R_2	X	Y	RBA
(40d)	6-OH	4-OH	N	S	0.70
(41d)	6-OH	3-OH	N	S	0.24
(42d)	5-OH	4-OH	N	S	<0.01
(72)	6-OH	4-OH	C-Me	N-Et	33.00
(73)	6-OH	3-OH	C-Me	N-Et	3.00
(23)	5-OH	4-OH	C-Me	N-Et	9.50
(74)	6-OH	4-OH	C-Et	S	27.60
(75)	5-OH	4-OH	C-Et	S	59.60
(76)	6-OH	4-OH	C-Et	O	0.60
(77)	5-OH	4-OH	C-Et	O	15.70
(78)	6-OH	4-OH	N	N-Pr	0.33
(79)	5-OH	4-OH	N	N-Pr	0.21

4.2 Aromatase Inhibition Assay

The compounds tested for aromatase inhibitory activity were the 2-phenylbenzothiazoles (40d), (51d) and (58d); (40b) a thioamide intermediate of (40d) and genistein (12). The fact that these compounds were potentially mimicking oestradiol and that oestradiol is produced by aromatase led us to examine the possibility that these compounds would inhibit aromatase. None of the compounds tested showed activity. As compound (40d), which had the highest RBA was tested, it is unlikely that any other 2-phenylbenzothiazoles will inhibit aromatase.

4.3 Cytotoxicity Assays

Evaluation of the selective cytotoxicity of potential anticancer agents is a useful indicator of potential antineoplastic activity. Our data (Tables 15 and 16) is for 3T3, ANN-1 , MCF-7 and WIDR cells (see Section 1.6). Of the test compounds, five were selectively toxic to the ANN-1 cells. 2-(2-Chloro-4-aminophenyl)-6-methoxybenzothiazole (63d) was fifteen times more toxic to "transformed" ANN-1 cells than "normal" 3T3 cells. The other compound showing increased toxicity towards ANN-1 cells were unsubsituted 2-phenylbenzothiazole (36), 2-(4-aminophenyl)benzothiazole (64d), 2-(3-aminophenyl)benzothiazole (63d) and 2,4,4,'-trihydroxyazobenzene (46).

Compound 63d was prepared as an intermediate in the synthesis of 2-(-2-chloro-4-hydroxyphenyl)-6-hydroxy-benzothiazole (44) which was predicted to be a tyrosine kinase inhibitor by our molecular modelling studies (see Section 2.3.2). It has previously been shown by Cunningham[72] that 3'-amino-4'-methoxyflavone (80) and its 3'-methoxy-4'-amino analogue (81) were selectively toxic towards ANN-1 cells. When compound (63d) was shown to be active we investigated whether a similar mechanism of action could be involved in the cytotoxicity of these compounds, using 2-(3-aminophenyl)benzothiazole (64d) and 2-(4-aminophenyl)-benzothiazole (65d).

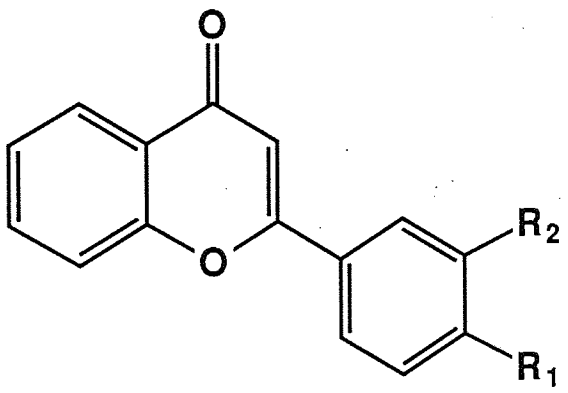

(80) R1 = OMe R2 = NH_2

(81) R1 = NH_2 R2 = OMe

In the flavones, 3'-amino substitution produced greatest cytotoxicity (IC_{50} ANN-1 cells 0.8-2.5μM) but was three times less toxic towards 3T3 cells. The 4'-amino

analogue was less toxic and only marginally selective. In the case of the 2-phenylbenzothiazole derivatives, the order was reversed with the 4-amino analogue (65d) being six fold more cytotoxic to ANN-1 cells than 3T3 cells (Table 15).

Table 15: Results of cytotoxicity tests of 2-phenylbenzothiazole derivatives

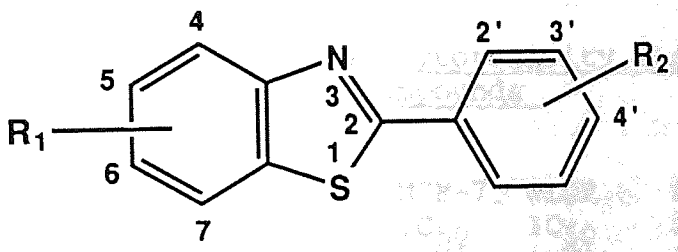

Comp. No.	R_1	R_2	MCF-7 IC_{50} (μM)	WIDR IC_{50} (μM)	ANN-1 IC_{50} (μM)	3T3 IC_{50} (μM
(35d)	H	4-OH	27.0	68.7	72,82	66,77
(36)	H	H	9.6	31.0	10,17	37,53
(38d)	5,6-di-OH	4-OH	-	-	8,10	10,17
(40d)	6-OH	4-OH	25.0	67.2	8,19	3,19
(41d)	6-OH	3-OH	-	-	15,19	25,36
(42d)	5-OH	4-OH	41.4	62.2	20,31	22,30
(51d)	6-OH	H	27.3	45.2	63,79	75,84
(56d)	4,6-di-OH	4-OH	33.3	31.2	16,27	15,25
(57d)	6-OH	3,4-di-OH	-	-	3,8	2,10
(58d)	4,6-di-OH	3,4-di-OH	41.3	47.7	32,85	40,55

Comp. No.	R_1	R_2	MCF-7 IC_{50} (μM)	WIDR IC_{50} (μM)	ANN-1 IC_{50} (μM)	3T3 IC_{50} (μM
(60d)	5,7-di-OH	3,4-di-OH	-	-	31,33	40,73
(63d)	6-OMe	2-Cl 4-NH_2	-	-	2(n=2)	23,28
(64d)	H	3-NH_2	-	-	2,3	16,32
(65d)	H	4-NH_2	-	-	16(n=2)	52,58

Table 16: Results of cytotoxicity tests on other compounds

Compound	MCF-7 IC_{50} (μM)	WIDR IC_{50} (μM)	ANN-1 IC_{50} (μM)	3T3 IC_{50} (μM
tamoxifen (1)[103]	5.0-7.5	-	3,4	3,5
quercetin (11)	24.0	40.2	24,43	29,50
genistein (12)	15.1	27.7	4,15	17,31
amiloride (13)	57.7	>223	50,88	>100
DES (31)[103]	5.0	-	1,5	1,4
2,4,4'-trihydroxy azobenzene (46)	-	-	1,3	5,6
3'-amino-4'-methoxy-flavone (80)	-	-	1,3	8(n=2)
3'-methoxy-4'-amino-flavone (81)	-	-	20,35	38,54

These results suggest that the amino substituted phenyl group is important in this selective cytotoxic effect but the mechanism of this effect is unclear.

Molecular modelling studies in the future may reveal whether the 3'-amino group on a flavone could be mimicked by a 4'-amino group on a 2-phenylbenzothiazole.

The hydroxylated 2-phenylbenzothiazoles were equitoxic to ANN-1, 3T3, MCF-7 and WIDR cells, with IC_{50} values spread from 2-85μM (Tables 15 and 16).

Quercetin (11), genistein (12) and amiloride (13), known tyrosine kinase inhibitors, were used as control compounds. Of these only amiloride (13) showed selective toxicity toward ANN-1 cells and this was at 50-88μM which is less than its IC_{50} for inhibition of EGFR tyrosine kinase (Table 2).

DES (31) and tamoxifen (1) were found to be very toxic to both 3T3 and ANN-1 cell lines (IC_{50} 0.5-5μM and 2.5-4.5μM respectively). These figures are comparable to those for inhibition of oestrogen dependent MCF-7 cell growth by DES (31) and tamoxifen (1)(Table 18)[103]. As DES (31) was 2-3 times less cytotoxic towards oestrogen independent MDA-MB-330 cells and tamoxifen (1) has an IC_{50} of 25μM against L1210 cells[104], it is possible that both 3T3 and ANN-1 cells are at least to some extent oestrogen dependent.

The oestrogen dependency of 3T3 and ANN-1 cells has not been documented but L-929 mouse fibroblasts have oestrogen and androgen receptors and their growth is stimulated by oestrogens and androgens and inhibited by antioestrogens and antiandrogens[105]. Skin fibroblasts have been shown to have aromatase activity[106], this may have some bearing on the cytotoxicity of quercetin, a known aromatase inhibitor (section 1.3) to fibroblast cell lines.

Although the ANN-1 cells are theoretically dependent on the $pp120^{gag-abl}$ protein tyrosine kinase we have not shown that under the conditions used differences in cytotxicity between 3T3 and ANN-1 cells is due to inhibition of this kinase.

4.4 Inhibition of EGF stimulated EGFR tyrosine kinase activity

This assay utilised a crude membrane preparation containing EGFR and as such only gives preliminary results. The results are given as percentage inhibition at 150μM as there was not enough data to calculate IC_{50} values. Six hydroxylated benzothiazoles and tamoxifen (1) were tested with quercetin (11), genistein (12) and amiloride (13) used as controls (Tables 17 and 18).

2-(4-Hydroxyphenyl)-6-hydroxybenzothiazole (40d) inhibited EGFR while 2-(3-hydroxyphenyl)-6-hydroxy-benzothiazole (41d) and 2-(4-hydroxyphenyl)-5-hydroxy-benzothiazole (42d) did not. The three other 2-phenyl-benzothiazoles tested were inhibitors there being essentially no difference between 2-(4-hydroxyphenyl)-4,6-dihydroxy-benzothiazole (56d), 2-(3,4-dihydroxyphenyl)-4,6-dihydroxy-benzothiazole (58d) and 2-(3,4-dihydroxyphenyl)-5,7-dihydroxybenzothiazole (60d). This would suggest that the benzothiazoles can interact with the receptor with either the nitrogen or the sulphur in the same position or that the binding site is non-specific.

Tamoxifen (1) was shown to inhibit EGFR tyrosine kinase to a similar extent as genistein (12) in our crude assay system (Table 18). This is an interesting result which may have some relevance to the action of tamoxifen as an anticancer agent.

The relationship between this data and the cytotoxicity of test compounds towards ANN-1 cells is not clear as the tyrosine kinases involved are different.

Table 17:

2-Phenylbenzothiazole derivatives as potential tyrosine kinase inhibitors

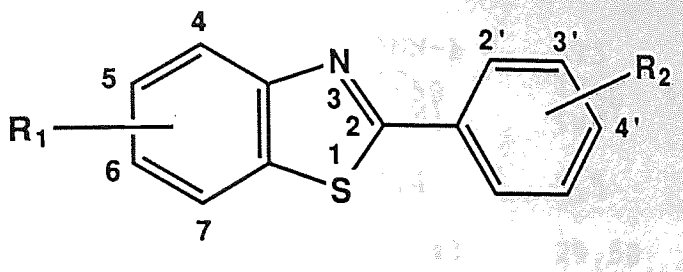

Comp No.	R_1	R_2	ANN-1 IC_{50} (μM)	3T3 IC_{50} (μM)	EGFR % inhibition at 150μM
(35d)	H	4-OH	72,82	66,77	n.d.
(36)	H	H	10,17	37,53	n.d.
(38d)	5,6-di-OH	4-OH	8,10	10,17	n.d.
(40d)	6-OH	4-OH	8,19	3,19	42
(41d)	6-OH	3-OH	15,19	25,36	-4
(42d)	5-OH	4-OH	20,31	22,30	5
(51d)	6-OH	H	63,79	75,84	n.d.
(56d)	4,6-di-OH	4-OH	16,27	15,25	47
(57d)	6-OH	3,4-di-OH	3,8	2,10	n.d.
(58d)	4,6-di-OH	3,4-di-OH	32,85	40,55	36
(60d)	5,7-di-OH	3,4-di-OH	31,33	40,73	38
(63d)	6-OMe	2-Cl, 4-NH_2	2(n=2)	23,28	n.d.
(64d)	H	3-NH_2	16(n=2)	52,58	n.d.
(65d)	H	4-NH_2	2,3	16,32	n.d.

Table 18:

Summary of biological results for control compounds and other potential tyrosine kinase inhibitors

Compound	ANN-1 IC_{50} (μM)	3T3 IC_{50} (μM)	EGFR % inhibition at 150μM
tamoxifen (1)	3,4	3,5	53§
quercetin (11)	24,43	29,50	30
genistein (12)	4,15	17,31	63
Amiloride (13)	50,88	>100	-24
DES (31)	1,5	0.5,4	n.d.
2,4,4'-trihydroxy benzylidene (46)	1,3	5,6.5	n.d.
3'-amino-4'-methoxy flavone (80) (ref. 72)	0.8,2.5	8(n=2)	
3'-methoxy-4'-amino flavone (81) (ref. 72)	20,35	38-54(n=3)	

§ = 100μM

None of the compounds tested showed any inhibition of aromatase but from the literature quercetin has IC_{50} of 12μM against human placental aromatase[39].

5 DISCUSSION AND FURTHER WORK

This project has covered areas from basic biochemistry to quantum pharmacology and has given rise to many more questions than it has solved. The use of chemical calculations has provided a useful adjunct to the standard synthesis and biological screening methods.

5.1 Production of Compounds for Evaluation as Potential Agents for the Treatment of Hormone Dependent Cancers

The hydroxy-substituted 2-phenylbenzothiazoles were produced as they were structurally similar to the 2-phenylindole antioestrogens already known and because of their possible similarity to genistein. The data so far available on these compounds show oestrogen receptor binding which is low but comparable to that of genistein and tamoxifen (see Section 4.1).

The test compounds which have shown oestrogen binding activity should now be assessed to see if this binding leads to oestrogenic or antioestrogenic effects.

Preliminary cytotoxicity data for substituted-2-phenylbenzothiazoles shows essentially no difference in cytotoxicity between ANN-1, 3T3, MCF-7 and WIDR cells. Despite some compounds showing oestrogen receptor binding

activity, no strong oestrogenic or antioestrogenic effect is apparent.

MCF-7 and WIDR cytotoxicity data for the amino substituted 2-phenylbenzothiazoles (63d, 64d, 65d) which showed greater toxicity to ANN-1 than 3T3 cells, is not available at present. This data would help show if any oestrogenic effects were involved in their activity.

ANN-1 and 3T3 cells should be tested for oestrogen dependency by growing them in oestrogen depleted medium and assessing the effect of adding exogenous oestrogens. The current culture system utilises medium containing phenol red, a known oestrogen[107], and supplemented with foetal calf serum.

5.2 Production of Potential Tyrosine Kinase Inhibitors

5.2.1 Molecular modelling studies

The molecular modelling study so far has shown a possible rational for producing potential tyrosine kinase inhibitors. Section 2.3 describes three rationally designed 2-phenylbenzothiazole analogues (43,44,45) (Table 8) which produce areas of negative electrostatic potential about the 2'-position of the 2-phenylbenzothiazoles. These should now be synthesised and tested for tyrosine

kinase inhibitory activity. The features we have shown to be present in both our model of kinase bound ATP and known kinase inhibitors can be used to assess other types of compounds. The usefulness of this model will become clear as further experimental results become available, especially x-ray crystal structure data for other binary complexes of tyrosine kinases with ATP. It is unlikely that this model will remain unchanged for very long as there is much research going on into the inhibition of tyrosine kinases.

It is not yet clear what effect inhibiting specific tyrosine kinases will have *in vivo* but this is a promising area for development as tyrosine kinase inhibition is not necessarily associated with general cytotoxicity[108].

5.2.2 Synthetic and biological studies

Due to the interesting *in vitro* activity of the amino-substituted 2-phenylbenzothiazole derivatives further work should be done to prepare further analogues with amino groups on the benzothiazole nucleus.

The production of 2-phenyl-5,6-dihydroxy-benzothiazoles needs some attention. The demethylation step to yield this catechol substitution pattern has not

been successful and a new work up procedure would probably increase the yield considerably.

As regards the testing of potential tyrosine kinase inhibitors, the assay procedures should be designed so that not only valid answers are produced but also that those answers can be related to each other. Any whole cell cytotoxicity assay should use cells dependent on an enzyme which can studied separately. Ideally, enzyme assays should use pure enzyme although this is not always possible, especially for routine screening, due the high cost of such enzymes.

The usefulness of compounds, both as research tools and as potential therapeutic agents will depend on their specificity to different tyrosine kinases. A battery of tests will be needed to assess any selectivity. As more selective inhibitors become available quercetin (11) will lose favour as a control compound due to its promiscuous nature ; effects seen in a complex biological system may not be due to tyrosine kinase inhibitory activity.

5.3 General Discussion

The present work has been wide ranging and included synthetic, theoretical and biological experiments. The aim of the work was to produce antioestrogenic and

tyrosine kinase inhibitory 2-phenylbenzothiazole derivatives. A few of the derivatives tested have shown the ability to bind to oestrogen receptors (Fig. 8) but this does not confer selective toxicity to oestrogen dependent MCF-7 cells. More interestingly four of the six hydroxy-substituted 2-phenylbenzothiazoles tested showed inhibitory activity towards EGFR tyrosine kinase. These results now need further investigation to characterise the nature of the enzyme inhibition and any selectivity towards different tyrosine kinases.

Serendipity played a part in finding that amino-substituted 2-phenylbenzothiazoles had potentially useful activity. 2-(2-Chloro-4-aminophenyl)-6-methoxy-benzothiazole (63d) was intermediate in the preparation of 2-(2-chloro-4-hydroxyphenyl)-6-hydroxybenzothiaole (44) which was predicted to be a tyrosine kinase inhibitor by our molecular modelling studies. Fortuitous testing of this compound gave a new lead into another area of potential activity.

The selective toxicity of certain compounds against ANN-1 and 3T3 cells should be investigated. The mechanism by which amino-substituted 2-phenylbenzothiazoles and flavones produce selective cytotoxicity may provide another target for the chemotherapy of cancer.

6 EXPERIMENTAL

6.1 Oestrogen Receptor Binding Assay

6.1.1 Materials

Compounds were prepared as described in section 6.5. Cytosol was obtained from a homogenate of calf uteri by centrifugation at 105,000g in 10.0mM Tris, 1.0mM EDTA, 3.0mM sodium azide buffer (pH 7.4).

6.1.2 Method

100µl aliquots of the cytosol preparation, containing 10mg of protein per ml, were mixed with 1 pmol of [^{3}H] oestradiol (specific activity 90-115 Ci nmol^{-1}) and either oestradiol or potential inhibitor. The final volume of each mixture was 0.5ml. Each potential inhibitor was tested in triplicate at four concentrations. The mixtures were incubated at 4°C for 16 hours after which 0.5ml of a suspension of dextran 60 0.008% and activated charcoal 0.8% in Tris-EDTA buffer. The mixture was shaken at 4°C for 90min and centrifuged at 700g for 10 min. 100µl Aliquots of the supernatent were assayed for specifically bound [^{3}H]- oestradiol by counting in a toluene scintilation mixture[109].

The concentration of inhibitor required to decrease the bound radioactivity by 50% was determined by plotting

the percentage of total activity bound versus the logarithm of the inhibitor concentration. From the values determined

$$\frac{IC_{50}E_2}{IC_{50}I_x} \times 100 = RBA$$

This work was performed by Prof. Erwin von Angerer at the Institut für Pharmzie, Regensburg University.

6.2 Aromatase Inhibition Assay

6.2.1 General

The aromatase enzyme is responsible for the conversion of testosterone to oestradiol (4) and of androstenedione to oestrone (5). The substrate is tritiated such that the radiolabel is released during the aromatisation reaction. The tritiated water produced can be assayed to give the rate of the reaction.

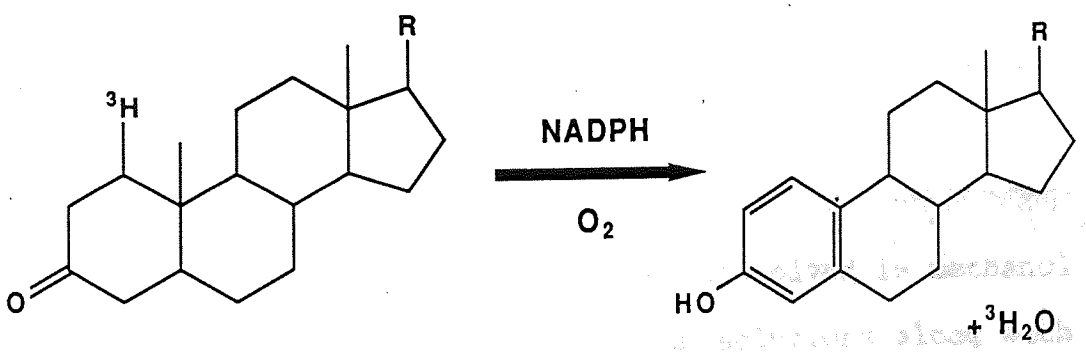

Androstenedione R = O
Testosterone R = OH

(4) Oestradiol R = OH
(5) Oestrone R = O

Fig. 10 Conversion of androgens to oestrogens by aromatase

6.2.2 Materials

Aromatase was obtained from the microsomal fraction of human placental tissue[110].

6.2.3 Method

Isolated microsomes were suspended in a minimum volume of 50mM phosphate buffer (pH 7.4) and stored at -30°C prior to use. Protein concentration was determined by the method of Lowry, as modified by Hartree[111]. [1-^{3}H]Androstenedione was used as substrate at a concentration of 1.5µM[112]. Stock substrate solution contained 60µl of 200µM androstenedione, 16µl of [1-^{3}H] androstenedione (16µCi) with 724µl propanediol. Cofactor solution contained 18mg NADP and 60mg glucose-6-phosphate in 2.4ml 50mM phosphate buffer (pH 7.4) with 2 x 25µl of glucose-6-phosphate dehydrogenase added immediately before use. Assays were in duplicate.

The potential inhibitors were dissolved in methanol to give 10µl of 5, 10, 20 and 50 µM solutions along with one tube containing only methanol. Substrate solution (25µl) was added to each assay tube with 3µl of [^{14}C]-sodium acetate as internal standard and 843µl of 50mM potassium phosphate (pH 7.4). Cofactor solution (100µl) was added to each tube and the reaction started by addition of 25µl placental microsomes in buffer equivalent to 100µg protein. The control was prepared using 973µl buffer, 3µl internal standard and 25µl of substrate solution. Incubation was at 37°C, 200µl samples being taken at 0, 5, 10 and 15 minutes and added to 0.2ml 1mM

$HgCl_2$ mercuric chloride, 1.0ml 1% activated charcoal in 0.1% Tween 80 on ice and allowed to stand for 30 minutes. After centrifugation (2,000g, 30 min), 0.5ml of supernatent was counted for ^3H_2O.

The amount of ^3H_2O released for each concentration are plotted against time. Comparison of the gradients of the lines compared to the control gives the percentage inhibition at each concentration. These can be used to determine the IC_{50}.

This assay was performed by Dr. Martin Rowlands at the Institute of Cancer Research, Sutton.

6.3 Cytotoxicity Assays

6.3.1 Materials

The preparation of genistein and benzothiazoles is shown in section 6.5.

6.3.2 Cells

American tissue culture collection (ATCC) 3T3 cells were obtained from Flo Laboratories. These are mouse fibroblast cells which are concidered to be normal displaying anchorage and density dependent growth. ANN-1 cells were a gift from Dr. J.G. Foulkes (NIMR, London). ANN-1 cells are grown in suspension culture and do not show density dependent growth. The cells express the Ableson gene product $pp^{120gag\text{-}abl}$ which has tyrosine kinase activity[72].

6.3.3 Method

ANN-1 cells were cultured in Dulbecco's modified Eagle medium (DMEM) (Gibco) supplemented with 10% foetal calf serum (Imperial Laboratories) and glutamine 1% (Gibco) under an atmosphere of 10% CO_2 in air and 100% humidity at 37°C.

3T3 cells were cultured in 45% DMEM (Gibco) with 10% foetal calf serum (Imperial Laboratories) under an atmosphere of 10% CO_2 in air and 100% humidity at 37°C.

Cells were seeded at a density of 4 x 10^4 cells per 2ml well and treated with drug dissolved in dimethyl-formamide (DMF). The final concentration of DMF in the medium was 0.5% $^{v}/_{v}$ and had no effect on the growth of cells. Cultures were incubated for 3 days and counted.

The IC50 is concentration of test compound required to reduce the growth of treated cell by 50% compared with control cells.

Cytotoxicity test on MCF-7 and WIDR cells were performed by Dr. Peter Lelieveld from EORTC Screening and Pharmacology Group, Rijswijk.

6.4 Determination of EGF-stimulated Tyrosine Kinase Inhibitory Activity

6.4.1 Materials

The preparation of genistein and benzothiazoles is shown in section 6.5. Tamoxifen and amiloride were purchased from Sigma and quercetin from Aldrich.

6.4.2 Cells

Human epidermoid carcinoma A431 cells were obtained from European Type Tissue Culture Collection (Porton Down).

6.4.3 Membrane Preparation

A crude membrane fraction was collected from 10^8 A431 cell equivalents per ml culture. The cells were washed (PBS) and hand homogenised (thirty strokes) in 2mM Hepes pH 7.4 (Sigma) buffer containing 150mM NaCl, 2mM MgCl and 4mM iodoacetic acid (Aldrich) then centrifuged (160,000g for 40min)[113]. The pellet was resuspended in buffer (20mM Hepes pH 7.5 (Sigma), 100mM NaCl, 0.1% $^{v}/_{v}$ Nonidet P-40 (Sigma)) and alliquots frozen at -20°C before use.

6.4.4 Method

The reactions were performed, in triplicate,in a final volume of 20 µl containing 100mM NaCl, 20mM Hepes pH

7.5 (Sigma), and 0.1% $^{v}/_{v}$ Nonidet P-40 (Sigma), 100μM {gamma^{32}p} ATP (0.001μCi/μM), with 4μl membrane preparation and 0.1μM EGF and test compound when required. The pre-incubation mixtures were prepared in microfuge tubes and preincubated at 30°C for 5 min. Labelled ATP was added. After 5 min the reaction was terminated by the addition of 184μl ice-cold 3.5% TCA. The mixture was microfuged (12,000 r.p.m., 2 min) and 100μl of supernatent spotted onto phosphocellulose paper, allowed to absorb but not dry then washed with phosphoric acid (4 x 10-20 min). The phosphocellulose papers were then added to a vial of distilled water and the ammount of radiolabelled phosphate incorporated into the proteins measured by liquid scintillation compared with 250μM of the labelled ATP.

6.5 Chemistry Experimental

U.v. spectra were recorded on a Pye Unicam SP8000 Ultraviolet Recording Spectrophotometer, 60MHz n.m.r. spectra on a Varian EM360A NMR Spectrometer and 300MHz n.m.r. spectra on a Bruker AM300 NMR Spectrometer. I.r. spectra were recorded on a Perkin-Elmer 1310 Infrared Spectrophotometer unless marked * when Perkin Elmer 1600 series FT IR, § when Nicolet 205 FT IR and ▵ when Mattson 4020 Galaxy Series FT IR were used. The t.l.c. systems employed Kieselgel $60F_{254}$ (0.25 mm) as the absorbant. Melting points are uncorrected. UV absorbances are given in nanometres.

General Method for the Preparation of Benzanilides

Substituted aniline (1 mol. equiv.) was added to a stirred solution of substituted benzoyl chloride (1 mol. equiv.) in excess pyridine. The mixture was stirred for 30 min at 20°C, then poured into water. The solid produced was filtered off and washed with water. Anilides were recrystalised from methanol.

General Method for the Preparation of Thiobenzanilides

Substituted anilide (1 mol. equiv.) was added to Lawesson's reagent (0.6 mol. equiv.) with sufficient chlorobenzene to dissolve the solids when hot. The mixture was heated under reflux for 3 hours then cooled and the solids filtered off.

General Method for the Preparation of 2-Phenylbenzothiazoles

Substituted thioamide (1 mol. equiv.) was finely powdered and a little ethanol added to wet the powder. Sodium hydroxide (8 mol. equiv.) was added in the form of a 30%$^{W}/_{V}$ solution. This was diluted with water to give a solution/suspension of thioamide in 10%$^{W}/_{V}$ sodium hydroxide solution. 1ml aliquots of this were added to a stirred solution of potassium ferricyanide (4 mol. equiv.) in water at 80-90°C, at 1 min intervals. The reaction mixture was heated for a further 30 min, then allowed to cool. The product was filtered off and washed with water.

Method A for the Demethylation of Methoxy-substituted 2-Phenylbenzothiazoles

To a stirred suspension of methoxy-substituted 2-phenylbenzothiazole (1 mol. equiv.) in dry dichloromethane (15-25ml), under nitrogen, at -70°C was added boron tribromide 1.0M in dichloromethane (2 mol. equiv. for each methoxy group plus 3 mol. equiv.) dropwise over 30-45 min. The mixture was kept at -70°C for a further 1h then allowed to warm slowly, in an ice-salt bath, to 20°C and then stirred overnight.

The reaction mixture was cooled to -70°C and methanol added dropwise until no further reaction was observed. The mixture was then poured into 50ml 8%$^{w}/_{v}$ sodium hydroxide solution and the aqueous phase was separated from the organic layer, made slightly acidic then extracted with 80% dichloromethane, 20% methanol (3 x 50ml). The solvent was the dried using sodium sulphate and evaporated under reduced pressure.

Method B for the Demethylation of Methoxy-substituted 2-Phenylbenzothiazoles

To a stirred suspension of methoxy-substituted 2-phenylbenzothiazole (1 mol. equiv. in dry dichloromethane (15-25ml), under nitrogen, at -70°C was added boron tribromide 1.0M in dichloromethane (excess) dropwise over 30-45 min. The mixture was kept at -70°C for a further 1h then allowed to warm slowly, in an ice-salt bath, to 20°C and stirred overnight.

The reaction mixture was cooled in to -70°C and the poured slowly (care!) into 75ml water cooled in an ice/salt bath. The product was extracted into the aqueous layer by addition of 40%$^{w}/_{v}$ sodium hydroxide solution (16ml). The aqueous phase was made slightly acidic and extracted with ethyl acetate or 80% dichloromethane, 20% methanol (3 x 50ml). The solvent was the dried using sodium sulphate and evaporated under reduced pressure.

Preparation of genistein (6)

Biochanin A (0.50g; 1.76×10^{-3}M) was reacted with boron tribromide 1.0M in dichloromethane (17.6ml) according to method B. Recrystallization from methanol gave beige needle crystals (0.53g, 56%), m.p. 286-287°C (lit. 297-298°C[114]); M+, 270.0528 gives $C_{15}H_{10}O_5$; $\lambda_{max.}$ (d.r.)* (KBr) 3414, 3198, 1654, 1519, 1310, 1274, 1203, 840 cm^{-1}; δ (DMSO-D_6) (300MHz) 12.94 (1H,s), 10.87 (1H,s), 9.58 (1H,s), 8.38 (1H,s), 7.34 (2H,d), 6.80 (2H,d), 6.38 (1H,s), 6.20 (1H,s) ppm; δ (DMSO + D_2O) (300MHz) 8.38 (1H,s), 7.37 (2H,d), 6.80 (2H,d), 6.36 (1H,s), 6.20 (1H,s) ppm; R_f ($CHCl_3$ + 2% EtOH) 0.53.

Preparation of 2-(4-methoxyphenyl)benzothiazole (35c)

2-Aminothiophenol (5.00g, 0.04M) was added to a stirred solution of 4-methoxybenzoyl chloride (6.80g, 0.04M) in pyridine (50ml). The mixture was stirred for 30 min then poured into water (200ml). The solid product was filtered and washed with water. Recrystallization from methanol gave white needle crystals (8.63g, 90%), m.p. 121-122°C (lit. 134°C[115]; M+, 241.; $\lambda_{max.}$ (nujol) 1600, 1300, 1260, 1220, 1180, 1020, 950, 820, 740 cm^{-1}; δ ($CDCl_3$) (300MHz) 8.01 (1H,s), 7.85 (1H,d), 7.45 (1H,t), 7.34 (1H,t), 6.97 (2H,d), 3.95 (3H,s) ppm; $\nu_{max.}$ (EtOH) 218, 313; R_f ($CHCl_3$) 0.33.

Preparation of 2-(4-hydroxyphenyl)benzothiazole (35d)

Compound 35c (1.00g, 0.00415M) was reacted with boron tribromide 1.0M in dichloromethane (16.6ml) according to method A. Recrystallization from methanol gave white plate crystals (0.53g, 56%), m.p. 220-221°C (lit. 229°C[116]; found C, 68.73; H, 3.96; N, 6.13% ($C_{13}H_9NOS$ requires C, 68.72; H, 3.96; N, 6.17%); M+, 227.; λ max. (nujol) 3400, 1600, 1460, 1290, 1220, 1160, 960, 820, 750 cm^{-1}; δ (DMSO-D_6) (300MHz) 10.23 (1H,s), 7.93 (4H,m), 7.48 (1H,t), 7.38 (1H,t), 6.92 (2H,d) ppm; δ (DMSO-D_6 + D_2O) (300MHz) 7.93 (4H,m), 7.48 (1H,t), 7.38 (1H,t), 6.92 (2H,d) ppm; ν max. (EtOH) 225, 282, 320; ν max. (EtOH + NaOH) 225, 354; R_f ($CHCl_3$ + 2% EtOH) 0.18.

Preparation of 3,4,4'-dimethoxybenzanilide (44)(38a)

3,4-dimethoxyaniline (5.00g, 0.0327M) was reacted with 4-methoxybenzoyl chloride (5.56g, 0.0327M) according to the general method. Recrystallization from methanol gave off-white needle crystals (8.24g, 88%); m.p. 148-150°C; found C, 63.23; H, 5.66; N, 4.39% ($C_{16}H_{17}NO_4$ requires C, 63.37; H, 5.61; N, 4.62%); M+, 287; λ max. (nujol) 3260, 1625, 1590, 1500, 1255, 1010, 840 cm^{-1}; δ (DMSO-D_6) (60MHz) 9.90 (1H,s), 7.80-8.10 (7H,m), 3.75 (9H,d) ppm; Rf ($CHCl_3$) 0.26.

Preparation of 3,4,4'-trimethoxythiobenzanilide (38b)

Compound 38a (4.00g, 0.0139M) was reacted with Lawesson's reagent according to the general method. Recrystallization from methanol gave yellow needle crystals (3.51g, 83%); m.p. 149-151°C; M+, 303; λ max. (nujol) 3160, 1590, 1500, 1250, 1220, 1020, 840, 700 cm^{-1}; δ ($CDCl_3$) (60MHz) 11.35 (1H,s), 7.80 (2H,d), 6.80-7.55 (5H,m), 3.80 (9H,t) ppm; ν max. (EtOH) 235, 328; ν max. (EtOH + NaOH) 241, 270; Rf ($CHCl_3$) 0.24.

Preparation of 2-(4-methoxyphenyl)-5,6-dimethoxy-benzothiazole (38c)

Compound 38b (1.00g, 0.0033M) was reacted with potassium ferricyanide according to the general method. Recrystallization from methanol gave cream needle crystals (0.90g, 91%), m.p. 159-160°C; M+, 301; found C, 63.67 H, 5.04 N, 4.73% ($C_{16}H_{15}NO_3S$ requires C, 63.81 H, 4.98, N, 4.65%); λ max. (KBr) 1590, 1280, 1240, 1210, 1150, 830 cm^{-1} ; δ ($CDCl_3$) (300MHz) 7.93 (2H,d), 7.49 (1H,s), 7.25 (1H,s), 6.94 (2H,d), 3.84 (9H,t) ppm; ν max. (EtOH) 239, 354; Rf ($CHCl_3$ + 2% EtOH) 0.32.

Preparation of 2-(4-hydroxyphenyl)-5,6-dihydroxy-benzothiazole (38d)

Compound 38c (0.85g, 0.00282M) was reacted with borom tribromide 1.0M in dichloromethane (17.0ml) according to general method A. Purification was by flash column

chromatography using 90% ethyl acetate, 9.9% methanol and 0.1% citric acid which gave a impure yellow solid (0.26g, 36%), m.p. >335°C; M+, 316 (285, 273, 259); $\lambda_{max.}$ (nujol) 3300 (broad), 1575, 1290, 1250, 1160, 955, 820 cm^{-1}; δ (DMSO-D_6) (300MHz) 9.88 (1H,s) (exchanges with D_2O), 9.38 (2H,d) (exchanges with D_2O), 7.79 (2H,d), 7.28 (2H,s), 6.87 (2H,d) ppm; $\nu_{max.}$ (EtOH) 239, 354; Rf ($CHCl_3$ + 2% EtOH) 0.00, 0.35.

Preparation of 4,4'-dimethoxybenzanilide (40a)

4-Methoxyaniline (36.18g, 0.294M) was reacted with 4-methoxybenzoyl chloride (50.00g, 0.294M) according to the general method. Recrystallization from methanol gave grey plate crystals (68.04g, 90%); m.p. 201-202°C (lit. 200-201°C[117]); M+, 273; $\lambda_{max.}$ (nujol) 3310, 1630, 1590, 1500, 1235, 1215, 1020, 820 cm^{-1}; δ (DMSO-D_6) (60MHz) 10.00 (1H,s), 8.00 (2H,d), 7.70 (2H,d), 7.00 (3H,t), 3.80 (6H,d) ppm; Rf ($CHCl_3$) 0.21.

Preparation of 4,4'-dimethoxythiobenzanilide (40b)

Compound 40a (10.00g, 0.0389M) was reacted with Lawesson's reagent according to the general method. Recrystallization from ethanol gave a yellow powder (9.22g, 89%); m.p. 151-152°C (lit. 157°C[118]); M+, 273; max. (nujol) 3120, 2960, 1590, 1500, 1340, 1230, 1160, 1010, 980, 835 cm^{-1}; δ ($CDCl_3$) (60MHz) 8.85 (1H,s), 6.65-

7.90 (8H,m), 3.75 (6H,d) pm; ν max. (EtOH) 226, 288; νmax. (EtOH + NaOH) 227; Rf ($CHCl_3$ + 2% EtOH) 0.35.

Preparation of 2-(4-methoxyphenyl)-6-methoxybenzothiazole (40c)

Compound 40c (2.00g, 0.00733M) was reacted with potassium ferricyanide according to the general method. Recrystallization from methanol gave cream needle crystals (1.42g, 71%), m.p. 156-158°C (lit. 163°C[115]); M+, 271; λ max. (KBr) 1600, 1460, 1255, 1220, 1015, 830 cm^{-1}; δ ($CDCl_3$) (300MHz) 7.95 (3H,m), 7.31 (1H,d), 6.97 (3H,m), 3.86 (6H,d) ppm; ν max. (EtOH) 217, 324; Rf ($CHCl_3$) 0.41.

Preparation of 2-(4-hydroxyphenyl)-6-hydroxybenzothiazole (40d)

Compound 40c (1.63g, 0.006M) was reacted with boron tribromide (30.0ml, 1.0M in dichloromethane) according to method A. Recrystallization from methanol gave a beige powder (0.95g, 65%), m.p. 275-276°C; found C, 64.05; H, 3.60; N, 5.56% ($C_{13}H_9NO_2S$ requires C, 64.20; H, 3.70; N, 5.76%); M+, 243.; λ max. (d.r.)§ (KBr) 3350, 1600, 1260, 1225, 840, 580, 520 cm^{-1}; δ (DMSO-D_6) (300MHz) 9.96 (2H,s), 7.76 (1H,d), 7.36 (1H,s), 6.98 (1H,d), 6.93 (2H,d) ppm; (DMSO-D_6 + D_2O) (300MHz) 7.83 (2H,d), 7.77 (1H,d), 7.34 (1H,s), 6.93 (1H,d), (6.88) (2H,d) ppm; ν max. (EtOH) 228, 275, 327; ν max. (EtOH + NaOH) 228, 274, 358; R_f ($CHCl_3$ + 5% MeOH) 0.33.

Preparation of 4,3'-dimethoxybenzanilide (41a)

4-Methoxyaniline (9.04g, 0.0735M) was reacted with 4-methoxybenzoyl chloride (12.50g, 0.0735M) according to the general method. Recrystallization from methanol gave large grey needle crystals (17.03g, 90%); m.p. 107-108°C (lit. 114°C[119]); λ max. (nujol) 3300, 1640, 1580, 1520, 1320, 1240, 1030, 810 cm^{-1}; δ ($CDCl_3$) (60MHz) 8.10 (1H,s), 6.70-7.55 (8H,m), 3.80 (6H,s) ppm; Rf ($CHCl_3$ + 2% EtOH) 0.34.

Preparation of 4,3'-dimethoxythiobenzanilide (41b)

Compound 41a (10.00g, 0.0389M) was reacted with Lawesson's reagent according to the general method. Water (50ml) was added to the reaction mixture and shaken periodically. After 5 days the precipitate was filtered and washed as far as possible with water. Recrystallization from methanol gave yellow crystals (5.05g, 47%); m.p. 75-76°C; found C, 64.29; H, 5.56; N, 4.70% ($C_{15}H_{15}NO_2S.\frac{1}{2}CH_3OH$ requires C, 64.36; H, 5.54; N, 4.84%); λ max. (nujol) 3120, 1580, 1500, 1240, 1030, 800, 710, 680 cm^{-1}; δ ($CDCl_3$) (60MHz) 9.00 (1H,s), 6.70-7.60 (8H,m), 3.80 (6H,s) ppm; ν max. (EtOH) 226, 275, ν max. (EtOH + NaOH) 226, 280; Rf ($CHCl_3$ + 2% EtOH) 0.50.

Preparation of 2-(3-methoxyphenyl)-6-methoxybenzothiazole (41c)

Compound 41b (2.50g, 0.00916M) was reacted with potassium ferricyanide according to the general method. Recrystallization from methanol gave beige crystals (1.75g, 71%), m.p. 98-99°C; M+, 271; found C, 66.29; H, 4.66; N, 5.33% ($C_{15}H_{13}NO_2S$ requires C, 66.42 H, 4.79, N, 5.17%); λ max. (KBr) 1600, 1520, 1290, 1270, 1220, 1170 cm^{-1}; δ ($CDCl_3$) (300MHz) 7.93 (1H,d), 7.57 (2H,m), 7.35 (1H,m), 7.05 (1H,d), 6.97 (1H,m), 3.87 (6H,d) ppm; ν max. (EtOH) 225, 325; Rf ($CHCl_3$ + 2% EtOH) 0.57.

Preparation of 2-(3-hydroxyphenyl)-6-hydroxybenzothiazole (41d)

Compound 41c (0.75g, 0.00277M) was reacted with boron tribromide 1.0M in dichloromethane (16.6ml) according to method A. Purification by flash column chromatography (10% methanol, 90% dichloromethane) gave a beige powder (0.49g, 73%), m.p. 200-201°C; M+, 243.0354000 gives $C_{13}H_9NO_2S$; λ max. (d.r.)$^{\Delta}$ 3230, 1600, 1567, 1517, 1433, 1283, 850, 685 cm^{-1}; δ (DMSO-D_6) (300MHz) 9.89 (1H,s), 9.83 (1H,s), 7.82 (1H,d), 7.34 (4H,m), 6.97 (1H,d), 6.88 (1H,d) ppm; δ (DMSO-D_6 + D_2O) (300MHz) 7.82 (1H,d), 7.34 (4H,m), 6.97 (1H,d), 6.88 (1H,d) ppm; ν max. (EtOH) 225, 324; ν max. (EtOH + NaOH) 222, 354; R_f ($CHCl_3$ 10% EtOH) 0.47.

Preparation of 3,4'-dimethoxybenzanilide (42a)

3-Methoxyaniline (10.00g, 0.0813M) was reacted with 4-methoxybenzoyl chloride (13.82g, 0.0813M) according to the general method. Recrystallization from methanol gave off-white needle crystals (17.22g, 82%); m.p. 135-136°C (lit. 144°C[119]); M+, 257; λ max. (nujol) 3260, 1600, 1280, 1250, 1180, 1020, 840 cm^{-1}; δ ($CDCl_3$) (60MHz) 6.80-8.10 (9H,m), 3.80 (3H,s) ppm; δ ($CDCl_3$ + D_2O) (60MHz) 6.80-8.00 (8H,m), 3.80 (3H,s) ppm; Rf ($CHCl_3$ + 2% EtOH) 0.38.

Preparation of 3,4'-dimethoxythiobenzanilide (42b)

Compound 42a (8.00g, 0.0311M) was reacted with Lawesson's reagent according to the general method. The solid formed after addition of water and a few drops of methanol to the reaction mixture was filtered off. The oily solid still heavily contaminated with chlorobenzene was purified by dry column chromatography with chloroform as solvent. Recrystallization from methanol gave a yellow powder (2.00g, 24%); m.p. 98-99°C; M+, 273; λ max. (d.r.)* (KBr) 3157, 1600, 1507, 1302, 1257, 1176, 842, 720 cm^{-1}; δ (DMSO-D_6) (300MHz) 11.52 (1H,s) (exchanges with D_2O), 7.85 (2H,d), 7.55 (1H,s), 7.34 (2H,m), 6.99 (2H,d), 6.83 (1H,d), 3.82 (3H,s), 3.75 (3H,s) ppm; ν max. (EtOH) 224, 285, ν max. (EtOH + NaOH) 224; Rf ($CHCl_3$ + 2% EtOH) 0.50.

Preparation of 2-(4-methoxyphenyl)-5-methoxybenzothiazole (42c) and 2-(4-methoxyphenyl)-7-methoxybenzothiazole ($42c^{i}$)

Compound 42b (1.50g, 0.00549M) was reacted with potassium ferricyanide according to the general method. Recrystallization from ethanol gave a mixture of the two compounds which were separated by flash column chromatography using dichloromethane as solvent.

Fractions 8-19 gave off-white crystals of 2-(4-methoxyphenyl)-7-methoxybenzothiazole ($42c^{i}$) (0.44g, 29%); m.p. 140-141°C ; M+, 271; found C, 66.07 H, 4.73 N, 5.08%; $C_{15}H_{13}NO_2S$ requires C, 66.42 H, 4.80, N, 5.17%; λ max. (d.r.)* (KBr) 2790, 1606, 1565, 1482, 1254, 1170, 1036, 840, 773 cm^{-1}; δ ($CDCl_3$) (300MHz) 8.03 (2H,d), 7.84 (1H,d), 7.38 (1H,t), 6.96 (2H,d), 6.79 (1H,d), 3.95 (6H,d) ppm; ν max. (EtOH) 220, 266, 309; Rf (CH_2Cl_2) 0.38.

Fractions 22-36 gave a white powder of 2-(4-methoxyphenyl)-5-methoxybenzothiazole (42c) (0.34g, 23%); m.p. 120-121°C ; M+, 271; found C, 66.10 H, 4.77 N, 5.06% ($C_{15}H_{13}NO_2S$ requires C, 66.42 H, 4.80, N, 5.17%); λ max. (d.r.)* (KBr) 2958, 1598, 1464, 1258, 1161, 1026, 830, 806 cm^{-1}; δ ($CDCl_3$) (300MHz) 8.03 (2H,d), 7.73 (1H,d), 7.56 (1H,s), 7.02 (3H,m), 3.91 (6H,d) ppm; ν max. (EtOH) 226, 298, 335; Rf (CH_2Cl_2) 0.30.

Preparation of 2-(4-hydroxyphenyl)-5-hydroxybenzothiazole (42d)

Compound 42c (1.00g, 0.00369M) was reacted with boron tribromide 1.0M in dichloromethane (21.0ml) according to method A. Removal of solvent gave a yellow powder (0.70g, 80%), m.p. 234-235°C; M+, 243.0354000 gives $C_{13}H_9NO_2S$; λ max. (d.r.)* (KBr) 3364, 1594, 1455, 1254, 1169, 982, 830 cm^{-1}; δ (DMSO-D_6) (300MHz) 10.19 (1H,d), 9.71 (1H,s), 7.87 (2H,d), 7.70 (1H,d), 7.31 (1H,s), 6.90 (3H,q) ppm; δ (DMSO-D_6 + D_2O) (300MHz) 7.85 (2H,d), 7.77 (2H,d), 7.30 (1H,s), 6.88 (3H,q) ppm; R_f ($CHCl_3$ + 10% EtOH) 0.44.

Preparation of 2,4,4'-trihydroxyazobenzene (46)

4-Hydroxyaniline (1.00g, 0.00917M) was diazotised by reaction with sodium nitrite (0.70g, 0.0101M) in 5N hydrochloric acid (10ml) at -10°C. To a cooled solution of resorcinol (1.00g, 0.00917M) in 10% $^{w}/_{v}$ sodium hydroxide (20ml) the diazotised amine was added dropwise. The solid produced was filtered off and recrystallization from methanol/water (1:1). Purification by flash column chromatography using 5%$^{v}/_{v}$ methanol in chloroform as solvent gave a red solid (0.45g, 21%); m.p. 241-242°C (lit. 226°C[120]; M+ 230; λ max. (d.r.)* (KBr) 3450, 3227, 1592, 1473, 1251, 1195, 1119, 835 cm^{-1}; δ (DMSO-D_6) (300MHz) 12.46 (1H,s), 10.23 (1H,s), 7.72 (2H,d), 7.60 (1H,d), 6.89 (2H,d), 6.46 (1H,d), 6.31 (1H,s) ppm; δ

(DMSO-D_6 + D_2O) (300MHz) 7.72 (2H,d), 7.60 (1H,d), 6.89 (2H,d), 6.46 (1H,d) ppm; R_f ($CHCl_3$ + 10% EtOH) 0.53.

Preparation of 3,4-dimethoxybenzoyl chloride (47)

3,4-Dimethoxy benzoic acid (31.90g, 0.160M) was refluxed in excess thionyl chloride (2h). The excess thionyl chloride was distilled off. Recrystallization of the residue from petrolium ether (b.p. 80-90°C) gave white needle crystals (26.03g, 74%), m.p. 158-159°C (lit 141-144°C [121]; M+, 243.; λ max. (nujol) 1680, 1590, 1515, 1270, 1025, 755 cm^{-1}; δ ($CDCl_3$) (60MHz) 7.60 (2H,m), 6.85 (1H,d), 3.90 (6H,s) ppm; R_f ($CHCl_3$ + 2% EtOH) 0.19.

Preparation of 2-methoxybenzanilide (49a)

2-Methoxyaniline (10.00g, 0.0813M) was reacted with benzoyl chloride (11.38g, 0.0813M) according to the general method. Recrystallization from ethanol gave a pink powder (14.72g, 80%); m.p. 55-56°C (lit. 66-67°C[122]); λ max. (nujol) 3320, 1630, 1490, 1020, 740, 700 cm^{-1}; δ ($CDCl_3$) (60MHz) 8.40 (2H,m), 7.80 (2H,m), 7.40 (3H,m), 6.80 (3H,m), 3.80 (3H,s) ppm; δ ($CDCl_3$ + D_2O) (60MHz) 8.40 (1H,m), 7.80 (2H,m), 7.40 (3H,m), 6.80 (3H,m), 3.80 (3H,s) ppm; Rf ($CHCl_3$ + 2% EtOH) 0.55.

Preparation of 2-methoxythiobenzanilide (49b)

Compound 49a (10.00g, 0.0440M) was reacted with Lawesson's reagent according to the general method.

Recrystallization from methanol gave yellow cubic crystals (8.16g, 76%); m.p. 121-122°C (lit. 76°C[123]); M+, 243; λ max. (nujol) 3100, 1580, 1520, 1240, 1180, 1010, 760, 715, 670 cm^{-1}; δ ($CDCl_3$) (60MHz) 8.40 (1H,d), 6.80-7.85 (9H,m), 3.90 (3H,s) ppm; ν max. (EtOH) 223, 312; ν max. (EtOH + NaOH) 223, 277; Rf ($CHCl_3$ + 2% EtOH) 0.69.

Preparation of 4-methoxy-2-phenylbenzothiazole (49c)

Compound 49b (5.00g, 0.0206M) was reacted with potassium ferricyanide according to the general method. Recrystallization from methanol gave cream plate crystals (3.78g, 76%), m.p. 103-104°C; M+, 241; λ max. (Nujol) 1580, 1280, 1240, 1110, 1010, 940, 740, 720 cm^{-1}; δ ($CDCl_3$) (60MHz) 8.53 (1H,d), 9.10 (1H,d), 7.91 (1H,d), 7.44 (3H,m), 7.13 (1H,t), 7.03 (1H,d), 4.02 (3H,s) ppm; ν max. (EtOH) 226, 257, 322; Rf ($CHCl_3$ + 2% EtOH) 0.65.

Preparation of 3-methoxybenzanilide (50a)

3-Methoxyaniline (10.00g, 0.0813M) was reacted with benzoyl chloride (11.38g, 0.0813M) according to the general method. Recrystallization from methanol gave an off-white powder (16,58g, 90%); m.p. 111°C (lit. 111°C[124]); λ max. (nujol) 3300, 1645, 1600, 1520, 1490, 1410, 1270, 1040, 830, 770 cm^{-1}; δ ($CDCl_3$) (60MHz) 9.15 (1H,s), 7.80 (2H,m), 7.20 (6H,m), 6.70 (1H,m), 3.75 (3H,s) ppm; Rf ($CHCl_3$ + 2% EtOH) 0.42.

Preparation of 3-methoxythiobenzanilide (50b)

Compound 50a (6.02g, 0.0265M) was reacted with Lawesson's reagent according to the general method. Recrystallization from methanol/water (1:1) gave lime green crystals (4.02g, 62%); m.p. 81-82°C; found C, 69.08; H, 5.57; N, 5.81% ($C_{14}H_{13}NOS$ requires C, 69.14; H, 5.35; N, 5.76%); M+, 243; λ max. (nujol) 3120, 1605, 1580, 1520, 1260, 1150, 1040, 700 cm^{-1}; δ ($CDCl_3$) (60MHz) 9.05 (1H,s), 6.55-7.90 (9H,m), 3.70 (3H,s) ppm; ν max. (EtOH) 223, 320; ν max. (EtOH + NaOH) 227, 280; Rf ($CHCl_3$ + 2% EtOH) 0.52.

Preparation of 4-methoxybenzanilide (51a)

4-Methoxyaniline (5.00g, 0.0407M) was reacted with benzoyl chloride (5.70g, 0.0407M) according to the general method. Recrystallization from methanol gave off-white plate crystals (7.66g, 83%); m.p. 155-157°C (lit. 157°C[125]); M+, 227; λ max. (nujol) 3310, 1630, 1500, 1240, 1030, 820cm^{-1}; δ (DMSO-D_6) (60MHz) 10.10 (1H,s), 9.95 (2H,d), 7.30-8.15 (7H,m), 3.75 (3H,s) ppm; Rf ($CHCl_3$) 0.44.

Preparation of 4-methoxythiobenzanilide (51b)

Compound 51a (6.50g, 0.0286M) was reacted with Lawesson's reagent according to the general method. Recrystalization from methanol gave yellow plate crystals (5.5g, 79%); m.p. 131-133°C (lit. 133°C[126]); M+, 243;

$\lambda_{max.}$ (nujol) 3150, 1600, 1500, 1240, 1020, 970, 740, 680 cm^{-1}; δ ($CDCl_3$) (60MHz) 9.00 (1H,s), 7.25-7.90 (7H,m), 6.85 (2H,d), 3.80 (3H,s) ppm; $\nu_{max.}$ (EtOH) 234, 273, 325, $\nu_{max.}$ (EtOH + NaOH) 230, 283; Rf ($CHCl_3$) 0.39.

Preparation of 2-phenyl-6-methoxybenzothiazole (51c)

Compound 51b (4.50g, 0.0185M) was reacted with potassium ferricyanide according to the general method. Recrystallization from methanol gave cream needle crystals (3.26g, 73%), m.p. 114-115°C (lit. 117°C[127]); M+, 241; $\lambda_{max.}$ (nujol) 1590, 1260, 1220, 1020, 800 cm^{-1}; δ ($CDCl_3$) (300MHz) 8.01 (2H,m), 7.93 (1H,d), 7.46 (3H,m), 7.32 (1H,s), 7.07 (1H,d), 3.98 (3H,s) ppm; $\nu_{max.}$ (EtOH) 230, 270, 322; Rf ($CHCl_3$ + 2% EtOH) 0.60.

Preparation of 2-phenyl-6-hydroxybenzothiazole (51d)

Compound 51c (1.00g, 0.00415M) was reacted with boron tribromide 1.0M in dichloromethane (16.6ml) according to method A. Recrystallization from methanol gave white cubic crystals (0.47g, 50%), m.p. 223-224°C; found C, 68.43; H, 3.89; N, 6.04%; $C_{13}H_9NOS$ requires C, 68.72; H, 3.96; N, 6.17%; M+, 227; $\lambda_{max.}$ (nujol) 3200, 1590, 1280, 1230, 960, 830, 750 cm^{-1}; δ (DMSO-D_6) (300MHz) 7.99 (2H,m), 7.86 (1H,d), 7.51 (5H,m), 7.00 (1H,d) ppm; (DMSO-D_6 + D_2O) (300MHz) 7.96 (2H,m), 7.83 (1H,d), 7.49 (4H,m), 6.98 (1H,d) ppm; $\nu_{max.}$ (EtOH) 228, 271, 323; $\nu_{max.}$ (EtOH + NaOH) 225, 280, 359; R_f ($CHCl_3$ + 5% MeOH) 0.43.

Preparation of 3'-methoxybenzanilide (52a)

Aniline (6.84g, 0.0735M) was reacted with 3-methoxybenzoyl chloride (12.50g, 0.0735M) according to the general method. Recrystallization from methanol gave an off white powder (15.73, 94%); m.p. 119-120°C (lit. 120°C[119]); λ max. (nujol) 3240, 1640, 1600, 1520, 1490, 1320, 1040, 750 cm^{-1}; δ ($CDCl_3$) (60MHz) 8.10 (1H,s), 6.90-7.70 (9H,m), 3.70 (3H,s) ppm; Rf ($CHCl_3$) 0.19.

Preparation of 3'-methoxythiobenzanilide (52b)

Compound 52a (10.00g, 0.0441M) was reacted with Lawesson's reagent according to the general method. Recrystallization from methanol gave large yellow needle crystals (7.93g, 74%); m.p. 93-96°C (lit. 97-98°C[123]); λ max. (nujol) 3150, 1590, 1500, 1310, 1260, 1190, 1030, 840, 700, 680 cm^{-1}; δ ($CDCl_3$) (60MHz) 9.10 (1H,s), 6.80-7.80 (9H,m), 3.80 (3H,s) ppm; ν max. (EtOH) 230, 282, 311, $\nu_{max.}$ (EtOH + NaOH) 228; Rf ($CHCl_3$) 0.43.

Preparation of 2-(3-methoxyphenyl)benzothiazole (52c)

Compound 52b (5.00g, 0.0206M) was reacted with potassium ferricyanide according to the general method. Recrystallization from methanol gave a yellow powder crystals (3.95g, 80%), m.p. 81-82°C (lit. 82-83°C[128]); M+, 241; λ max. (Nujol) 1600, 1570, 1430, 1280, 1260, 1040, 990, 880, 740, 710, 680 cm^{-1}; δ ($CDCl_3$) (300MHz) 8.08 (1H,d), 7.88 (1H,d), 7.63 (2H,t), 7.48 (1H,t), 7.36

(2H,t), 7.01 (1H,d) ppm; ν max. (EtOH) 225, 295; Rf ($CHCl_3$ + 2%, EtOH) 0.60.

Preparation of 2,4'-dimethoxybenzanilide (53a)

2-Methoxyaniline (10.00g, 0.0813M) was reacted with 4-methoxybenzoyl chloride (13.82g, 0.0813M) according to the general method. Recrystallization from methanol gave off white needle crystals (19.70g, 94%); m.p. 91-92°C (lit. 99-100°C[119]); λ max. (nujol) 3320, 1650, 1600, 1500, 1250, 1170, 1020, 840, 740, 610 cm^{-1}; δ ($CDCl_3$) (60MHz) 8.50 (2H,m), 7.80 (2H,d), 6.90 (5H,m), 3.85 (3H,s) ppm; Rf ($CHCl_3$ + 2% EtOH) 0.38.

Preparation of 2,4'-dimethoxythiobenzanilide (53b)

Compound 53a (10.00g, 0.0389M) was reacted with Lawesson's reagent according to the general method. Dry column chromatography using chloroform as eluent followed by recrystallization from ethanol gave yellow crystals (2.67g, 25%); m.p. 69-71°C; M+, 273; λ max. (nujol) 3200, 1580, 1340, 1240, 1170, 1025, 830, 730 cm^{-1}; δ ($CDCl_3$) (60MHz) 9.50 (1H,s), 8.9 (1H,s), 7.85 (2H,d), 6.95 (5H,m), 3.90 (6H,d) ppm; ν max. (EtOH) 224, 283; ν max. (EtOH + NaOH) 226; Rf ($CHCl_3$ + 2% EtOH) 0.57.

Preparation of 3,4-dimethoxybenzanilide (54a)

3,4-Methoxyaniline (5.00g, 0.0327M) was reacted with benzoyl chloride (4.58g, 0.0327M) according to the general

method. Recrystallization from methanol gave off-white crystals (6.98g, 83%); m.p. 177-178°C; M+, 257; λ max. (nujol) 3220, 1630, 1590, 1500, 1400, 1220, 1020, 830, 800, 700 cm^{-1}; δ (DMSO-D_6) (60MHz) 10.10 (1H,s), 7.95 (2H,q), 7.45 (5H,m), 6.90 (1H,d), 3.70 (3H,s) ppm; Rf ($CHCl_3$) 0.14.

Preparation of 3,4-dimethoxythiobenzanilide (54b)

Compound 54a (2.50g, 0.00923M) was reacted with Lawesson's reagent according to the general method. Recrystallization from methanol gave yellow plate crystals (1.90g, 75%); m.p. 154°C; found C, 66.21; H, 5.53; N, 5.27% ($C_{15}H_{14}NO_2S$ requires C, 65.94; H, 5.49; N, 5.12%); M+, 273; λ max. (nujol) 3140, 1590, 1500, 1260, 1220, 1130, 1020, 1000, 790, 690 cm^{-1}; δ ($CDCl_3$) (60MHz) 9.05 (1H,s), 6.70-7.90 (8H,m), 3.75 (6H,s) pm; ν max. (EtOH) 237, 277, 333, ν max. (EtOH + NaOH) 238, 287; Rf ($CHCl_3$ + 2% EtOH) 0.41.

Preparation of 2-pheny-5,6-dimethoxybenzothiazole (54c)

Compound 54b (1.50g, 0.00549M) was reacted with potassium ferricyanide according to the general method. Recrystallization from methanol gave cream needle crystals (0.59g, 40%), m.p. 142-144°C (lit. 152°C[129]); M+, 271; $\lambda_{max.}$ (Nujol) 1290, 1220, 1000, 820 cm^{-1}; δ ($CDCl_3$) (300MHz) 8.01 (2H,m), 7.53 (1H,s), 7.45 (3H,m), 7.28

(1H,s), 3.86 (6H,d) ppm; ν max. (EtOH) 236, 272, 335; Rf ($CHCl_3$ + 2% EtOH) 0.46.

Preparation of 3,5-dimethoxybenzanilide (55a)

3,5-Dimethoxyaniline (10.00g, 0.0653M) was reacted with benzoyl chloride (9.15g, 0.0653M) according to the general method. Recrystallization from methanol gave off-white crystals (16.01g, 95%); m.p. 134-135°C; λ max. (nujol) 3220, 1645, 1590, 1420, 1280, 1200, 1150, 1050, 820, 700 cm^{-1}; δ ($CDCl_3$) (60MHz) 8.00 (1H,s), 7.75 (2H,m), 7.40 (3H,m), 6.80 (2H,d), 6.20 (1H,t), 3.70 (3H,s) ppm; Rf ($CHCl_3$ + 2% EtOH) 0.30.

Preparation of 3,5-dimethoxythiobenzanilide (55b)

Compound 55a (7.00g, 0.0272M) was reacted with Lawesson's reagent according to the general method. Recrystallization from methanol gave yellow plate crystals (5.48g, 74%); m.p. 135-136°C; M+, 273; λ max. (nujol) 3200, 3090, 1600, 1320, 1150, 1060, 715, 700 cm^{-1}; δ ($CDCl_3$) (60MHz) 8.95 (1H,s), 7.75 (2H,m), 7.40 (3H,m), 6.90 (2H,m), 6.30 (1H,m), 3.75 (6H,s) ppm; ν max. (EtOH) 220, 267, 330; ν max. (EtOH + NaOH) 228; Rf ($CHCl_3$) 0.39.

Preparation of 2,4,4'-trimethoxybenzanilide (56a)

2,4-Dimethoxyaniline (10.22g, 0.0650M) was reacted with 4-methoxybenzoyl chloride (11.11g, 0.0650M) according to the general method. Recrystallization from

methanol gave off-white needle crystals (15.73g, 82%); m.p. 124°; found C, 66.65; H, 6.04; N, 4.85%; $C_{16}H_{17}NO_4$ requires C, 66.90; H, 5.92; N, 4.88%; M^+, 287; λ max. (nujol) 3320, 1630, 1600, 1500, 1250, 1200, 1030, 820 cm^{-1}; δ ($CDCl_3$) (60MHz) 8.40 (1H,s), 8.25 (1H,s), 7.80 (2H,d), 6.90 (2H,d) 6.45 (2H,m), 3.80 (9H,t) ppm; Rf ($CHCl_3$) 0.12.

Preparation of 2,4,4'-trimethoxythiobenzanilide (56b)

Compound 56a (5.00g, 0.0174M) was reacted with Lawesson's reagent according to the general method. Water (50ml) was added to the reaction mixture and shaken periodically. After 3 days the precipitate was filtered and washed as far as possible with water. Recrystallization from methanol gave yellow crystals (2.28g, 43%); m.p. 103-104°C; found C, 63.11, H, 5.41; N, 4.50% ($C_{16}H_{17}NO_3S$ requires C, 63.37; H, 5.61; N, 4.62%); M+, 303; λ max. (nujol) 3380, 1590, 1500, 1380, 1350, 1270, 1030, 810 cm^{-1}; δ ($CDCl_3$) (60MHz) 9.25 (1H,s), 8.80 (1H,d), 7.80 (2H,d), 6.80 (2H,d), 6.45 (2H,m), 3.80 (9H,t) ppm; ν max. (EtOH) 224, 291, ν max. (EtOH + NaOH) 225; Rf ($CHCl_3$) 0.23.

Preparation of 2-(4-methoxyphenyl)-4,6-dimethoxy-benzothiazole (56c)

Compound 56b (1.60g, 0.00528M) was reacted with potassium ferricyanide according to the general method.

Recrystallization from methanol gave a yellow solid (1.04g, 66%), m.p. 123-124°C; M+, 301; found C, 63.61 H, 4.90 N, 4.58%; $C_{16}H_{15}NO_3S$ requires C, 63.67; H, 5.04; N, 4.73%; λ max. (d.r.)* (KBr) 3020, 1609, 1571, 1525, 1272, 129, 1210, 1150, 1036, 826 cm^{-1}; δ ($CDCl_3$) (300MHz) 7.97 (2H,d), 6.87 (2H,d), 6.88 (1H,s), 6.51 (1H,s), 4.01 (3H,s), 3.87 (6H,d) ppm; ν max. (EtOH) 225, 286, 320; Rf ($CHCl_3$ + 2% EtOH) 0.51.

Preparation of 2-(4-hydroxyphenyl)-4,6-dihydroxy-benzothiazole (56d)

Compound 56c (0.50g, 0.00166M) was reacted with boron tribromide 1.0M in dichloromethane (10.0ml) according to method A. Recrystallization from methanol gave a beige solid (0.22g, 51%), m.p. 236-237°C; M+, 259.0303 gives $C_{13}H_9NO_3S$; λ max. (d.r)* (KBr) 3381, 1614, 1585, 1452, 1305, 1216, 1172, 1005, 843 cm^{-1}; δ ($DMSO-D_6$) (300MHz) 9.95 (2H,broad s), 9.55 (1H, broad s), 7.79 (2H,d), 6.87 (2H,d), 6.76 (1H,s), 6.37 (1H,s) ppm; δ ($DMSO-D_6$ + D_2O) (300MHz) 7.79 (2H,d), 6.87 (2H,d), 6.76 (1H,s), 6.37 (1H,s) ppm; R_f ($CHCl_3$ + 10% MeOH) 0.31.

Preparation of 3',4,4'-trimethoxybenzanilide (57a)

4-methoxyaniline (6.00g,0.0488M) was reacted with 3,4-dimethoxybenzoyl chloride (47) (9.76g, 0.0407M) according to the general method. Recrystallization from methanol gave off-white needle crystals (10.83g, 77%);

m.p. 180°C; found C, 66.82; H, 6.17; N, 4.93% ($C_{16}H_{17}NO_4$ requires C, 66.90; H, 5.92; N, 4.88%); M+, 287; $\lambda_{max.}$ (nujol) 3300, 1640, 1600, 1500, 1260, 1170, 1020, 800 cm^{-1}; δ ($CHCl_3$) (60MHz) 8.10 (1H,s), 7.40 (4H,m), 6.75 (3H,m), 3.80 (9H,t) ppm; Rf ($CHCl_3$ + 2% EtOH) 0.29.

Preparation of 3',4,4'-trimethoxythiobenzanilide (57b)

Compound 57a (5.00g, 0.01742M) was reacted with Lawesson's reagent according to the general method. Recrystallization from methanol gave a yellow solid (4.58g, 87%); m.p. 154-155°C; found C, 63.27; H, 5.51; N, 4.57% ($C_{16}H_{17}NO_3S$ requires C, 63.37; H, 5.61; N, 4.62%); M+, 303; $\lambda_{max.}$ (d.r.)* (KBr) 3156, 2992, 1597, 1510, 1269, 1168, 1144, 1024, 815 cm^{-1}; δ ($CDCl_3$) (60MHz) 9.00 (1H,s), 6.70-7.70 (7H,m), 3.85 (9H,d) ppm; $\nu_{max.}$ (EtOH) 230, 310; $\nu_{max.}$ (EtOH + NaOH) 228; Rf ($CHCl_3$ + 2% EtOH) 0.38.

Preparation of 2-(3,4-dimethoxyphenyl)-6-methoxy-benzothiazole (57c)

Compound 57b (4.00g, 0.0132M) was reacted with potassium ferricyanide according to the general method. Recrystallization from methanol gave cream needle crystals (3.42g, 86%), m.p. 123-124°C; M+, 301; found C, 63.61; H, 5.01; N, 4.73% ($C_{16}H_{15}NO_3S$ requires C, 63.79; H, 4.98; N, 4.65%); $\lambda_{max.}$ (nujol) 1580, 1260, 1240, 1220, 1190, 1010, 830 cm^{-1}; δ ($CDCl_3$) (300MHz) 7.89 (1H,d), 7.64 (1H,s),

7.51 (1H,d), 7.30 (1H,s), 7.05 (1H,d), 6.91 (1H,d), 3.99 (3H,s), 3.93 (3H,s), 3.86 (3H,s) ppm; ν max. (EtOH) 225, 332; Rf ($CHCl_3$ + 2% EtOH) 0.46.

Preparation of 2-(3,4-dihydroxyphenyl)-6-hydroxy-benzothiazole (57d)

Compound 57c (1.00g, 0.00332M) was reacted with boron tribromide 1.0M in dichloromethane (20.0ml) according to method A. Separation using flash column chromatography (solvent 80% dichloromethane, 10% methanol) gave a beige solid crystals (0.18g, 21%), m.p. 261-265°C with decomposition; found C, 57.52; H, 3.94; N, 5.15%; $C_{13}H_9NO_3S.CH_3OH$ requires C, 57.73; H, 4.12; N, 4.81%; M+, 259.0303 gives $C_{13}H_9NO_3S$; λ max. (d.r.)* (KBr) 3558, 3324, 1599, 1566, 1536, 1434, 1295, 1277, 1216, 1122, 875, 813 cm^{-1}; δ (DMSO-D_6) (300MHz) 9.76 (1H,s), 9.57 (1H,s), 9.40 (1H,s), 7.73 (1H,d), 7.41 (1H,s), 7.33 (1H,s), 7.26 (1H,d), 6.92 (1H,d), 6.83 (1H,d) ppm; δ (DMSO-D_6 + D_2O) (300MHz) 7.73 (1H,d), 7.41 (1H,s), 7.33 (1H,s), 7.26 (1H,d), 6.92 (1H,d), 6.83 (1H,d) ppm; ν max. (EtOH) 225, 334; ν max. (EtOH + NaOH) 225, 267; R_f (CH_2Cl_2 + 20% MeOH) 0.66.

Preparation of 2,3'4,4'-tetramethoxybenzanilide (58a)

4-Methoxyaniline (8.00g, 0.0522M) was reacted with 3,4-dimethoxybenzoyl chloride (47) (10.45g, 0.0407M) according to the general method. Recrystallization from

methanol gave off-white needle crystals (10.34g, 62%); m.p. 120°C; M+, 317; λ max. (d.r.)$^{\Delta}$ (KBr) 3267, 2900, 1700, 1642, 1533, 1033, 767, 580 cm^{-1}; δ ($CHCl_3$) (60MHz) 8.30 (2H,d), 7.30 (2H,m), 6.80 (1H,d), 6.45 (2H,m), 3.80 (12H,q) ppm; δ ($CHCl_3$ + H_2O) (60MHz) 8.30 (1H,d), 7.30 (2H,m), 6.80 (1H,d), 6.45 (2H,m), 3.80 (12H,q) ppm; Rf ($CHCl_3$ + 2% EtOH) 0.43.

Preparation of 2,3',4,4'-tetramethoxythiobenzanilide (58b)

Compound 58a (7.00g, 0.0220M) was reacted with Lawesson's reagent according to the general method. Recrystallization from methanol gave yellow plate crystals (6.21g, 84%); m.p. 128-129°C; M+, 333; λ max. (d.r.)* (KBr) 3302, 1615, 1509, 1289, 1265, 1211, 1169, 1045, 788, 711 cm^{-1}; δ ($CDCl_3$) (60MHz) 9.30 (1H,s), 6.35-7.65 (6H,m), 3.85 (12H,q) ppm; Rf ($CHCl_3$ + 2% EtOH) 0.40.

Preparation of 2-(3,4-dimethoxyphenyl)-4,6-dimethoxybenzothiazole (58c)

Compound 58b (4.00g, 0.0120M) was reacted with potassium ferricyanide according to the general method B. Recrystallization from methanol gave orange powder (1.84g, 48%), m.p. 148-149°C; M+, 331; λ max. (d.r.)* (KBr) 1585, 1462, 1418, 1265, 1147, 1054, 1019, 808 cm^{-1}; δ (DMSO-D_6) (300MHz) 7.51 (2H,m), 7.20 (1H,s), 7.08 (1H,d), 6.64 (1H,s), 3.94 (3H,s), 3.87 (3H,s) ppm; Rf ($CHCl_3$ + 2% EtOH) 0.45.

Preparation of 2-(3,4-dihydroxyphenyl)-4,6-dihydroxy-benzothiazole (58d)

Compound 58c (0.50g, 0.00150M) was reacted with boron tribromide 1.0M in dichloromethane (18.2ml) according to method B. Removal of solvent gave a yellow solid crystals (0.20g, 48%), m.p. >330°C; MH+, 276.0330000 gives $C_{13}H_9NO_4S$; λ max. (d.r.)$^{\Delta}$ (KBr) 3200, 1600, 1275, 1065, 810 cm^{-1}; δ (DMSO-D_6) (300MHz) 9.43 (1H,broad s), 7.34 (1H,s), 7.16 (1H,t), 6.76 (1H,d), 6.68 (1H,s), 6.31 (1H,s), 3.90 (3H, broad s) ppm; δ (DMSO-D_6 + D_2O) (300MHz) 7.33 (1H,s), 7.18 (1H,d), 6.83 (1H,d), 6.69 (1H,s), 6.31 (1H,s) ppm; R_f ($CHCl_3$ + 10% EtOH) 0.11.

Preparation of 3,4,3',4'-tetramethoxybenzanilide (59a)

3,4-Dimethoxyaniline (8.00g, 0.0523M) was reacted with 3,4-dimethoxybenzoyl chloride (47) (10.45g, 0.0523M) according to the general method. Recrystallization from methanol gave white needle crystals (12.09g, 73%); m.p. 187-188°C; λ max. (nujol) 3300, 1640, 1600, 1500, 1270, 1230, 1020, 820, 790, 760 cm^{-1}; δ ($CDCl_3$) (60MHz) 7.80 (1H,s), 6.75-7.50 (6H,m), 3.90 (12H,d) ppm; Rf ($CHCl_3$ + 2% EtOH) 0.25.

Preparation of 3,3',4,4'-tetramethoxythiobenzanilide (59b)

Compound 59a (7.00g, 0.0221M) was reacted with Lawesson's reagent according to the general method. Recrystallization from methanol gave yellow needle

crystals (6.33g, 86%); m.p. 165-166°C; λ max. (nujol) 3140, 1590, 1500, 1400, 1260, 1130, 1020, 840, 790, 690 cm^{-1}; δ ($CDCl_3$) (60MHz) 9.05 (1H,s), 6.50-7.60 (6H,m), 3.80 (12H,d) ppm; ν max. (EtOH) 229, 312; ν max. (EtOH + NaOH) 225, 290; Rf ($CHCl_3$ + 2% EtOH) 0.32.

Preparation of 2-(3,4-dimethoxyphenyl)-5,6-dimethoxybenzothiazole (59c)

Compound 59b (5.00g, 0.0150M) was reacted with potassium ferricyanide according to the general method. Recrystallization from methanol gave cream needles crystals (2.35g, 47%), m.p. 176-177°C; M+, 331; found C, 61.76, H, 4.88, N, 4.21 ($C_{17}H_{17}NO_4S$ requires C, 61.63 H, 5.14, N, 4.23%); λ max. (nujol) 1590, 1515, 1410, 1265, 1230, 1145, 1005, 830 cm^{-1}; δ ($CDCl_3$) (300MHz) 7.62 (1H,s), 7.51 (2H,d), 7.26 (1H,s), 6.90 (1H,d), 3.97 (12H,q) ppm; ν max. (EtOH) 226, 273, 343; Rf ($CHCl_3$ + 2% EtOH) 0.34.

Preparation of 3,3',4',5-tetramethoxybenzanilide (60a)

3,5-dimethoxyaniline (8.00g, 0.0522M) was reacted with 3,4-dimethoxybenzoyl chloride (47) (10.45g, 0.0522M) according to the general method. Recrystallization from methanol gave off-white needle crystals (10.35g, 62%); m.p. 123-124°C; M+, 317; λ max. (d.r.)* (KBr) 3300, 1645, 1601, 1422, 1273, 1204, 1156, 1022, 828 cm^{-1}; δ ($CDCl_3$)

(60MHz) 8.20 (1H,s), 7.35 (2H,d), 6.80 (3H,m), 6.20 (1H,s), 3.80 (12H,t) ppm; Rf ($CHCl_3$ + 2% EtOH) 0.28.

Preparation of 3,3',4',5-tetramethoxythiobenzanilide (60b)

Compound 60a (7.00g, 0.0220M) was reacted with Lawesson's reagent according to the general method. Recrystallization from methanol gave yellow needle crystals (5.52g, 75%); m.p. 155-156°C; M+, 333; λ max. (d.r.)* (KBr) 1611, 1597, 1515, 1274, 1209, 1148, 1024, 812 cm^{-1}; δ ($CDCl_3$) (60MHz) 9.00 (1H,s), 7.30 (2H,m), 6.80 (3H,m), 6.25 (1H,s), 3.90 (6H,s), 3.75 (6H,s) ppm; Rf ($CHCl_3$ + 2% EtOH) 0.34.

Preparation of 2-(3,4-dimethoxyphenyl)-5,7-dimethoxybenzothiazole (60c)

Compound 60b (4.00g, 0.0120M) was reacted with potassium ferricyanide according to the general method. Recrystallization from methanol gave cream needles crystals (1.08g, 27%), m.p. 159-160°C; M+, 331; λ max. (d.r.)* (KBr) 1596, 1574, 1470, 1413, 1260, 1145, 1120, 1022, 818 cm^{-1}; δ ($CDCl_3$) (300MHz) 7.57 (2H,d), 7.20 (1H,s), 7.10 (1H,d), 6.64 (1H,s), 3.93 (3H,s) ppm; Rf ($CHCl_3$) 0.38.

Preparation of 2-(3,4-dihydroxyphenyl)-5,7-dihydroxy-benzothiazole (60d)

Compound 60c (0.50g, 0.00151M) was reacted with boron tribromide 1.0M in dichloromethane (18.1ml) according to method B. Removal of solvent gave a yellow powder (0.39g, 94%), m.p. >320°C; MH+, 276.0331 gives $C_{13}H_{10}NO_4S$; λ max. (d.r.)* (KBr) 3225, 1613, 1469, 1263, 1061 cm^{-1}; δ (DMSO-D_6) (300MHz) 11.00 (1H,s) (exchanges with D_2O), 10.34 (1H,s) (exchanges with D_2O), 9.48 (2H,s) (exchanges with D_2O), 7.44 (1H,s), 7.32 (1H,d), 6.85 (1H,d), 6.78 (1H,s), 6.36 (1H,s) ppm; R_f ($CHCl_3$ + 2% EtOH) 0.11.

Preparation of 4-nitro-4'-methoxybenzanilide (61a)

4-Nitroaniline (4.06g, 0.0294M) was reacted with 4-methoxybenzoyl chloride (5.00g, 0.0294M) according to the general method. Recrystallization from methanol gave cream needle crystals (5.59g, 70%); m.p. 177-178°C (lit. 183-185°C[130]); M+, 272; λ max. (nujol) 3400, 3310, 1640, 1580, 1340, 1240, 1170, 1100, 1010, 845, 745 cm^{-1}; δ ($CDCl_3$ + DMSO-D_6) (60MHz) 10.25 (1H,s), 7.95 (6H,m), 6.90 (2H,d), 3.80 (3H,s) ppm; Rf ($CHCl_3$) 0.17.

Preparation of 4-methoxy-4'-nitrothiobenzanilide (61b)

Compound 61a (5.00g, 0.0184M) was reacted with Lawesson's reagent according to the general method. Recrystallization from methanol gave a yellow powder

(4.55g, 86%); m.p. 187-188°C (lit. 194-195°C[131]); M+, 288; λ max. (KBr) 3110, 2970, 1590, 1500, 1335, 1300, 1250, 1160, 1005, 980, 850 cm^{-1}; δ ($DMSO-D_6$) (300MHz) 11.90 (1H,s), 8.28 (2H,d), 8.18 (2H,d), 7.87 (2H,d), 7.02 (2H,d), 3.38 (3H,s) ppm; ν max. (EtOH) 210, 235, 313; ν_{max}. (EtOH + NaOH) 220; Rf ($CHCl_3$) 0.27.

Preparation of 4-methoxy-4'-nitrobenzanilide (62a)

4-Methoxyaniline (5.00g, 0.0407M) was reacted with 4-nitrobenzoyl chloride (7.52g, 0.0407M) according to the general method. Recrystallization from methanol gave yellow needle crystals (7.29g, 66%); m.p. 192-194°C (lit. 199-200°C[132]); M+, 272; λ max. (KBr) 3250, 1650, 1600, 1515, 1345, 1320, 1250, 840 cm^{-1}; δ ($DMSO-D_6$) (60MHz) 10.40 (1H,s), 8.25 (4H,q), 7.65 (2H,d), 6.90 (2H,d), 3.75 (3H,s) ppm; Rf ($CHCl_3$) 0.16.

Preparation of 4-methoxy-4'-nitrothiobenzanilide (62b)

Compound 62a (5.00g, 0.0184M) was reacted with Lawesson's reagent according to the general method. The reaction mixture was extracted with 3 x 20ml 5% NaOH(aq). After neutralisation with glacial acetic acid, the solid was filtered off. Recrystallization from ethoxyethanol gave an orange powder (3.38g, 64%); m.p. 164-166°C (lit. 133-134°C[133]); M+, 288; λ max. (nujol) 3130, 1600, 1510, 1340, 1250, 820 cm^{-1}; δ ($DMSO-D_6$) (60MHz) 12.00 (1H,s),

7.60-8.25 (6H,m), 6.90 (2H,d), 3.70 (3H,s) ppm; Rf ($CHCl_3$) 0.66.

Preparation of 2-(4-nitrophenyl)-6-methoxybenzothiazole (62c)

Compound 62b (1.00g, 0.00347M) was reacted with potassium ferricyanide according to the general method. Recrystallization from 2-ethoxyethanol gave a green powder (0.67g, 68%), m.p. 204-205°C; M+, 272; $\lambda_{max.}$ (KBr) 3450, 1600, 1510, 1340, 1320, 1260, 1220, 850, 690 cm^{-1}; δ (DMSO-D_6) (300MHz) 8.35 (4H,q), 8.15 (1H,d), 7.80 (1H,s), 7.19 (1H,d), 3.87 (3H,s) ppm; Rf ($CHCl_3$) 0.75.

Preparation of 4-methoxy-2'-chloro-4'-nitrobenzanilide (63a)

2-chloro-4-nitrobenzoyl chloride (9.30g, 0.429M) was heated under reflux with excess thionyl chloride (2h). The residue left on distilling off of the thionyl chloride, was recrystallized from petrolium ether and promptly reacted with 4-methoxyaniline (6.12g, 0.0497M) according to the general method. Recrystallization from methanol gave grey needle crystals (6.03g, 40%); m.p. 172°C; $\lambda_{max.}$ (nujol) 3250, 1640, 1590, 1510, 1240, 1020 cm^{-1}; δ (DMSO-D_6) (60MHz) 10.45 (1H,s) (exchanges with D_2O), 8.15 (2H,t), 8.85 (1H,s), 7.55 (2H,d), 6.85 (2H,d), 3.70 (3H,s) ppm; Rf ($CHCl_3$ + 5% MeOH) 0.53.

Preparation of 4-methoxy-2'-chloro-4'-nitrothiobenzanilide (63b)

Compound 63a (5.00g, 0.0163M) was reacted with Lawesson's reagent according to the general method. Recrystallization from methanol gave a yellow powder (3.15g, 60%); m.p. 176°C; $\lambda_{max.}$ (nujol) 3060, 1500, 1390, 1240, 1020, 980, 810, 730 cm^{-1}; δ ($DMSO-D_6$) (60MHz) 13.20 (1H,s)(exchanges with D_2O), 8.30 (2H,d), 7.80 (3H,m, 7.00 (2H,d), 3.80 (3H,s) ppm; Rf ($CHCl_3$ + 5% MeOH) 0.63.

Preparation of 2-(2-chloro-4-nitrophenyl)-6-methoxy-benzothiazole (63c)

Compound 63b (2.00g,0.0062M) was reacted with potassium ferricyanide according to the general method. Recrystallzation from ethanol gave small yellow needle crystals (1.09g, 55%), m.p. 174°C; $\lambda_{max.}$ (nujol) 1590, 1510, 1250, 1010, 815 cm^{-1}; δ ($CDCl_3$) (300MHz) 8.44 (2H,t), 8.28 (1H,d), 8.03 (1H,d), 7.75 (1H,s), 7.20 (1H,d), 3.87 (3H,s) ppm; Rf ($CHCl_3$ + 5% MeOH) 0.86.

Preparation of 2-(2-chloro-4-aminophenyl)-6-methoxy-benzothiazole (63d)

Compound 63c (0.50g, 0.00156M) was heated under reflux (2h) in an ethanolic solution of tin (II) chloride (1.76g, 0.00782M) under of nitrogen. The ethanol was removed under vacuum and the residue washed with 2x40ml 20% sodium hydroxide solution then 2x40ml water. The

residue was filtered and recrystallized from methanol to give beige needle crystals (0.39g, 86%), m.p. 182-183°C; M^+, 292; λ max. (nujol) 3400, 3340, 1615, 1585, 1250, 1200, 1040, 800 cm^{-1}; δ (DMSO-D_6) (300MHz) 7.95 (1H,d), 7.84 (1H,d), 7.64 (1H,d), 7.09 (1H,d), 6.73 (1H,s), 6.64 (1H,d), 6.05 (2H,s), 3.83 (3H,s) ppm; δ (DMSO-D_6 + D_2O) (300MHz) 7.88 (2H,q), 7.60 (1H,s), 7.08 (1H,d), 6.72 (1H,s), 6.65 (1H,d), 3.81 (3H,s) ppm; Rf ($CHCl_3$ + 5% EtOH) 0.51.

Preparation of 3'-nitrobenzanilide (64a)

Aniline (10.04g, 0.108M) was reacted with 3-nitrobenzoyl chloride (20.00g, 0.108M) according to the general method. Recrystallization from methanol gave cream needle crystals (18.92g, 72%); m.p. 178-180°C (lit. 207-211[134]; λ max. (nujol) 3300, 1600, 1510, 1315, 1070, 890, 750, 705 cm^{-1}; δ ($CDCl_3$) (300MHz) 8.67 (1H,s), 8.39 (1H,d), 8.36 (1H,d), 7.65 (3H,m), 7.38 (2H,t), 7.19 (1H,q) ppm; Rf ($CHCl_3$ + 2% EtOH) 0.37.

Preparation of 3'-nitrothiobenzanilide (64b)

Compound 64a (15.00g, 0.0620M) was reacted with Lawesson's reagent according to the general method. Recrystallization from methanol gave a yellow solid (9.96g, 62%); m.p. 124-126°C (lit. 134°C[135]); M+, 243; λ max. (nujol) 3240, 1595, 1520, 1370, 1340, 1000, 760, 700 cm^{-1}; δ ($CDCl_3$) (60MHz) 9.15 (1H,s), 7.20-8.30 (9H,m) ppm; Rf ($CHCl_3$) 0.35.

Preparation of 2-(3-nitrophenyl)benzothiazole (64c)

Compound 64b (7.00g, 0.0271M) was reacted with potassium ferricyanide according to the general method. Recrystallization from methanol gave colourless needle crystals (6.56g, 94%), m.p. 144-145°C (lit. 187°C[116]); M+, 256; max. (nujol) 1520, 1330, 980, 960, 870, 740 cm^{-1}; δ ($CDCl_3$) (300MHz) 8.91 (1H,s), 8.38 (1H,d), 8.30 (1H,d), 8.09 (1H,d), 7.94 (1H,d), 7.67 (1H,t), 7.50 (1H,t), 7.43 (1H,t) ppm; ν max. (EtOH) 239, 354; Rf ($CHCl_3$) 0.65.

Preparation of 2-(3-aminophenyl)benzothiazole (64d)

Compound 64c (2.00g, 0.00781M) was heated under reflux (4h) in an ethanolic solution of tin (II) chloride (8.79g, 0.0391M) under nitrogen. The ethanol was removed under reduced pressure and the residue dissolved in ethyl acetate. The organic phase was washed with 2x40ml 20% sodium hydroxide solution then 2x40ml water. Removal of the ethyl acetate gave a residue which when recrystallized from methanol gave a beige solid (1.54g, 88%), m.p. 143°C (lit. 141°C[116]); M+, 256 (minor) 226 (major); λ max. (nujol) 3410, 3380, 3180, 1560, 1300, 750 cm^{-1}; δ (DMSO-D_6) (300MHz) 9.08 (1H,d), 9.00 (1H,d), 7.44 (3H,m), 7.19 (2H,m), 6.74 (1H,m), 5.47 (2H,s) (exchanges with D_2O) ppm; Rf ($CHCl_3$ + 2% EtOH) 0.28.

Preparation of 4'-nitrobenzanilide (65a)

Aniline (2.96g, 0.0318M) was reacted with 4-nitrobenzoyl chloride (5.88g, 0.0318M) according to the general method. Recrystallization from methanol gave white needle crystals (5.55g, 72%); m.p. 209-211°C (lit. 213°C[125]); M+, 242; λ max. (nujol) 3310, 1655, 1600, 1520, 1350, 1320, 760, 700 cm^{-1}; δ (DMSO-D_6) (60MHz) 10.45 (1H,s), 7.00-8.45 (9H,m) ppm; Rf ($CHCl_3$) 0.25.

Preparation of 4'-nitrothiobenzanilide (65b)

Compound 65a (4.50g, 0.0186M) was reacted with Lawesson's reagent according to the general method. Recrystalisation from methanol gave a yellow powder (1.54g, 32%); m.p. 149-150°C (lit. 155°C[135]); M+, 258; $\lambda_{max.}$ (KBr) 3260, 1600, 1530, 1370, 1345, 860, 760 cm^{-1}; δ ($CDCl_3$) (60MHz) 9.10 (1H,s), 7.10-8.25 (9H,m) ppm; ν max. (EtOH) 210, 275; ν max. (EtOH + NaOH) 215, 272; Rf ($CHCl_3$) 0.40.

Preparation of 2-(4-nitrophenyl)benzothiazole (65c)

Compound 65b (3.00g, 0.0116M) was reacted with potassium ferricyanide according to the general method. Recrystallization from dimethylformamide gave a pale yellow solid (0.35g, 10%), m.p. 224-226°C (lit. 230-232°C[136]); M+, 256; λ max. (KBr) 1590, 1510, 1330, 1105, 850, 760, 680 cm^{-1}; δ ($CDCl_3$) (300MHz) 8.35 (2H,d), 8.25

(2H,d), 8.10 (1H,d), 7.93 (1H,d), 7.50 (2H,m) ppm; Rf ($CHCl_3$) 0.39.

Preparation of 2-(4-aminophenyl)benzothiazole (65d)

Compound 65c (0.34g, 0.00133M) was heated under reflux (4h) in an ethanolic solution of tin (II) chloride (8.79g, 0.0391M) under of nitrogen. The ethanol was removed under reduced pressure and the residue dissolved in ethyl acetate. The organic phase was washed with 2x40ml 20% sodium hydroxide solution then 2x40ml water. Removal of the ethyl acetate gave a residue which when recrystallized from methanol gave beige needle crystals (0.22g, 73%), m.p. 155-156°C (lit. 156°C[135]); λ max. (nujol) 3440, 3290, 3170, 1600, 1470, 1440, 1300, 1220, 1170, 830, 760 cm^{-1}; δ (DMSO-D_6) (300MHz) 7.99 (1H,d), 7.88 (1H,d), 7.75 (2H,d), 7.44 (1H,d), 7.32 (1H,t), 6.65 (2H,d), 5.90 (2H,s) (exchanges with D_2O) ppm; Rf ($CHCl_3$ + 2% EtOH) 0.29.

Preparation of 4-chloro-4'-methoxybenzanilide (66a)

4-Chloroaniline (5.00g, 0.0394M) was reacted with 4-methox ybenzoyl chloride (6.69g, 0.0394M) according to the general method. Recrystallization from methanol gave white plate crystals (7.97g, 78%); m.p. 205-206°C (lit. 207-208°C[119]); M+, 261; λ max. (nujol) 3340, 1640, 1580, 1490, 1250, 1020, 820, 760 cm^{-1}; δ (DMSO-D_6) (60MHz) 10.20 (1H,s), 7.85 (4H,t), 7.20 (2H,d), 7.00 (2H,d), 3.85 (3H,s) ppm; Rf ($CHCl_3$) 0.34.

Preparation of 4-chloro-4'-methoxythiobenzanilide (66b)

Compound 66a (5.00g, 0.0192M) was reacted with Lawesson's reagent according to the general method. Recrystallization from methanol gave yellow needle crystals (4.83g, 91%); m.p. 180-183°C; found C, 60.73; H, 4.42; N, 5.40% ($C_{14}H_{12}ClNOS$ requires C, 60.54; H, 4.33; N, 5.05%); M+, 277; λ max. (nujol) 3120, 1585, 1240, 1170, 1010, 980, 840 cm^{-1}; δ ($CDCl_3$ + DMSO-D_6) (60MHz) 11.40 (1H,s), 7.95 (4H,d), 7.40 (2H,d), 6.95 (2H,d), 3.90 (3H,s) ppm; ν max. (EtOH) 225, 283; ν max. (EtOH + NaOH) 218, 270; Rf ($CHCl_3$) 0.75.

Preparation of 2-(4-methoxyphenyl)-6-chlorobenzothiazole (66c)

Compound 66b (1.00g, 0.00360M) was reacted with potassium ferricyanide according to the general method. Recrystallization from methanol gave a white solid (0.89g, 90%), m.p. 145-146°C; M+, 275; found C, 61.30; H, 3.79; N, 5.14 ($C_{14}H_{10}ClNOS$ requires C, 61.00; H, 3.63; N, 5.08%); λmax. (nujol) 1590, 1485, 1305, 1260, 1170, 835 cm^{-1}; δ ($CDCl_3$) (300MHz) 8.28 (1H,s), 8.00 (3H,t), 7.55 (1H,d), 7.12 (2H,d), 3.85 (3H,s) ppm; ν max. (EtOH) 220, 321; Rf ($CHCl_3$) 0.84.

Preparation of 2-methyl-4'-methoxybenzanilide (67a)

2-Methylaniline (2.50g, 0.0234M) was reacted with 4-methoxybenzoyl chloride (3.97g, 0.0234M) according to the

general method. Recrystallization from methanol gave white needle crystals (4.42g, 78%); m.p. 164-165°C (lit. 167-168°C[119]); M+, 241; λ max. (nujol) 3260, 1630, 1590, 1560, 1500, 1290, 1240, 1160, 1020, 840, 740, 680 cm^{-1}; δ (DMSO-D_6) (60MHz) 9.65 (1H,s), 7.95 (2H,d), 6.85-7.30 (6H,t), 3.75 (3H,s), 2.20 (3H,s) ppm; Rf ($CHCl_3$) 0.45.

Preparation of 2-methyl-4'-methoxythiobenzanilide (67b)

Compound 67a (3.00g, 0.0125M) was reacted with Lawesson's reagent according to the general method. Recrystallization from methanol gave large yellow needle crystals (2.11g, 65%); m.p. 119-120°C; M+, 257; λ max. (nujol) 3140, 1580, 1485, 1330, 1295, 1240, 1160, 980, 830, 715 cm^{-1}; δ ($CDCl_3$) (60MHz) 8.80 (1H,s), 7.85 (2H,d), 7.25 (4H,s), 6.85 (2H,d), 3.80 (3H,s), 2.25 (3H,s) ppm; νmax. (EtOH) 241, 303; ν max. (EtOH + NaOH) 249, 268; Rf ($CHCl_3$) 0.81.

Preparation of 2-(4-methoxyphenyl)-4-methylbenzothiazole (67c)

Compound 67b (1.00g, 0.00389M) was reacted with potassium ferricyanide according to the general method. Recrystallization from methanol gave an orange solid (0.89g, 90%), m.p. 87-88°C; M+, 255; λ max. (nujol) 1590, 1250, 1160, 830 cm^{-1}; δ (DMSO-D_6) (300MHz) 7.99 (2H,d), 7.85 (1H,s), 7.30 (2H,s), 7.08 (2H,d), 3.83 (3H,s) ppm; νmax. (EtOH) 217, 310; Rf ($CHCl_3$ + 2% EtOH) 0.67.

Preparation of 2,6-dimethyl-4'-methoxybenzanilide (68a)

2,6-Dimethylaniline (3.56g, 0.0294M) was reacted with 4-methoxybenzoyl chloride (5.00g, 0.0294M) according to the general method. Recrystallization from methanol gave white needle crystals (6.30g, 84%); m.p. 166-167°C (lit. 169°C[119]); M+, 255; $\lambda_{max.}$ (nujol) 3215, 1630, 1590, 1490, 1350, 1025, 840, 770 cm^{-1}; δ (DMSO-D_6) (60MHz) 9.55 (1H,s), 7.95 (2H,d), 6.95 (5H,d), 3.80 (3H,s), 2.25 (6H,s) ppm; Rf ($CHCl_3$) 0.12.

Preparation of 2,6-dimethyl-4'-methoxythiobenzanilide (68b)

Compound 68a (5.00g, 0.0196M) was reacted with Lawesson's reagent according to the general method. Recrystallization from methanol gave large yellow crystals (4.60g, 87%); m.p. 158-160°C; M+, 271; $\lambda_{max.}$ (nujol) 3340, 1590, 1470, 1335, 1295, 1005, 975, 855, 780 cm^{-1}; δ ($CDCl_3$) (60MHz) 10.90 (1H,s), 8.10 (2H,d), 6.80-7.20 (5H,t), 3.80 (3H,s), 2.20 (3H,s) ppm; δ ($CDCl_3$ + D_2O) (60MHz) 8.10 (2H,d), 6.80-7.20 (5H,t), 3.80 (3H,s), 2.20 (3H,s) ppm; $\nu_{max.}$ (EtOH) 212, 275; $\nu_{max.}$ (EtOH + NaOH) 215; Rf ($CHCl_3$ + 2% EtOH) 0.67.

Preparation of N-methyl-4'-methoxybenzanilide (69a)

N-Methylaniline (3.15g, 0.0294M) was reacted with 4-methoxybenzoyl chloride (5.00g, 0.0294M) according to the general method. Recrystallization from ethanol gave a

white solid (4.04g, 57%); m.p. 55-56°C (lit. 80°C[119]); λ max. (nujol) 1635, 1590, 1370, 1260, 1030, 840 cm^{-1}; δ ($CDCl_3$) (60MHz) 7.30-6.80 (7H,m), 6.50 (1H,d), 3.65 (3H,s), 3.40 (3H,s) ppm; Rf ($CHCl_3$) 0.20.

Preparation of N-methyl-4'-methoxythiobenzanilide (69b)

Compound 69a (2.00g, 0.00830M) was reacted with Lawesson's reagent according to the general method. Recrystallization from methanol gave a yellow powder (1.06g, 50%); m.p. 100-101°C; M+, 257; λ max. (nujol) 1590, 1285, 1250, 1170, 1090, 1035, 820 cm^{-1}; δ ($CDCl_3$) (60MHz) 6.90-7.30 (7H,m), 6.50 (1H,d), 3.85 (3H,s), 3.65 (3H,s) ppm; Rf ($CHCl_3$) 0.75.

Preparation of N-(4-methoxybenzoyl)1,2,3,4-tetrahydroquinoline (70a)

1,2,3,4-Tetrahydroquinoline (4.00g, 0.0308M) was reacted with 4-methoxybenzoyl chloride (5.23g, 0.0308M) according to the general method. Recrystallization from methanol gave white needle crystals (6.93g, 85%); m.p. 98-99°C; M+, 267; λ max. (nujol) 1615, 1585, 1295, 1250, 1160, 1015, 850, 750 cm^{-1}; δ (DMSO-D_6) (60MHz) 6.70-7.45 (8H,m), 3.75 (5H,q), 2.85 (2H,t), 2.0 (2H,q) ppm; Rf ($CHCl_3$) 0.38.

Preparation of N-(4-methoxythiobenzoyl)tetrahydroquinoline (70b)

Compound 70a (4.00g, 0.0150M) was reacted with Lawesson's reagent according to the general method. Recrystallization from methanol gave large yellow crystals (2.46g, 58%); m.p. 146-147°C; found C, 71.80; H, 5.89; N, 5.01% ($C_{17}H_{17}NOS$ requires C, 72.10; H, 6.00; N, 4.94%); M+, 283; $\lambda_{max.}$ (nujol) 1580, 1480, 1240, 1160, 1020, 840, 750 cm^{-1}; δ (DMSO-D_6) (300MHz) 7.19 (3H,q), 7.02 (1H,t), 6.84 (1H,t), 6.72 (2H,d), 6.50 (1H,d), 4.26 (2H,t), 3.70 (3H,s), 2.81 (2H,t), 2.04 (2H,m) ppm; $\nu_{max.}$ (EtOH) 210, 310; $\nu_{max.}$ (EtOH + NaOH) 215, 310; Rf ($CHCl_3$) 0.85.

Preparation of N-(4-methoxybenzoyl)indoline (71a)

Indoline (3.50g, 0.0294M) was reacted with 4-methoxybenzoyl chloride (5.00g, 0.0294M) according to the general method. Recrystallization from methanol gave a pink solid (6.43g, 86%); m.p. 111°C; M+, 253; found C, 76.25, H, 6.18; N, 5.47% ($C_{16}H_{15}NO_2$ requires C, 75.90; H, 5.92; N, 5.52%); $\lambda_{max.}$ (nujol) 1620, 1580, 1240, 1020, 840, 750 cm^{-1}; δ ($CDCl_3$) (60MHz) 6.70-7.60 (8H,m), 3.80-4.30 (5H,m), 3.10 (2H,m) ppm; Rf ($CHCl_3$) 0.14.

Preparation of N-(4'-methoxythiobenzoyl)indoline (71b)

Compound 71a (5.00g, 0.0198M) was reacted with Lawesson's reagent according to the general method. Recrystallization from methanol gave yellow needle

crystals (2.25g, 42%); m.p. 120-122°C; M+, 269.0874000 gives $C_{16}H_{15}NOS$; $\lambda_{max.}$ (KBr) 1600, 1580, 1400, 1275, 1250, 1170, 1020, 830, 750 cm^{-1}; δ (DMSO-D_6) (300MHz) 7.33 (3H,t), 6.94 (4H,d), 5.85 (1H,s), 4.42 (2H,s), 3.80 (3H,s), 3.16 (2H,d) ppm; $\nu_{max.}$ (EtOH) 230, 292, 326, $\nu_{max.}$ (EtOH + NaOH) 218, 292, 326; Rf ($CHCl_3$) 0.73.

7 REFERENCES

Ref.

1 An assessment of current achievements in the systemic management of breast cancer.
Lippman M.E.
Breast Canc. Res. Treat. 4, 69-77, 1984.

2 Antioestrogens in the management of hormone dependent cancer.
Litherland S., Jackson I.M.
Cancer Treat. Rev. 15, 183-194, 1988.

3 Endocrine therapy of advanced breast cancer.
Rose C., Mouridsen H.T.
Acta Oncologica 27, 721-728, 1988.

4 Steroid hormone receptors in breast cancer.
Wittliff J.L.
Cancer 53, 630-643, 1984.

5 Hormone receptor assays: Clinical usefulness in the management of carcinoma of the breast.
Jordan V.C., Wolf M.F., Mirecki D.M., Whitford D.A., Welshons W.V.
CRC Critical Reviews in Clinical Laboratory Sciences 26, (2), 97-152, 1988.

6 Specific and direct binding of protein kinase C to an immobilised tamoxifen analogue.
O'Brian C.A., Housey G.M., Weinstein I.B.
Cancer Research 48, 3626-3629, 1988.

7 A phase II trial of tamoxifen, premarin, methotrexate and 5-fluorouracil in metastatic breast cancer.
Allegra J.C., Woodcock T.M., Richman S.P.
Breast Cancer Treat. Rep. 2, 93-100, 1982.

8 Estrogen priming in advanced breast cancer.
Maghsoodnia M., Holleran W.M., DeGregorio M.W.,
Drug Intelligence and Clinical Pharmacy 22, 672-675, 1988.

9 Hormone prevention of mammary carcinogenesis: A new approach in anticancer research.
Russo I.H., Russo J.
Anticancer Research 8, 1247-1264, 1988.

10 Tamoxifen: transition from the laboratory to clinical preventative chemosuppression.
Tormey D.C.
Cancer Investigation 6 (5), 597-600, 1988.

Ref.

11 Effects of anti-estrogens on bone in castrated and intact female rats.
Jordan V.C., Phelps E., Lindgren J.U.
Breast Cancer Res. Treat. 10, 31-35, 1987.

12 Evaluation of the antitumour activity of the non-steroidal antioestrogen monohydroxytamoxifen in the DMBA-induced rat mammary carcinoma model.
Jordan V.C., Allen K.E.
Eur. J. Cancer 16, 239-251, 1980.

13 Differential regulation of growth and invasiveness of MCF-7 breast cancer cells by antiestrogens.
Thompson E.W., Reich R., Shima T.B., Albini A., Graf J., Martin G.R., Dickson R.B., Lippman M.E.
Cancer Research 48, 6764-6768, 1988.

14 Inhibition of aromatase as treatment of breast carcinoma in postmenopausal women.
Santen R.J., Boucher A.E., Santner S.J., Herderson I.C., Harvey H., Lipton A.
J. Lab. Clin. Med. 109, 278-289, 1987.

15 The Extra Pharmacopoeia 29th Edition.
Edited by Reynolds J.E.F.
The Pharmaceutical Press, 1989.

16 Analogues of 3-ethyl-3-(4-pyridyl)piperidine-2,6-dione as selective inhibitors of aromatase. Derivatives with variable 1-alkyl substituents.
Leung C-S., Rowlands M.G., Jarman M., Foster A.B., Griggs L.Y., Wilman D.E.
J. Med. Chem. 30, 1550, 1987.

17 Evidence that the phosphorylation of tyrosine is essential for cellular transformation by Rous sarcoma virus.
Sefton B.M., Hunter T., Beemon K., Eckhart W.
Cell 20, 807-816, 1980.

18 Stimulation of 3T3 cells induces transcription of the c-fos proto-oncogene.
Greenberg M.E., Ziff E.B.
Nature 311, 433-437,1984.

19 Regulation of cell growth and transformation by the epidermal growth factor receptor.
Schlessinger J.
Advances in Experimental Medicine and Biology 234, 65-73, 1988.

Ref.

20 C-kinase phosphorylates the epidermal growth factor receptor and reduces its epidermal growth factor-stimulated tyrosine protein kinase activity.
Cochet C., Gill G.N., Meisenhelder J., Cooper J.A., Hunter T.,
J. Biol. Chem. 259, 2553-2558,1984

21 Close similarity of epidermal growth factor receptor and v-erb-B oncogene protein sequences.
Downyard J., Yarden Y., Mayers E., Scrace G., Totty N., Stockwell P., Ullrich A., Schlessinger J., Wakefield M.D.
Nature 307, 521-526, 1984

22 Antibodies against a synthetic peptide as a probe for the kinase activity of the avian EGF receptor and v-erbB protein.
Kris R.M., Lax I., Gullick W., Waterfield M.D., Ullrich A., Fridkin M., Schlessinger J.
Cell 40, 619-625, 1985.

23 Differential expression of cellular oncogenes during pre- and postnatal development of the mouse.
Müller R., Salmon D.J., Tremblay J.M., Cline M.J., Verma I.M.
Nature 299, 640-644, 1982.

24 Human breast cancer: Correlation of relapse and survival with amplification of the HER-2/neu oncogene.
Salmon D.J., Clark G.M., Wong S.G., Levin W.J., Ullrich A., McGuire W.L.
Science 235, 177-182, 1987.

25 The role of oestrogen receptors and c-erb-B_2 in the long term prognosis of breast cancer.
Winstanley J.H.R., Holt S.M., Rudland R.S., Baraclough B.R., Platt-Higgins A.M., George W.D., Griffiths K., Nicolson R., Cooke T.G.
31st Annual Meeting of the British Assoc. of Cancer Res. 12.1, 1990.

26 Protein tyrosine kinase associated with human malignancies.
Cromoglio P.M., Di Renzo M.F., Gaudino G.
Ann. N.Y. Acad. Sci. 511, 256-261, 1987.

Ref.

27 Immunological detection of proteins phosphorylated at tyrosine in cells stimulated by growth factors or transformed by retroviral-oncogene-coded tyrosine kinases.
Di Renzo M.F., Ferracini R., Naldini L., Giordano S., Comoglio P.M.
Eur. J. Biochem. 158, 383-391, 1986.

28 Proteins phosphorylated on tyrosine as markers of human tumour cell lines.
Giordano S., Di Renzo M.F., Cirillo D., Naldini L., Chiado'Piat L., Comoglio P.M.
Int. J. Cancer 39, 482-487, 1987.

29 Tyrophostins I: Synthesis and biological activity of protein tyrosine kinase inhibitors.
Gazit A., Yaish P., Gilon C., Levitzki A.
J. Med. Chem. 32, 2344-2352, 1989.

30 Specific inhibitors of tyrosine – specific protein kinases: Properties of 4-hydroxycinnamide derivatives in vitro.
Shiraishi T., Owada M.K., Tatsuka M., Yamashita T., Watenabe K., Kakunaga T.
Cancer research 49, 2374-2378, 1989.

31 Design of kinase inhibitors.
Kenyon G.L., Garcia G.A.
Medical Research Reviews 7, (4), 389-416, 1987.

32 The effect of quercetin on the phosphorylation activity of the Rous Sarcoma virus transforming gene product in vitro and in vivo.
Graziani Y., Erikson E., Erikson R.L.
Eur. J. Biochem. 135, 583-589, 1983.

33 Genistein, a specific inhibitor of tyrosine-specific protein kinases.
Akiyama T., Ishida J., Nakagawa S., Ogawara H., Watanabe S., Itoh N., Shibuya M., Fukami Y.
J. Biol. Chem. 262, (12), 5592-5595, 1987.

34 Amiloride directly inhibits growth factor receptor tyrosine kinase activity.
Davis R.J., Czech M.P.
J. Biol. Chem. 260, (4) 2543-25515, 1985.

35 Inhibition of protein-kinase activity by flavenoids and related compounds.
Geahlen R.L., Koonchanok N.M., McLaughlin J.L.
J. Natural Products 52, (5), 982-986, 1989.

Ref.

36 Potential value of plants as sources of new antifertility agents II.
Farnsworth N.R., Bingel A.S., Cordell G.A., Crane F.A., Fong H.H.S.
J. Pharm. Sci. 64, (5), 717-754, 1975.

37 Naturally occurring oestrogens in foods - a review.
Price K.R., Fenwick G.R.
Food Additives and Contaminants 2, (2), 73-106, 1985.

38 Flavenoids. 8. Synthesis and antifertility and estrogen receptor binding activities of coumarins and Δ^3-isoflavenes.
Wani C.W., Rector D.H., Christensen H.D., Kimmel G.L., Cook C.E.
J. Med. Chem. 18, (10), 982-985.

39 Inhibition of human estrogen synthetase (aromatase) by flavones.
Kellis J.T. Jn., Vickery L.E.
Science 225, 1032-1034, 1984.

40 Inactivation of oestrogen receptor in vitro by nuclear dephosphorylation.
Auricchio F., Migliaccio A., Rotondi A.
Biochem. J. 194, 569-574, 1981.

41 Oestradiol stimulates tyrosine phosphorylation and hormone binding of its own receptor in a cell free system.
Auricchio F., Migliaccio A., Di Domenico M., Nola E.
EMBO J. 6, (10), 2923-2929, 1987.

42 Evidence that in vivo estradiol receptor translocated into nuclei is dephosphorylated and released into cytoplasm.
Auricchio F., Migliaccio A., Castoria S., Lastoria S., Rotondi A.
Biochem. Biophys. Res. Commun. 106, (1), 149-157, 1982.

43 Dephosphorylation of oestradiol nuclear receptor in vitro. A hypothesis on the mechanism of action of non-steroidal anti-oestrogens.
Auricchio F., Migliaccio A., Castoria G.
Biochem. J. 198, 699-702, 1981.

Ref.

44 Effects of diabetes and sex steroid hormones on insulin receptor tyrosine kinase activity in R3230AC mammary adenocarcinomas.
Hilf R., Livingston J.N., Crofton D.H.
Cancer Research 48, 3742-3750, 1988.

45 Regulation of epidermal growth factor receptor by estrogen.
Mukku V.R., Stancel G.M.
J. Biol. Chem. 260, (17), 9820-9824, 1985.

46 Interactions between estrogen and EGF in uterine growth.
Stancel G.M., Gardner R.M., Kirkland J.L., Lin T.H., Lingham R.B., Loose-Mitchell D.S., Mukku V.R. Orengo C.A., Verner G.
Advances in Experimental Medicine and Biology 230, 99-118, 1987.

47 2-Phenylindoles. Relationship between structure, estrogen receptor affinity, and mammary tumour inhibiting activity in the rat.
von Angerer E., Prekajac J., Strohmeier J.
J. Med. Chem. 27, 1439-1447, 1984.

48 2-Phenylindenes: Development of a new mammary tumour inhibiting antiestrogen by combination of estrogenic side effect lowering structural elements.
Schneider M.R., Ball H.
J. Med. Chem. 29, 75-79, 1986.

49 The inhibitory effect of 5-acetoxy-2-(4-acetoxyphenyl)-1-ethyl-3-methylindole (D16726) on estrogen-dependent mammary tumours.
von Angerer E., Prekajac J., Berger M.
Eur. J. Cancer Clin. Oncol. 21, (4), 531-537, 1985.

50 Benzo[a]carbazole derivatives. Synthesis, estrogen receptor binding affinities, and mammary tumour inhibiting activity.
von Angerer E., Prekajac J.
J. Med. Chem. 29, 380-386, 1986.

51 Diethylstilbestrol metabolites and analogues. Stereochemical probes for the estrogen receptor binding site.
Korach K.S., Chea K., Levy L.A., Duax W.L., Sarver P.J.
J. Biol. Chem. 264, 5642-5647, 1989.

Ref.

52 Synthese und testung mammatumorhemmender derivate des 2-phenylindoles, benzo[b]furans und benzo[b]thiophenes.
Erber S.
PhD Thesis, Regensburg University, 1989.

53 Catechol oestrogens inhibit oestrogen elicited accumulation of hypothalamic cyclic AMP suggesting role as endogenous antioestrogens.
Paul S.M., Skolnick P.
Nature 266, 559, 1977.

54 Antiestrogen action of 2-hydroxyestrone on MCF-7 breast cancer cells.
Schneider J., Huh M.M., Bradlow H.L., Fishman J.
J. Biol. Chem. 258, 4840-4845, 1984.

55 Isolation and purification of rat mammary tumour peroxidase.
DeSomber E.R., Lyttle C.R.
Cancer Res. 38, 4086-4090, 1978.

56 Cytochrome P-450 mediated oxidation of 2-hydroxyestrogens to reactive intermediates.
Nelson S.D., Mitchell J.R., Dybing E., Sasame H.A.
Biochem. Biophys. Res. Commun. 70, 1157-1165, 1976.

57 Thionation reactions of Lawesson's reagent.
Cava M.P., Levinson M.I.
Tetrahedron 41, (22), 5061-5087, 1985.

58 Comprehensive heterocyclic chemistry. The structure, reactions, synthesis and uses of heterocyclic compounds. Part XI. Five-membered rings with two of more O,S or N atoms.
Katritzky A.R., Rees C.W.
Pergamon Press, 1984.

59 Reagents for organic synthesis. Volume 1.
Fieser L.F., Fieser M.
John Wiley & sons inc., 1967.

60 Heterocyclic compounds. Vol. 5.
Elderfield R.C.
John Wiley & Sons Ltd, 1957.

61 Cleavage of ethers.
Bhatt M.V., Kulkarni S.U.
Synthesis 4, 249-282, 1983.

Ref.

62 Selective reduction of aromatic nitro compounds with stannous chloride in non-acidic and non-aqueous media.
Bellamy F.D., Ou K.
Tet. Lett. 25, (8), 839-842, 1984.

63 Operation manual for control of selection, production, preclinical and phase I trials of endocrine agents for patients with cancer.
CRC Joint Committee
British J. Cancer 60, 265-269, 1989.

64 Laboratory models of breast cancer to aid the elucidation of antiestrogen action.
Jordan V.C.
J. Lab. Clin. Med. 109, (3), 267-277, 1987.

65 Required presence of both estrogen and pituitary factors for the growth of human breast cancer cells in athymic nude mice.
Leung C.K.H., Shiu R.P.C.
Cancer Res 41, 546-551, 1981.

66 Induction of mammary carcinomas in rats by nitrosomethylurea involves malignant activation of H-ras-1 locus by single point mutations.
Sukumar S., Notario V., Martin Zanca D.
Nature 306, 658-661, 1983.

67 N-Nitrosomethylurea as mammary gland carcinogen in rats.
Gullino P.M., Pettigrew H.M., Grantham F.H.
J. Natl. Cancer Inst. 54, 401-414, 1975.

68 Hormone dependency in N-methylnitrosourea-induced rat mammary tumours.
Arafah B.M. Finegan H.M., Roe J., Manni A., Pearson O.H.
Endocrinol. 111, 584-588, 1982.

69 Estrogen receptor characteristics in a transplantable mouse mammary tumour.
Watson C., Medina D., Clark J.H.
Cancer Res. 37, 3344, 1977.

70 Human breast carcinoma cells in continuous culture: A review
Engel L.W., Young N.A.
Cancer Res. 38, 4327-4339, 1978.

Ref.

71 Role of receptors in mediating steroid hormone effects in human breast cancer.
Lippman M.E., Kasid A.
Cancer Treat. Rep. 68, (1) 265-279, 1984.

72 Flavones and related compounds as inhibitors of protein tyrosine kinases
Cunningham B.D.M.
Ph.D. thesis, Aston University, 1987.

73 Direct transformation of 3T3 cells by Ableson murine leukaemia virus.
Scher C.D., Siegler R.
Nature 253, 729-731, 1975.

74 Cytogenetic and phenotypic analysis of a human colon carcinoma cell line resistant to mitoxantrone.
Dalton W.S., Cress A.E., Alberts D.S., Trent J.M.
Cancer Res. 48, 1882-1888, 1988.

75 A handbook of computational chemistry. A practical guide to chemical structure and energy calculations.
Clark T.
John Wiley & Sons, Inc., 1985.

76 Concerning the conformation of isolated benzylidene-aniline.
Bally T., Haselbach E., Lanyiova S., Marschner F., Rossi M.
Helv. Chim. Acta. 59, 486-498, 1976.

77 AM1: A new general purpose quantum mechanical molecular model.
Dewar M.J.S., Zoebisch E.G., Healy E.F., Stewart J.J.P.
J. Am. Chem. Soc. 107, 3902-3909, 1980.

78 Optimisation of parameters for semi-empirical methods II. Applications.
Stewart J.J.P.
J. Comp. Chem. 10, (2), 221-264, 1989.

79 CHEM-X.
Developed and distributed by Chemical Design Ltd, Oxford, England.

80 MOPAC 5.0.
QCPE Bulletin 9, (4), 116, 1989. Quantum Chemistry Program Exchange, Dept. of Chemistry, Indiana University, Bloomington, IN., U.S.A.

Ref.

81 QUANTA
Copyright Polygen Corporation, Waltham, MA., U.S.A.

82 Crystal clear data.
Kennard O., Watson D.G., Allen F.H., Motherwell W.D.S., Town W.G., Rodgers J.
Chemistry in Britain 11, 313, 1975.

83 The protein data bank: A computer-based archive file for macromolecular structures
Bernstein F.C., Koetzle T.F., Williams G.J.B., Meyer E.F. Jn., Brice M.D., Rodgers J.R., Kennard O., Shimanouchi T., Tasumi M.
J. Mol. Biol. 112, 535-542, 1977.

84 Polymorphs of tamoxifen citrate: Detailed structural characteristics of the stable form.
Goldberg I., Becker Y.
J. Pharm. Sci. 76, 259, 1987

85 Structure cristalline et moléculaire de l'oestradiol hemihydrate.
Busetta B., Hospital M.
Acta cryst B28, 560, 1973

86 The crystal and molecular structure of adenosine triphosphate.
Kennard O., Isaacs N.W., Motherwell W.D.S., Coppola J.C., Wampler D.L., Larson A.C., Watson D.G.
Proc. R. Soc. Lond. Sect. A, 325, 401-436, 1971.

87 Restrained refinement of disodium adenosine 5'-triphosphate trihydrate.
Larson A.C.
Acta Cryst. Section B, 34, 3601-3604, 1978.

88 Sequence and structure of yeast phosphoglycerate kinase.
Watson H.C., Walker N.P.C., Shaw P.J., Bryant T.N., Wendell P.L., Fothergill L.A., Perkin R.E., Conroy S.C., Dobson M.J., Tuite M.F., Kingsman A.J., Kingsman S.M.
EMBO J. 1, (12), 1635-1640, 1982.

89 The Crystal and molecular structure of quercetin: A biologically active naturally occurring flavonoid.
Ross M., Rickles L.F., Halpin W.A.
Bioorg. Chem. 14, 55-69, 1986.

90 Génistein
Breton M., Precigoux G., Courseille C., Hospital M.
Acta Cryst. Sect. B, 31, 921-923, 1975.

Ref.

91 Amiloride and epithelial sodium transport.
Eds. Cuthbert A.W., Farelli G.M. Jn., Scriabine A.
Urban and Schwarzenberg Inc., 1979.

92 Investigation of the Bischler indole synthesis from 3,5-dimethoxyaniline.
Black D. St. C., Gatehouse B.M.K.C., Theobald F., Wong L.C.H.
Aust. J. Chem. 33, 343, 1980.

93 D-16726
von Angerer E., Engle J., Schneider M.R., Sheldrick W.S.
Drugs of the Future 10, (4), 281-285, 1985.

94 The crystal and molecular structure of diethylstilbestrol.
Weeks C.M., Cooper A., Norton D.A.
Acta Cryst. Sect. B, 26, 429-433, 1970.

95 A refinement of the crystal structure of azobenzene.
Brown C.J.
Acta. Cryst. 21, 146-152, 1966.

96 Sheldrick, W.S.
Personal communication, 1990.

97 Direct evidence that oncogenic tyrosine kinases and cyclic AMP-dependent protein kinases have homologous ATP-binding sites.
Kamps M.P., Taylor S.S., Seftom B.M.
Nature 310, 589-592, 1984.

98 Why is Mg^{2+} necessary for specific cleavage of the terminal phosphoryl group of ATP?
Yoshikawa K., Shinohara Y., Terada H., Kato S.
Biophys. Chem. 27, 251-254, 1987.

99 Structure/activity studies of flavenoids as inhibitors of cyclic AMP phosphodiesterase and relationship to quantum chemical indices.
Ferrell J.E. Jn., Chang Sing D.G., Loew G., King R., Mansour J.M., Mansour T.E.
Molecular Pharmacology 16, 556-568, 1979.

100 Direct synthesis of 2,2-diaryl-3-methyl-2,3-dihydrobenzothiazoles from 3-methyl- 2,3-dihydrobenzothiazole-2-thione and some mechanistic aspects.
Akibe K., Shiriaishi H., Inamoto N.
Bull. Chem. Soc. Japan 52, (1), 156-159, 1979.

Ref.

101 Studies on heteroaromatic N-oxides IX. The synthesis and structure of benzothiazole N-oxides.
Takahashi S., Kano H.
Chem. Pharm. Bull. 17, (8), 1598-1604, 1969.

102 The synthesis and reactions of organic compounds.
Barton D., Ollis W.D.
Pergamon Press, 1979.

103 Effects of pharmacological concentrations of estrogens on proliferation and cell cycle kinetics of human breast cancer cell lines in vitro.
Reddel R.R., Sutherland R.L.
Cancer Research 47, 5323-5329, 1987.

104 Rowlands M.G., Parr I.B., M^{c}Cague R., Jarman M., Goddard P.H.
Biochem. Pharmacol. "in press"

105 Effects of steroid hormones and antihormones in cultured cells.
Jung-Testas I., Baulieu E-E.
Exp. Clin. Endocrinol. 86, (2), 151-164, 1985.

106 Increased aromatase activity in pubic skin fibroblasts from patients with isolated gynacomastia.
Bulard J., Mowszowicz I., Schaison G.
J. Clin. Endo. Metab. 64, (2), 1987.

107 Estrogenic activity of phenol red.
Welshons W.V., Wolf M.F., Murphy C.S., Jordan V.C.
Mol. Cell. Endocrinol. 57, (3), 169-178

108 Regulation of biosynthesis and phosphorylation of $p210^{bcr/abl}$ protein during differentiation induction of K 562 cells.
Nishimura J., Takahira H., Shibata K., Muta K., Yamamoto M., Ideguchi H., Umemura T., Nawata H.
Leukaemia Research 12 (11/12), 875-885, 1988.

109 3,4-Bis-(3'-hydroxyphenyl)-hexane - A new mammary tumour-inhibiting compound.
Kranzfelder G., Hartmann R.W., von Angerer E., Schonenberger H., Bogden A.E.
J. Cancer Res. Clin. Oncol., 103, 165-180, 1982.

110 Biological aromatization of steroids.
Ryan K.J.
J. Biol. Chem. 234, 268-272, 1959.

Ref.

111 Determination of protein: a modification of the Lowry method that gives a linear photometric response.
Hartree E.F.
Anal. Biochem. 48, 422-427, 1972.

112 Analogues of aminoglutethimide based on 1-phenyl-3-azabicyclo[3.1.0]heane-2,4-dione: Selective inhibition of aromatase activity.
Rowlands M.G., Bunnett M.A., Foster A.B., Jarman M., Stanek J., Schweizer E.
J. Med. Chem. 31, 971-976, 1988.

113 Isolation of a calcium-dependent 35-kilodalton substrate for the epidermal growth factor receptor/kinase from A-431 cells.
Fava R.A., Cohen S.
J. Biol. Chem. 259, (4), 2636-2645, 1984.

114 The Merck Index. 10th Edition
Ed Windholz M.
Merck & Co Inc., 1983.

115 Organic photoconductive materials for electrophotography.
Sues O., Tomanek M., Lind E.
U.S. Patent 3 257 204, 21 June, 1966.

116 Researches on thiazoles. IX. Further studies on derivatives of 2-phenylbenzothiazole.
Bogert M.T., Corbitt H.B.
J. Am. Chem. Soc. 48, 783-788, 1926.

117 Studies on heterocyclic chemistry part XVIII. Thermally induced isomerisation of 3-p-alkoxyphenyl-5-methoxy isoxazoles in aryl aldehydes and dehydration of 5-amino-3,4-diarylisoxazoles in hexamethylphosphoric triamide.
Nishiwaki T., Azechi K., Fujiyama F.
J. Chem Soc. Perkin I 15, 1867-1870, 1974.

118 Friedel crafts reaction of isothiocyanates I. Aryl isothiocyanates.
Ginwala K.K., Trivedi J.P.
J. Ind. Chem. Soc. 40, (10), 897-898, 1963.

119 Medium ultraviolet and visible absorption of N- aroyl amines III. o-, m-, and p-methoxybenzoylarylamines.
Grammaticakis P.
Bull. Soc. Chim. Fra. 5, 924-935, 1964.

Ref.

120 Uber die Behiehungen zwischen dinonhydrazonen und p-oxyazoverbindung V: Uber p-arylsulfan-azo-phenole
Borsche W., Frank R.
Justus Liebig's Ann. Chem. 450, 79, 75-84, 1926.

121 Derivatives of p-alkoxybenzoic acids XXIII. Synthesis of amino esters of 3-methoxy-4-alkoxybenzoic acids.
Mndzhoyan A.L., Afrikyin V.G., Khorenyan R.A., Aleksanyan R.A., Stepanyon N.O.
Izv. Akad. Nauk. Arm. SSR. Khim. 18, (2), 193-9, 1965.

122 The preparation of some secondary and tertiary selenoamides and study of their spectra.
Rae I.D., Wade M.J.
Int. J. Sulfur Chem. 8, (4), 519-528, 1977.

123 Ortho effects in organic molecules on electron impact XI. The interesting ortho effect of a methoxy group in O-methoxy aromatic thioamides.
Ramana D.V., Viswanadham S.K.
Org. Mass. Sectrom. 18, (10), 418-422, 1983.

124 Anodic oxidation of some anilides in trifluoroacetic acid.
Hess U., Gross T., Jahn B.
Z. Chem. 19, (1), 25-26, 1979.

125 Etude cinétique de l'hydrolyse des amides XV. Hydrolyse acide et lieu de protonation des benanilides.
Rysman de Lockerent P.S., van Brant P., Bruylants A., de Theux T.
Bull. Soc. Chim. Fra. 2207-2210, 1970.

126 Thioamides IV. Reaction of O-ethyl thioesters with aliphatic and aromatic amines. Preparation of mono- and disubstituted thioamides.
Reynaud P., Moreau R.C., Samama J.P.
Bull. Soc. Chim. Fra. 12, 3623-3628, 1965.

127 Bicyclic compounds and their comparison with napthalene.
Fries K.
Justus Liebig's Annalen der Chemie 454, 121-324, 1927.

Ref.

128 2-Benzothiazolyl alkanoic acids and their derivatives VIII. Condensation of unsymmetrically substituted phthalic anhydrides and pyridinedicarboxylic anhydrides with o-aminothiophenol.
Babichev E.S., Kiripanova L.A., Dashevskaya T.A.
Ukr. Khim. Zh. 32, (7), 706-715, 1966.

129 Untersuchungen in der Reihe des Benzothiazols.
Fries K., Wolter A.
Justus Liebig's Ann. Chem. 527, (193), 60-71, 1936.

130 Basic methanolysis of some substituted 4'-nitrobenzanilides.
Broxton T.J., Cardane C.J., Deady L.W.
Aust. J. Chem. 28, (2), 451-454, 1975.

131 Direct preparation of thioamides form acid chlorides and amines.
Voss J., Walter W.
Justus Liebig's Ann. Chem. 716, 209-211, 1968.

132 The aminolysis of N-hydroxysuccinamide esters. A structure-reactivity study.
Cline G.W., Hanna S.B.
J. Am. Chem. Soc. 109, 3087-3091, 1987.

133 Synthesis of n-substituted thioamides of p-nitrobenzoic acid.
Golovinski E., Arnaudov M., Spasov A.L.
Compt. Rend. Acad. Bulgare Sci. 16, (7), 717-720, 1963.

134 Some nitro and amino derivatives of benzanilide, thiobenzanilide and 2-phenylbenzothiazole and the azo dyes derived therefrom.
Rivier H. Zeltner J.
Helv. Chim. Acta. 20, 691-704, 1937.

135 Carbithioic acid studies I. Tolyl-4-carbithioic acid and certain derivatives.
Bost R.W., Mattox W.J.
J. Am. Chem. Soc. (52), 332-335, 1930.

136 Copper (I) oxide promoted arylation of benzothiazole with iodoarenes.
Chodowska-Palicka J.
Synthesis 2, 128-129, 1974.

137 International tables for X-ray crystallography. Vol 4
Kynoch Press, Birmingham, 1974.

APPENDIX 1

Crystal Structure of 2-(4-Methoxyphenyl)-5,6-dimethoxybenzothiazole (38c)

Cream needle crystals of 2-(4-methoxyphenyl)-5,6-dimethoxybenzothiazole were grown from a methanolic solution. The crystal had dimensions 0.35 x 0.35 x 1.25 mm. The data were collected on an Enraf-Nonius CAD4 diffractometer with monochromated Mo-K_α radiation, (lambda)=0.71069 Å.

Crystal Data

$C_{16}H_{15}O_3NS$, M=301.4, monoclinic, a=17.142(1), b=11.165(1), c=7.683(2) Å, β=101.34(1) °, V=1441.7(9) $Å^3$, Z=4, D_m=1.35(2) g cm^{-3}, D_x=1.39 g cm^{-3}, F(000)=632, μ(Mo-K_α)=1.88 cm^{-1}, space group $P2_1/c$.

The 3134 unique intensity data were collected by the ω-2Θ scan technique, and of these 2307 reflections were deemed observed with $F_o > 2.5\sigma$. Using SHELX-76[7], an E-map was produced in which all but four of the non-hydrogen atoms were located. These remaining atoms were located in a subsequent Fourier map. Hydrogen atoms were included in calculated positions and all atoms refined isotropically. Further refinement with anisotropic non-hydrogen atoms

reduced the unweighted discrepancy index to R = 0.039. In the latter stages of refinement, reflections were weighted according to $w = K/[\sigma^2(F)+0.003F^2]$. Finally a difference electron density map was calculated which showed no feature greater than 0.28 e $Å^{-3}$. Calculations were performed on the VAX 8650 Cluster at Aston University. Observed and calculated structure factors, and atom thermal parameters are given in Table 24. Scattering factors were taken from ref. 137.

This structure was determined by Dr. P. C. Yates.

Table 19: Final atomic coordinates (x 10^4) for 2-(4-methoxyphenyl)-5,6-dimethoxybenzothiazole (38c) with estimated standard deviations (e.s.d.'s.) in parentheses

Atom	x/a	y/b	z/c
C(1)	-2210(2)	3059(3)	-1640(4)
O(2)	-1921(1)	3803(1)	-0154(2)
C(3)	-1124(1)	3773(2)	0531(3)
C(4)	-0840(1)	4664(2)	1774(3)
C(5)	-0050(1)	4707(2)	2549(2)
C(6)	0489(1)	3861(2)	2115(2)
C(7)	0193(1)	2975(2)	0891(3)
C(8)	-0601(1)	2925(2)	0098(3)
C(9)	1326(1)	3918(2)	2974(2)
N(10)	1593(1)	4455(1)	4482(2)
C(11)	2410(1)	4326(2)	4980(2)
S(12)	2053(0)	3225(0)	2000(1)
C(13)	2772(1)	3685(2)	3786(3)
C(14)	3592(1)	3466(2)	4132(3)
C(15)	4038(1)	3877(2)	5712(3)
C(16)	3669(1)	4487(2)	6963(3)
C(17)	2870(1)	4718(2)	6597(3)
O(18)	4175(1)	4790(2)	8514(2)
C(19)	3817(1)	5172(3)	9944(3)
O(20)	4840(1)	3733(2)	6228(2)
C(21)	5246(1)	3157(3)	5010(4)
H(40)	-1245(1)	5323(2)	2119(3)
H(50)	0164(1)	5401(2)	3502(2)
H(70)	0597(1)	2314(2)	0545(3)
H(80)	-0818(1)	2227(2)	-0846(3)
H(101)	-2827(2)	3237(3)	-2206(4)
H(102)	-2146(2)	2141(3)	-1194(4)
H(103)	-1854(2)	3208(3)	-2633(4)
H(140)	3865(1)	2985(2)	3189(3)
H(170)	2596(1)	5198(2)	7541(3)
H(191)	4317(1)	5227(3)	11043(3)
H(192)	3407(1)	4495(3)	10218(3)
H(193)	3518(1)	6028(3)	9766(3)
H(211)	5878(1)	3155(3)	5539(4)
H(212)	5131(1)	3601(3)	3736(4)
H(213)	5033(1)	2245(3)	4852(4)

Table 20: Interatomic distances for 2-(4-methoxyphenyl)-5,6-dimethoxybenzothiazole (38c) with e.s.d.s in parentheses.

Bond	Interatomic distance (Å)
C(1)-O(2)	1.420(3)
O(2)-C(3)	1.364(2)
C(3)-C(4)	1.398(3)
C(3)-C(8)	1.388(3)
C(4)-C(5)	1.368(3)
C(5)-C(6)	1.407(3)
C(6)-C(7)	1.391(2)
C(6)-C(9)	1.457(3)
C(7)-C(8)	1.379(3)
C(9)-N(10)	1.305(2)
C(9)-S(12)	1.754(2)
N(10)-C(11)	1.385(2)
C(11)-C(13)	1.401(3)
C(11)-C(17)	1.404(3)
S(12)-C(13)	1.732(2)
C(13)-C(14)	1.400(3)
C(14)-C(15)	1.380(3)
C(15)-C(16)	1.423(3)
C(15)-O(20)	1.363(2)
C(16)-C(17)	1.368(3)
C(16)-O(18)	1.372(2)
C(18)-C(19)	1.425(3)
O(20)-C(21)	1.426(3)

Table 21: Interatomic angles for 2-(4-methoxyphenyl)-5,6-dimethoxybenzothiazole (38c)

Atoms	Bond angle (°)
C(1)-O(2)-C(3)	117.5(2)
O(2)-C(3)-C(4)	115.7(2)
O(2)-C(3)-C(8)	124.7(2)
C(3)-C(4)-C(5)	120.2(2)
C(4)-C(5)-C(6)	120.9(2)
C(5)-C(6)-C(7)	117.9(2)
C(5)-C(6)-C(9)	119.8(2)
C(7)-C(6)-C(9)	122.2(2)
C(6)-C(7)-C(8)	121.7(2)
C(3)-C(8)-C(7)	119.6(2)
C(6)-C(9)-N(10)	124.4(2)
C(6)-C(9)-S(12)	120.4(1)
N(10)-C(9)-S(12)	115.2(1)
C(9)-N(10)-C(11)	110.9(2)
N(10)-C(11)-C(17)	125.0(2)
N(10)-C(11)-C(13)	115.2(2)
C(13)-C(11)-C(17)	119.7(2)
C(9)-S(12)-C(13)	89.2(1)
C(11)-C(13)-S(12)	109.4(1)
C(11)-C(13)-C(14)	121.5(2)
S(12)-C(13)-C(14)	129.0(2)
C(13)-C(14)-C(15)	118.1(2)
C(14)-C(15)-C(16)	120.7(2)
C(14)-C(15)-O(20)	124.7(2)
C(16)-C(15)-O(20)	114.6(2)
C(15)-C(16)-C(17)	120.8(2)
C(15)-C(16)-O(18)	114.6(2)
C(11)-C(17)-C(16)	119.2(2)
C(16)-O(18)-C(19)	116.7(2)
C(15)-O(20)-C(21)	117.2(2)

Table 22: Torsion angles for bonds in 2-(4-methoxyphenyl)-5,6-dimethoxy-benzothiazole (38c) involving non-hydrogen atoms

Atoms	Torsion angle (°)
C(1)-O(2)-C(3)-C(4)	168.9
C(1)-O(2)-C(3)-C(8)	-12.1
O(2)-C(3)-C(4)-C(5)	179.6
C(8)-C(3)-C(4)-C(5)	0.6
O(2)-C(3)-C(8)-C(7)	-179.3
C(4)-C(3)-C(8)-C(7)	-0.4
C(3)-C(4)-C(5)-C(6)	0.0
C(4)-C(5)-C(6)-C(7)	-0.6
C(4)-C(5)-C(6)-C(9)	-179.3
C(5)-C(6)-C(7)-C(8)	0.9
C(9)-C(6)-C(7)-C(8)	179.5
C(5)-C(6)-C(9)-N(10)	21.3
C(7)-C(6)-C(9)-N(10)	-157.3
C(5)-C(6)-C(9)-S(12)	-159.4
C(7)-C(6)-C(9)-S(12)	22.0
C(6)-C(7)-C(8)-C(3)	-0.4
C(6)-C(9)-N(10)-C(11)	178.3
S(12)-C(9)-N(10)-C(11)	-1.1
C(6)-C(9)-S(12)-C(13)	-178.7
N(10)-C(9)-S(12)-C(13)	0.6
C(9)-N(10)-C(11)-C(13)	1.1
C(9)-N(10)-C(11)-C(17)	-174.8
N(10)-C(11)-C(13)-S(12)	-0.6
C(17)-C(11)-C(13)-S(12)	175.5
N(10)-C(11)-C(13)-C(14)	-178.8
C(17)-C(11)-C(13)-C(14)	-2.7
N(10)-C(11)-C(17)-C(16)	177.0
C(13)-C(11)-C(17)-C(16)	1.3
C(9)-S(12)-C(13)-C(11)	0.0
C(9)-S(12)-C(13)-C(14)	178.0
C(11)-C(13)-C(14)-C(15)	1.4
S(12)-C(13)-C(14)-C(15)	-176.4
C(13)-C(14)-C(15)-C(16)	1.1
C(13)-C(14)-C(15)-O(20)	-179.9
C(14)-C(15)-C(16)-C(17)	-2.5
O(20)-C(15)-C(16)-C(17)	178.4
C(14)-C(15)-C(16)-O(18)	176.7
O(20)-C(15)-C(16)-O(18)	-2.4
C(14)-C(15)-O(20)-C(21)	2.6
C(16)-C(15)-O(20)-C(21)	-178.4
C(15)-C(16)-C(17)-C(11)	1.2
O(18)-C(16)-C(17)-C(11)	-177.9
C(15)-C(16)-O(18)-C(19)	-167.3
C(17)-C(16)-O(18)-C(19)	11.8

Table 23: Close interatomic contacts in 5,6-dimethoxy-2-(4-methoxyphenyl)benzothiazole (38c)

Atoms*	Distance (Å)
O(18)...C(19)^{I}	3.414
O(2)....S(12)^{I}	3.598
S(12)...S(12)^{II}	4.169
N(10)...S(12)^{II}	3.566
S(12)...C(17)^{II}	3.609
C(11)...S(12)^{II}	3.357
S(12)...C(13)^{II}	3.656

* Roman numerals as superscript denote atoms in the following equivalent positions with respect to those at x,y,z (Table 1):

I	1-x,1-y,1-z
II	x,0.5-y,0.5+z

Table 24: Atomic Thermal Parameters

Anisotropic values are in the form $\exp\{-2\pi^2(U_{11}a^{*2}h^2 + ... + 2U_{23}b^*c^*kl)\}$

Atom	U_{11}	U_{22}	U_{33}	U_{23}	U_{13}	U_{12}
C(1)	558	921	659	-272	-87	-25
O(2)	480	643	501	-119	9	12
C(3)	448	453	320	16	72	-37
C(4)	512	433	397	-32	88	35
C(5)	521	407	320	-58	74	-14
C(6)	471	383	274	9	86	-30
C(7)	511	423	363	-75	97	14
C(8)	541	432	356	-82	66	-30
C(9)	478	379	316	-22	112	-20
N(10)	447	441	334	-47	77	-8
C(11)	424	389	357	-10	98	-30
S(12)	498	580	365	-132	90	26
C(13)	500	419	355	-25	101	-15
C(14)	481	486	437	-65	131	5
C(15)	421	482	439	9	102	0
C(16)	448	464	376	-29	61	-54
C(17)	424	469	387	-51	98	-23
O(18)	433	803	405	-118	32	-43
C(19)	508	977	399	-167	66	-87
O(20)	439	785	566	-110	88	72
C(21)	464	893	817	-223	161	71

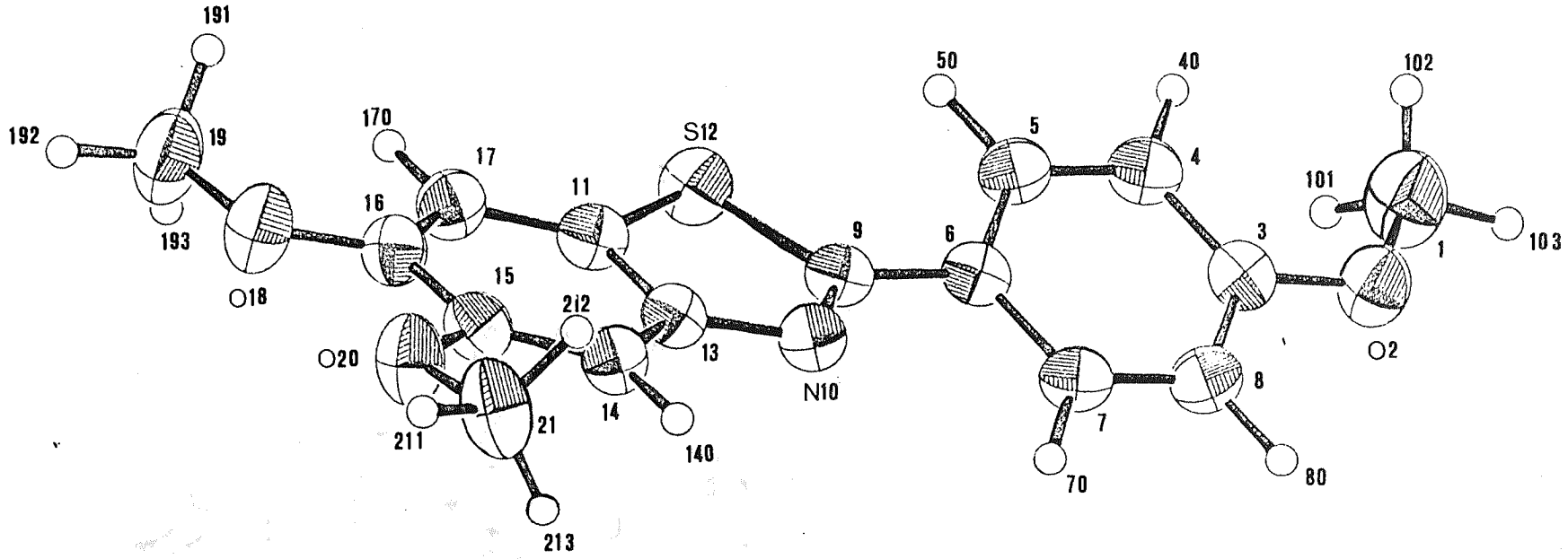

Fig. 11: Crystal structure of 2-(4-methoxyphenyl)-5,6-dimethoxybenzothiazole (38c) as determined by X-ray diffraction, showing the atomic numbering scheme.

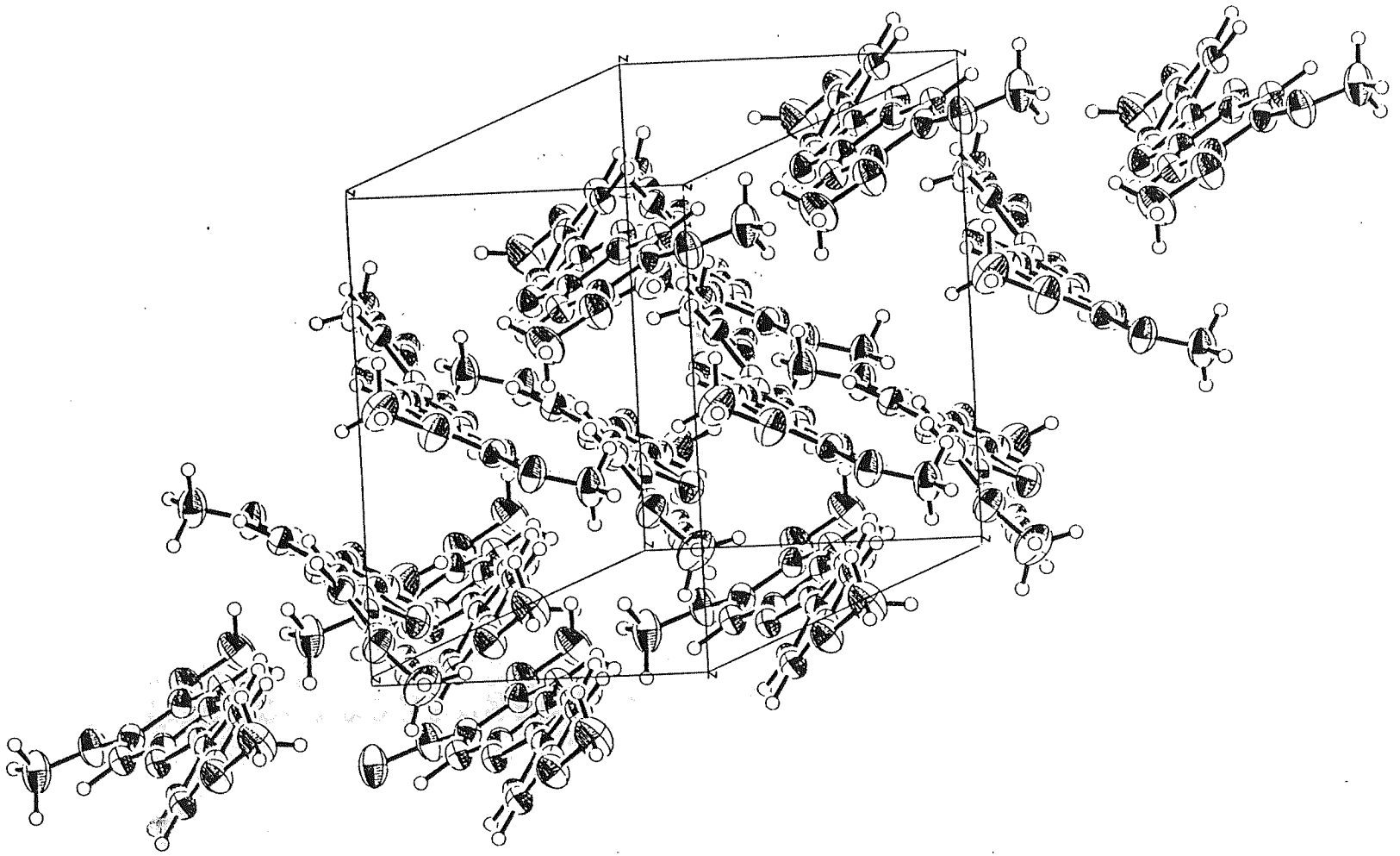

Fig.12: The unit cell of the crystal structure of 2-(4-methoxyphenyl)-5,6-dimethoxybenzothiazole (38c) showing the close packing of the moleclues. The b and c axis are in the plane of the paper.

APPENDIX 2

Table 25: Cartesian co-ordinates and net atomic charges of adenosine triphosphate complexed to two magnesium-like sparkles

Atom	X	Y	Z	Charge
P(1)	-6.0438	-2.4205	0.5942	1.4480
O(2)	-4.4444	-2.4205	0.4137	-0.8187
P(3)	-3.3357	-1.1394	1.0326	1.4340
O(4)	-2.9094	-1.5821	2.4004	-0.7187
O(5)	-6.6549	-1.2340	1.3058	-0.8445
O(6)	-3.7627	0.2866	0.7413	-0.9298
O(7)	-6.0274	-3.8824	1.0076	-0.8386
O(8)	-2.1059	-1.4749	-0.0301	-0.5673
C(9)	-0.7764	-1.1996	0.1757	0.2435
C(10)	-0.2728	0.0085	-0.7177	0.0947
C(11)	0.7824	-0.3694	-1.8315	0.0670
C(12)	1.9525	0.6923	-1.6710	0.0665
C(13)	1.5951	1.4389	-0.3114	0.2979
O(14)	0.3433	0.9853	0.1041	-0.3276
O(15)	-6.5703	-2.4412	-0.8928	-0.8665
H(16)	-0.1880	-2.1223	-0.0956	-0.0374
P(17)	-6.5970	-1.9141	-2.4740	1.4312
O(18)	-7.9920	-2.1819	-2.9849	-0.7806
O(19)	0.1683	-0.3675	-3.0808	-0.3026
O(20)	2.1335	1.5489	-2.7498	-0.2937
N(21)	2.5820	1.1723	0.7636	-0.3001
C(22)	3.8842	1.6855	0.8070	0.1445
H(23)	1.3993	2.1286	-2.8987	0.1887
H(24)	0.6763	-0.8539	-3.7167	0.1869
N(25)	4.5311	2.4596	-0.1037	-0.2849
C(26)	5.8086	2.7383	0.2367	0.1784
N(27)	6.4740	2.3213	1.3534	-0.3524
C(28)	5.8205	1.5710	2.2796	0.2740
H(29)	-0.5294	-1.0015	1.2502	0.0145
O(30)	-5.5031	-2.8472	-3.0212	-1.0414
C(31)	2.4210	0.4674	1.9916	0.1300
C(32)	4.4651	1.2193	2.0305	-0.1785
N(33)	3.5208	0.4713	2.7415	-0.1998
H(34)	6.3861	3.3597	-0.4633	0.1124
N(35)	6.5070	1.2746	3.4574	-0.2468
H(36)	7.5086	1.3256	3.3932	0.1583
O(37)	-6.2217	-0.4367	-2.3342	-1.0321
H(38)	1.4911	-0.0154	2.2822	0.1489
H(39)	6.2308	0.4143	3.8949	0.1601
H(40)	1.5461	2.5587	-0.4379	0.0523
H(41)	-1.1609	0.5037	-1.1966	0.0578
H(42)	2.9189	0.1297	-1.5807	0.0610
Mg(43)	-4.5867	-4.8879	-1.6814	2.0000
H(44)	1.2327	-1.3773	-1.6182	0.0111
Mg(45)	-6.1207	1.3411	-0.4092	2.0000

Table 26: Interatomic distances for adenosine triphosphate complexed with two magnesium-like sparkles

Atoms	Interatomic distance (Å)
O(2) - P(1)	1.63978
P(3) - O(2)	1.59650
O(4) - P(3)	1.49948
O(5) - P(1)	1.51240
O(6) - P(3)	1.51681
O(7) - P(1)	1.51929
O(8) - P(3)	1.65970
C(9) - O(8)	1.37324
C(10) - C(9)	1.58468
C(11) - C(10)	1.58018
C(12) - C(11)	1.58812
C(13) - C(12)	1.59180
O(14) - C(13)	1.39469
O(15) - P(1)	1.57766
H(16) - C(9)	1.12738
P(17) - O(15)	1.66689
O(18) - P(17)	1.50960
O(19) - C(11)	1.39212
O(20) - C(12)	1.38933
N(21) - C(13)	1.48345
C(22) - N(21)	1.40037
H(23) - O(20)	0.94720
H(24) - O(19)	0.94811
N(25) - C(22)	1.35908
C(26) - N(25)	1.35114
N(27) - C(26)	1.36515
C(28) - N(27)	1.35933
H(29) - C(9)	1.12021
O(30) - P(17)	1.53844
C(31) - N(21)	1.42502
C(32) - C(28)	1.42228
N(33) - C(31)	1.33113
H(34) - C(26)	1.09983
N(35) - C(28)	1.39511
H(36) - N(35)	1.00503
O(37) - P(17)	1.53073
H(38) - C(31)	1.08735
H(39) - N(35)	1.00397
H(40) - C(13)	1.12806
H(41) - C(10)	1.12394
H(42) - C(12)	1.12186
Mg(43) - O(30)	2.60756
H(44) - C(11)	1.12432
Mg(45) - O(37)	2.62225

Table 27: Interatomic angles for adenosine triphosphate complexed with two magnesium-like sparkles

Atoms	Bond Angle (°)
P(3) - O(2) - P(1)	138.63
O(4) - P(3) - O(2)	111.84
O(5) - P(1) - O(2)	107.21
O(6) - P(3) - O(2)	107.54
O(7) - P(1) - O(2)	101.73
O(8) - P(3) - O(2)	98.27
C(9) - O(8) - P(3)	125.52
C(10) - C(9) - O(8)	112.08
C(11) - C(10) - C(9)	115.29
C(12) - C(11) - C(10)	105.12
C(13) - C(12) - C(11)	103.56
O(14) - C(13) - C(12)	107.67
O(15) - P(1) - (O2)	102.96
H(16) - C(9) - O(8)	107.77
P(17) - O(15) - P(1)	153.54
O(18) - P(17) - O(15)	106.24
O(19) - C(11) - C(10)	109.73
O(20) - C(12) - C(11)	115.45
N(21) - C(13) - C(12)	112.66
C(22) - N(21) - C(13)	125.12
H(23) - O(20) - C(12)	113.48
H(24) - O(19) - C(11)	111.40
N(25) - C(22) - N(21)	129.09
C(26) - N(25) - C(22)	113.50
N(27) - C(26) - N(25)	127.15
C(28) - N(27) - C(26)	119.45
H(29) - C(9) - O(8)	113.12
O(30) - P(17) - O(15)	97.72
C(31) - N(21) - C(13)	129.66
C(32) - C(28) - N(27)	118.38
N(33) - C(31) - N(21)	112.99
H(34) - C(26) - N(25)	116.91
N(35) - C(28) - N(27)	117.13
H(36) - N(35) - C(28)	115.20
O(37) - P(17) - O(15)	102.39
H(38) - C(31) - N(21)	123.13
H(39) - N(35) - C(28)	114.49
H(40) - C(13) - C(12)	112.30
H(41) - C(10) - C(9)	108.97
H(42) - C(12) - C(11)	107.91
Mg(43) - O(30) - P(17)	122.80
H(44) - C(11) - C(10)	110.37
Mg(45) - O(37) - P(17)	136.95

Table 28: Torsion angles for adenosine triphosphate complexed with two magnesium-like sparkles

Atoms	Torsion angle (°)
O(4) - P(3) - O(2) - P(1)	75.00
O(5) - P(1) - O(2) - P(3)	18.26
O(6) - P(3) - O(2) - P(1)	298.30
O(7) - P(1) - O(2) - P(3)	240.50
O(8) - P(3) - O(2) - P(1)	188.56
C(9) - O(8) - P(3) - O(2)	197.45
C(10) - C(9) - O(8) - P(3)	252.73
C(11) - C(10) - C(9) - O(8)	246.63
C(12) - C(11) - C(10) - C(9)	228.76
C(13) - C(12) - C(11) - C(10)	9.58
O(14) - C(13) - C(12) - C(11)	353.16
O(15) - P(1) - (O2) - P(3)	132.71
H(16) - C(9) - O(8) - P(3)	133.03
P(17) - O(15) - P(1) - O(2)	323.71
O(18) - P(17) - O(15) - P(1)	207.53
O(19) - C(11) - C(10) - C(9)	105.16
O(20) - C(12) - C(11) - C(10)	244.54
N(21) - C(13) - C(12) - C(11)	113.17
C(22) - N(21) - C(13) - C(12)	72.09
H(23) - O(20) - C(12) - C(11)	65.08
H(24) - O(19) - C(11) - C(10)	198.73
N(25) - C(22) - N(21) - C(13)	357.08
C(26) - N(25) - C(22) - N(21)	182.24
N(27) - C(26) - N(25) - C(22)	0.57
C(28) - N(27) - C(26) - N(25)	357.99
H(29) - C(9) - O(8) - P(3)	17.30
O(30) - P(17) - O(15) - P(1)	88.16
C(31) - N(21) - C(13) - C(12)	246.48
C(32) - C(28) - N(27) - C(26)	1.52
N(33) - C(31) - N(21) - C(13)	182.47
H(34) - C(26) - N(25) - C(22)	179.83
N(35) - C(28) - N(27) - C(26)	185.72
H(36) - N(35) - C(28) - N(27)	337.63
O(37) - P(17) - O(15) - P(1)	328.95
H(38) - C(31) - N(21) - C(13)	2.08
H(39) - N(35) - C(28) - N(27)	208.30
H(40) - C(13) - C(12) - C(11)	233.78
H(41) - C(10) - C(9) - O(8)	10.10
H(42) - C(12) - C(11) - C(10)	127.42
Mg(43) - O(30) - P(17) - O(15)	12.48
H(44) - C(11) - C(10) - C(9)	343.31
Mg(45) - O(37) - P(17) - O(15)	343.57